2018

Simulation of Gas Dynamic Cold Spray Process

Sai Rajkumar Vadla
South Dakota State University

SIMULATION OF GAS DYNAMIC COLD SPRAY PROCESS

BY

SAI RAJKUMAR VADLA

A thesis submitted in partial fulfillment of the requirements of the

Master of Science

Major in Mechanical Engineering

South Dakota State University

2018

SIMULATION OF GAS DYNAMIC COLD SPRAY PROCESS

SAI RAJKUMAR VADLA

This thesis is approved as a creditable and independent investigation by a candidate for the Master of Science in Mechanical Engineering degree and is acceptable for meeting the thesis requirements for this degree. Acceptance of this thesis does not imply that the conclusions reached by the candidate are necessarily the conclusions of the major department.

Jeffrey Doom, Ph.D. Date
Thesis Advisor

Kurt Bassett, Ph.D. Date
Head, Department of Mechanical Engineering

Kinchel Doerner, Ph.D. Date
Dean, Graduate School

ACKNOWLEDGEMENTS

The first person I would like to thank is my advisor Dr. Jeffrey Doom. I cannot possibly thank him enough for providing me with the support and direction to complete this work. He was the one who ignited my passion for the CFD research and set me on the path of pursuing my Masters, and I will always be grateful for that. I would like to express my sincere gratitude to Dr. Fereidoon Delfanian for his excellent guidance and giving me the opportunity of taking part in Materials Evaluation and Testing Laboratory. I will always be grateful for his affection and support. I would also prefer to acknowledge the support of the faculty of the Department of Mechanical Engineering for giving me such wonderful education and place to work at South Dakota State University.

Masters education would be a dream for me unless Mr. Surendra Babu and Mrs. Girija gave financial support. I would like to thank Mrs. Sandra Nilges and Mrs. Lori Jacobson who took care of me like family during my stay in Brooking, SD. I would like to thank my friends, especially Ms. Kavya Ramineni for her accompany and support during my education at SDSU. Finally, to my beautiful grandmother Mrs. Suseela Devi and awesome parents Mr. Janakiram and Mrs. Rama Prada who cannot be here for my graduation but always keep me in their minds and hearts, I have more than just heartfelt gratitude for all the years of encouragement and support.

The Surface Engineering Research Collaboration grant supports this work through the Graduate Research Assistantship. Computing resources were provided by University Networking and Research Computing and Department of Mechanical Engineering at South Dakota State University. Simulation parameters were provided by AMP Laboratory, South Dakota School of Mines and Technology.

TABLE OF CONTENTS

NOMENCLATURE

V_0: Inlet velocity of the carrier gas, m/s

P_0: Inlet Pressure of the carrier gas, pa

T_0: Inlet Temperature of the carrier gas, ºC

ρ_0: Density at Inlet of the carrier gas, kg/m^3

c_p: Specific heat at constant-pressure, J/kg K

c_v: Specific heat constant-volume, J/kg K

V*: Carrier gas velocity at nozzle throat, m/s

P*: Carrier gas pressure at nozzle throat, pa

T*: Carrier gas temperature at nozzle throat, ºC

ρ^*: Density of the carrier gas at the nozzle throat, kg/m^3

A^*: Cross-sectional area at the nozzle throat, m^2

R: Gas constant, J/mol·K (8.314 J/mol·K)

$\dot{m}$: Mass flow rate, kg/s

M: Mach number

γ: Adiabatic Index

LIST OF FIGURES

LIST OF TABLES

ABSTRACT

SIMULATION OF GAS DYNAMIC COLD SPRAY PROCESS

SAI RAJKUMAR VADLA

2018

The utilization of computational fluid dynamics (CFD) as a study tool in the aerodynamics and turbomachinery industry reinforces efficiency in the design of aircraft or for understanding the flow through pipes. CFD offer tools to model different geometries and perform a more extensive study of the flow phenomena. This gives the opportunity to model a variety of geometries and analyze their behavior under different operating conditions. A similar approach can be applied to coating technologies. Coating technologies play an essential role in the manufacturing industry. Their ability to form layers of specific materials onto engineering components to enhance mechanical and physical properties has numerous applications. The applications include corrosion protection, repair, and thermal protection, etc., In recent years, CFD simulations are increasingly used in Cold Spray Technology which is a relatively new and novel coating technology used to manufacture coatings in the solid state fully preserving feedstock material properties.

This thesis is conducted mainly to verify the results of changing the cold spray nozzle profile shape. However, this study presents the theoretical and practical aspects of Cold Spray process modeling, discusses various numerical analysis research areas, and determines the significant parameters to be considered while developing a custom cold spray setup and exhibits analysis based correlations.

The simulations were performed on some meshes of different density using the k-Omega turbulent model in StarCCM+ solver. To assess the modeling requirements including mesh, numerical algorithm, and turbulence model, it is critical to validate the calculations against the experimental data. Hence, the numerical results were compared with Muhammad Faizan Ur Rab's simulation results [25], and they were in good agreement.

CHAPTER 1: INTRODUCTION

Cold spray refers to a direct material deposition process, the kinetic energy of the particles sprayed at very high velocities leads to the bonding of the particles to the substrate. In this process, small powdered particles in a range of 5 to 100 μm are accelerated to a high velocity in the range of 300 to 1200 m/s in a supersonic jet of heated gas and then impinged onto a substrate surface in solid state without significant fusion, undergoing intensive plastic deformation. Cold spray produces coatings based on a wide selection of materials with superior characteristics. Before cold spray technology, it was necessary to either dissolve the metal in a chemical bath, melt them or vaporize them. Now, through cold spray technology, metals can be deposited rapidly in the solid state, and thus, drawbacks connected with melting, such as oxidation and undesirable phase transformations can be avoided.

Cold spraying is recognized as a promising spray coating technique capable of producing thick metal and in some cases metal-ceramic coatings on metal or ceramic substrates at relatively low temperatures. Cold Spray has moved from a scientific curiosity to an established and integrated manufacturing process in a short span (30 years). Special material powders with specific characteristics, required for cold spray processing are readily available. Today, Cold Spray systems are being utilized in a wide range of applications including performance-enhancing coatings, protective layers, manufacturing new components and repairing fabricated parts, etc., The number of industries adapting to cold spray technology is increasing, from aerospace to automobile to turbine and defense to power to sputter targets, etc.,

History

Even though the cold spray is a relatively new technology, this process was mentioned over a century ago. In 1900, Thurston [2] filed a patent for a method in which metal particles are thrown upon against a metal plate by a blast of pressurized gas with such force to cause the particles to become embedded in the surface of the metal article and to form a permanent coating. The schematic of this invention is shown in Fig.

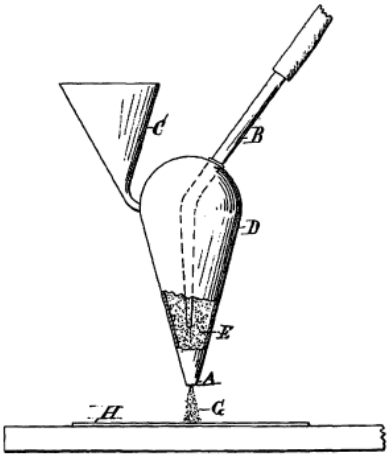

Figure 1: Schematic of Thurston's design [2]

In 1958, Rocheville [3] filed a patent to protect a device that mostly uses the method patented by Thurston but using a DeLaval type nozzle with high-pressure air to propel the fine powder particles at a higher velocity to form a coating. In his method, powder particles were powered by the supersonic blast of air directed against a substrate, and as a result, the powder adheres to the surface where it is firmly retained. He mentioned that a thin uniform layer is formed over the entire surface, the coating is built up only over the surface of the part but not upon the coat itself. Even with the use of a supersonic nozzle the device,

Rocheville could not propel the particles to high enough velocities to produce thick layers on a substrate.

In the mid-1980s, a group of scientists at the Institute of Theoretical and Applied Mechanics of the Siberian Division of the Russian Academy of Sciences in Novosibirsk, Russia, were performing supersonic wind tunnel tests to study two-phase flow around bodies using small tracers in the flow. They have observed that above a certain velocity (critical particle velocity) there was a transition from particle erosion of the target surface to rapidly increasing deposition. They named the phenomenon as ‘‘gas dynamic cold spray’’ [4]. Although some others had observed this phenomenon, the Russians developed the process as a coating technology.

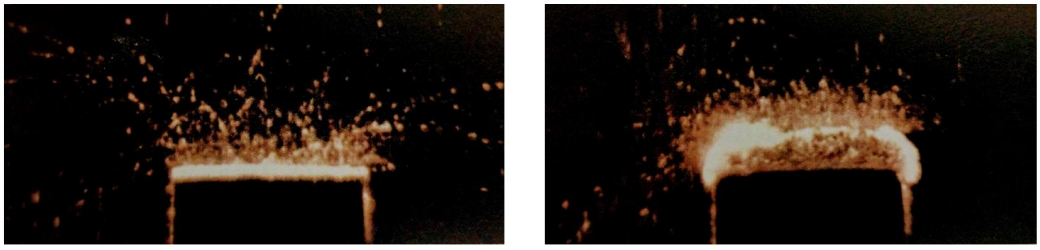

Figure 2: Early Russian Tunnel Experiments (a) Copper particles at 250m/s: Erosion (b) Copper particles at 900m/s: Deposition [4]

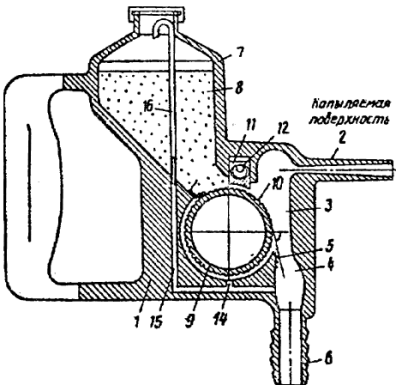

Figure 3: The First device for applying a coating by cold spray patented in 1986 [4]

Working Principle

The principle of cold spray is based on the metal particle deformation behavior during high-velocity impact with a solid subtract. In the process, the propellant gas is accelerated to supersonic velocity in a convergent-divergent (de ’Laval) nozzle. The coating powdered material is injected into the gas stream, stimulated by the propellant gas in the nozzle and propelled towards the substrate to be coated. If impact velocity of the particle exceeds a specific critical value, the impact energy from the particle provokes an intense plastic deformation of the particle. Upon impact, the particle breaks thin film on the substrate which helps to establish intimate, clean contact between the particle and substrate which leads to the creation of intense bonding. Hence, a dense and solid adhesive coating on the substrate surface is formed [10].

The main components of Cold Spray system include:

- Powder feeder
- Propellant Gas
- Gas heater to preheat the gas
- Supersonic nozzle
- Spraying chamber with a motion system
- Method for controlling spray parameters

The equipment used for cold spray has been continuously developed to achieve optimum impact conditions for a large variety of materials. Materials that have low melting temperatures can be successfully deposited by moderate conditions, using less expensive low pressure/temperature equipment. There is a necessity of having the more powerful

hardware for providing higher pressures and temperatures for processing high strength materials.

Various thermal spray techniques are compared with cold spray and discussed at more detailed in terms of impact velocity and temperature by Ang. [9] In the particle temperature and velocity map, one can observe that the process temperature of cold spray technology is much lower (below 1000 C) and impact velocity can get much higher (over 1000 m/s) when compared with other thermal spray processes.

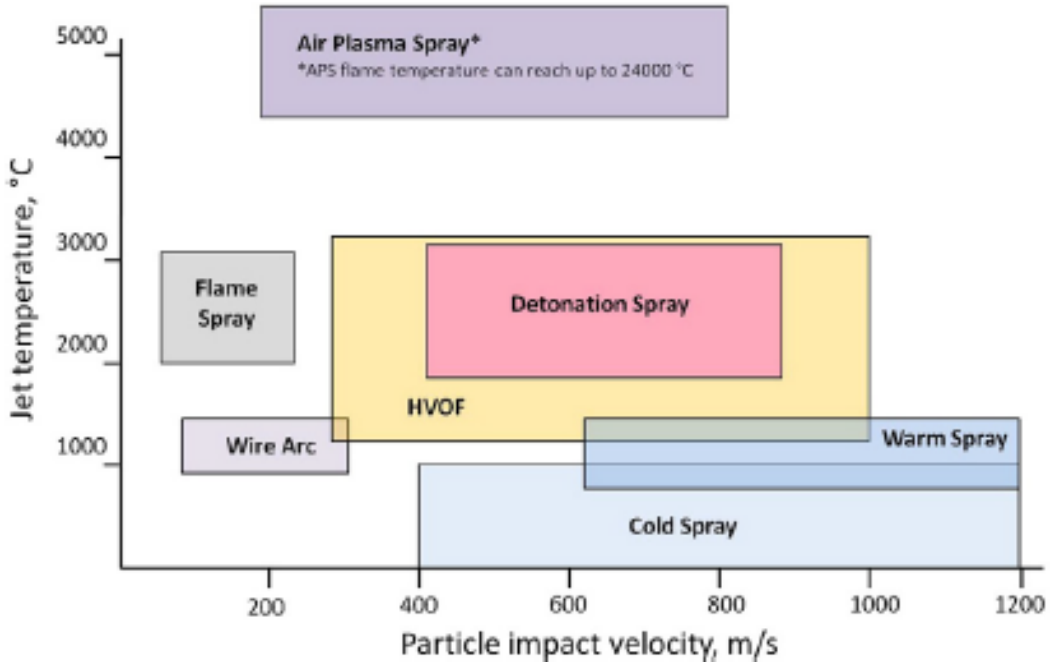

Figure 4: Particle temperature and velocity map [7]

Cold Spray Systems

A Cold Spray System can be designed in fixed, manual, portable or robotic systems.

There are majorly two main categories of cold spray systems,

1. Low-Pressure Cold Spray System,

2. High-Pressure Cold Spray System

1 *Low-Pressure Cold Spray System (LPCS)*

In the Low-Pressure cold spray system, the powder is injected in the diverging section of the nozzle where the gas is expanded [5]. Atmospheric pressure air supplied to transport powder from the feeder. Hence, the LPCS does not require a pressurized feeder. LPCS is typically smaller and often found in portable systems. The range of particle velocities that can be achieved through this system usually ranges between 300 to 600 m/s. They are used for the application of lighter materials and are generally available with air or nitrogen as a propellant gas at pressures on the order of 0.5 to 1.0 MPa.

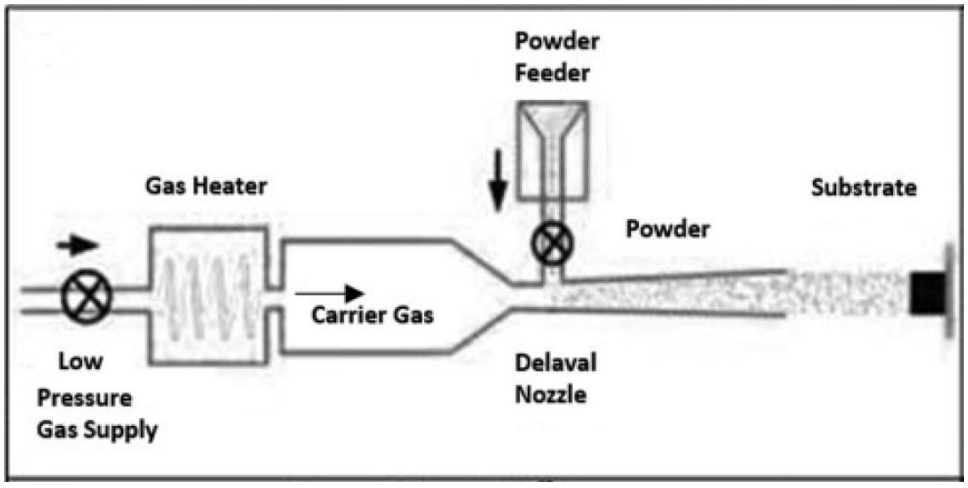

Figure 5: Low-Pressure Cold Spray system [6]

2 *High-Pressure Cold Spray system (HPCS)*

In High-Pressure Cold Spray, small particles can generate relatively higher particle velocities compared to LPCS ranging from 800 to 1400 m/s. Lower density gasses like helium or nitrogen are usually preferred for this system. The gases are pressurized high,

typically high in the range of 1 to 5 MPa through the converging-diverging nozzle to achieve high particle impact velocities.

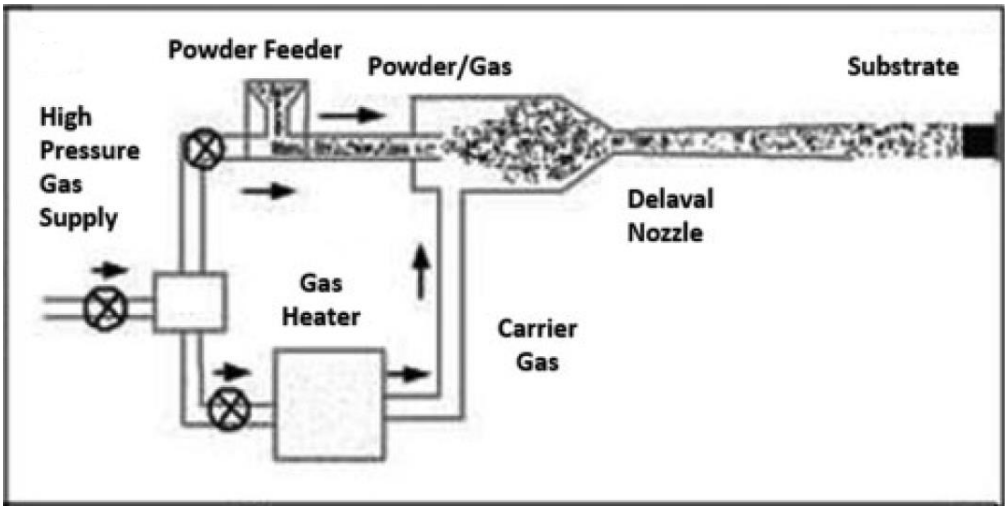

Figure 6: High-Pressure Cold Spray system [6]

For HPCS, high-pressure powder feeder running at a higher pressure than main gas stream is required to avoid powder backflow. High-pressure powder feeders are usually very expensive and big. Nozzle clogging is the other major problem with HPCS. When the particle velocity and temperature are increased, it can get worse. To overcome this problem, either a larger average particle diameter or higher yield strength second particle population with should be mixed with the first particle population. [7] Due to particle erosion, severe wear will occur at nozzle throat which affects the operation of the nozzle and leads to more considerable variations in deposit quantity. It gets worse when particles of harder material are sprayed. On the other hand, the LPCS has the simpler equipment. However, LPCS can only achieve relatively fewer particle velocities compared to HPCS as the exit Mach number, and inlet pressure is low, usually below 3 and 1MPa respectively.

Otherwise the atm. Pressure can no longer be able to supply powders into the supersonic nozzle.

Cold Sprayed Coatings

Cold spray offers many technical benefits when compared with other coating processes. Because cold spray does not use a high-temperature heat source, such as a flame or plasma, to melt the feed material, it does not deposit large amounts of heat into a coated part does it degrade thermally sensitive coating materials through oxidation or other in-flight chemical reactions. For this reason, cold spray seems very attractive for depositing oxygen-sensitive materials, such as copper or titanium.

Other properties include:

No powder melting, No grain growth, No phase changes, No oxidation, High dense coatings, Low porosity, High thermal conductivity, High electrical conductivity, Corrosion resistant, High bond strength, High compressive residual stress

Similarly, cold spray offers exciting new possibilities of building thick coatings and even free-standing shapes, from Nanophase materials, intermetallic, or amorphous materials.

Coating materials include:

Used to produce dense, pure, thick and well bonded deposits of many metals and alloys, such as Aluminum (Al), Copper (Cu), Nickel (Ni), Silver (Ag), Tantalum (Ta), Pure titanium (Ti), Zinc (Zn), Stainless steel, Nickel based alloys (Hastalloys, Inconel) and Bondcoats such as MCrAIYs

Manufacturing Advantages

- No masking is required for this process
- Flexibility in substrate
- Dissimilar materials can be coated on a substrate
- High Deposition efficiency can be obtained
- Ultra-thick coatings can be produced

Limitations

- Very less ductility
- Line of sight
- Limited sprayable materials
- The substrate must be hard enough
- High gas consumption

Applications of cold spray technology

Thermally sprayed coatings are usually evaluated by considering 1. Adhesion to the substrate, 2. Porosity and 3. Oxide contents in the layer. Presently cold spray enables the obtainment of coatings characterized by very low porosity, oxide content and high adhesion. Also, the lack of thermal stress in the layer and substrate increases the spectrum of cold spray method application in comparison with other thermal spraying methods. Cold spray can be used for applying coatings on most engineering materials. Cold spray applications are vast and primarily includes, the following areas:

Coatings

- Oxidation protection coatings
    - Copper-chrome layers
- Corrosion resistant coatings
    - Aluminum and zinc
- Composites
    - Metal-metal: copper-tungsten
    - Metal-carbide: aluminum-silicon carbide
    - Metal-oxide: aluminum-alumina
- Wear-resistant coatings
- Fretting Fatigue resistant coatings
- Self-lubrication coatings
- High-temperature protection coatings

Repairs and restoration in the following industries

- Aerospace
- Agriculture
- Automotive
- Tooling

Essential Parameters to be controlled in Cold Spray

To meet strong bonding, setting up the process, and powder parameters are vital. The following are the significant parameters to be monitored in a typical Cold Spray system:

- *Impact conditions*: Impact velocity, Impact temperature
- *Nozzle design*: Nozzle Throat diameter, Nozzle Exit diameter, Convergent length, Divergent Length and Profile Shape
- *Propellant Gas*: Gas temperature, pressure and Gas type
- *Particle*: Particle Velocity, Particle Temperature, Particle Size, Particle type and Critical Velocity of the particle
- *Substrate:* Standoff distance, Substrate temperature, Substrate type
- Deposition Efficiency

Modeling and simulation of Cold Spray

To ensure optimized and successful cold spraying, the influence of various process and powder parameters on the critical velocity, deposition efficiency should be well understood. Application of modeling and simulation in cold spray research is a feasible and robust way to reach this goal. Works related to modeling of the cold spray powder spraying process cover two primary research areas, i.e., modeling of powder particle deformation and modeling of powder particle velocity. Other research areas include modeling of substrate heating and building up residual stress in cold spraying. [11]

The numerical simulation of gas/powder velocity enables the determination of the gas state parameters inside the nozzle and once the gas has left it as well as the distribution of powder particle velocity and temperature.

Particle velocity is an important factor that determines whether particles can adhere on the substrate surface. It is known that particle in flight velocity is highly dependent on the character of the gas flow field inside and outside the nozzle because the powders are only dragged and accelerated by the compressed driving gas during the process. As for the gas flow field, it is influenced by several factors, including operating parameters, nozzle geometry, and standoff distance. Therefore, to achieve a high particle impact velocity, a large body of works has been carried out to optimize the parameters of nozzle geometry and operating parameters, and the following flow field. Among these studies, Computational fluid dynamics (CFD) technique was always adopted to predict the gas flow field and particle velocity due to its lower cost and time consuming compared to experimental implementations.

CHAPTER 2: LITERATURE REVIEW

This chapter contains a literature review related to the optimization of various parameters of the cold spray process and internal profile of the De Laval nozzle used for the cold spray process. The study done in this thesis is aimed to add more knowledge on cold spray simulation and to solve potential problems or questions not answered by the literature available on cold spray technology.

The exponential increase of industrial demand in the past two decades has led scientists to develop alternative technologies for the fast manufacturing of engineering components, aside from standard time-consuming techniques such as casting or forging.

Shuo Yin [12] conducted a numerical investigation to study the effect of nozzle cross-section shape on gas flow and particle acceleration in cold spraying. He presented a comprehensive comparison between rectangular nozzles and elliptical nozzles. Based on his calculation results, he concluded that the nozzle cross-section shape could affect the gas flow field, particle acceleration and thus particle impact velocity. His works showed that rectangular nozzles, result in slightly lower mean particle impact velocity than elliptical nozzles. However, for rectangular nozzles, more particles may achieve relatively high velocity due to the larger sectional area of their potential core. Furthermore, he found from the numerical results that the mean particle impact velocity increases gradually with the decrease in Width/Length ratio (W/L) of the cross-section because of the diminishing bow shock size. Moreover, his symmetric study on the power release position shows that releasing particles from the nozzle inlet can ensure that particles achieve a high impact velocity and temperature.

Masahiro Fukumoto [13] has carried out optimization in nozzle design by numerical simulation to improve the deposition efficiency of copper fine particles in cold spray process onto a metallic substrate. His team developed a special nozzle to reduce the bow shock effect on the substrate surface. By using his newly designed nozzle, he could able to decrease the pressure level on the substrate effectively when compared to the conventional nozzle. His research achieved a remarkable improvement in deposition efficiency, almost eight times higher than the traditional nozzle.

Wen-Ya Li [14] numerically investigated the optimization of exit diameter of a cold spray nozzle under different spray conditions. He showed that the gas conditions, particle size, and the divergent section length of the nozzle influence the optimal expansion ratio. He found that the optimal expansion ratio decreases with the increase in gas temperature, particle size, and nozzle throat diameter. His experiment with 316L stainless steel powder indicates that a thick 316L stainless steel coating with a high microhardness could be deposited with an optimized nozzle using air as an accelerating gas owing to the high particle velocity. His analysis showed a good correlation of particle velocity with the coating microstructure and microhardness.

Wen-Ya Li [15] designed a convergent barrel cold spray nozzle through numerical simulation. He found that the main factors influencing are particle velocity and temperature including the length and diameter of the barrel section, nature of the accelerating gas, pressure, and temperature of the accelerating gas, and the particle size. His analysis showed that under constant gas pressure, particles could achieve high temperature but relatively low velocity when the convergent-barrel nozzle is used compared to a convergent-

divergent nozzle. His experiments with Cu powder using convergent-barrel nozzle confirmed the feasibility to deposit thick, dense coating under a low gas inlet pressure.

Zheng-Dong, Zhou [16] compared the Laval orifice and straight orifice nozzles. In their work, they calculated gas flow field inside and outside of the nozzles. His numerical simulations show that the flow generated by the Laval nozzle had a higher exit velocity in comparison with that of the straight nozzle. He found that, in the Laval nozzle, the gas is compressed and the pressure is reduced at the throat part, whereas, at the accelerative part, the gas is almost entirely expanded and the velocity is driven close to the maximum. Moreover, the static outlet pressure of the Laval nozzle is close to the ambient pressure, whereas, the static pressure of the straight nozzle is much higher than ambient pressure and needs the further expansion of the nozzle. He also concluded that the gas flow field of the straight nozzle is somewhat convergent, but a comparatively broader flow field could be generated through a Laval nozzle.

Shuo Yin [17] investigated the effect of total pressure and the divergent length of the nozzle on the flow character and particle impact velocity in cold spraying. His simulated results indicate that the total pressure and the length of the divergent nozzle significantly influence the flow regime and particle acceleration. With gradually increasing total pressure, the nozzle exit Mach number firstly increases and then fluctuates after total pressure exceeds a critical value, finally exit Mach reaches the maximum value and maintains stable. Differing from the exit Mach, the particle impact velocity continuously goes up with total pressure due to the increasing gas density which can improve the drag force, but the growth rate levels out gradually. He also found that the exit shows a downward trend with

increasing divergent nozzle length. His works show that there exists an optimal divergent nozzle length which can guarantee the maximum particle velocity.

V. Varadaraajan [18] numerically modeled and experimentally validated a cold spray nozzle with radially injected powder. He simulated the gas flow field and particle trajectories for various injection angles and expansion ratios. He found that the injection angle influenced particle distribution and injection pressures but did not affect particle velocities significantly. He studied the effect of expansion ratio on gas flow and particle velocities in four cases. He observed the highest deposition efficiency at an over-expanded flow regime. Also, he assessed the effect of traverse speed experimentally. He concluded that the speed did not affect bond strength and coating hardness. He observed that the deposition rate was increasing until 4.5 mm/s after which it was reduced.

M. Meyer [19] experimented with three different nozzle designs under constant conditions and simulated their performance using Ansys v14.0. The deposition efficiency was measured using titanium as a feedstock material, and it was shown that it decreases with the cross-sectional throat area of the nozzle. He found that one-way coupled multiphase results could not agree with his experiments whereas more sophisticated modeling techniques with two way couplings could partially provide high-quality outcomes.

S. Yin [20] investigated the effect of carrier gas temperature on the particle acceleration and deposition by both numerical and experimental methods. He found that the carrier gas temperature significantly influences the supersonic driving gas flow and the resulting particle acceleration. The velocity and temperature of the driving gas at the throat and divergent section of the nozzle exhibit an increasing trend with gas temperature.

His results showed that higher carrier gas temperature results in increased particle velocity as well as the final impact temperature. From his analysis, it found out that the particle impact velocity is more influential than critical velocity reduction.

M Karimi, [21] presented a computational fluid dynamics model of the cold gas-dynamic spray process. The gas dynamic flow field and particle trajectories within an oval-shaped supersonic nozzle as well as in the immediate surrounding of the nozzle exit, before and after the impact with the target plane are simulated. Their predicted values of the particle nozzle wall pressure compare well with experimental data. Their works showed that the particle distribution is considerably asymmetric about the major axis but relatively symmetric about the minor axis. Their preliminary wear pattern on the nozzles sides supports this finding.

Details of the particle release pattern into the surroundings are conveniently depicted. However, their works underestimated velocity magnitudes.

R. Lupoi and O'Neill [22] investigated the powder stream characteristics in Cold spray supersonic nozzles. In his experiment, he varied the powder insertion location within the carrier gas flow, along with the geometry of the powder injector, to identify their relation with particle trajectories. R. Lupoi performed the experiment as well as CFD simulations for his analysis. He used Fluent v6.3.26 for running CFD simulation and results obtained compared to the experimental results. He modeled and tested for configurations with various acceleration channel lengths, powder injector geometry, and locations. They found out that when the powder is released axially and upstream from the nozzle throat, particle trajectories do not stay close to the centerline, but tend to spread over the entire volume of the channel. Their CFD analysis has shown that the leading causes for this effect are a

relatively high gas turbulence level generated at the vicinity of the nozzle throat which affects particle trajectories, and particle deflections due to impacts against channel walls. They also found that by employing a smaller diameter injector, a narrower beam can be achieved.

X.K. Suo [23] performed a numerical study on the effect of nozzle dimension on particle distribution in cold spraying. In his analysis, he systematically changed the hight of rectangular nozzle's exit, throat and powder injector keeping nozzle expansion ratio as a constant to study their effects on the distribution and velocity of magnesium particles using three-dimensional models of cold spraying systems. He also examined the effect of particle size on the particle distribution. He found that the particle distribution is mainly influenced by the turbulent kinetic energy of the gas flow at the nozzle exit. He also showed that changing the height of the exit or throat can control the particle distribution, i.e., 1. As the exit height increases, the particle distribution broadens and flattens along the transverse direction, 2. As the throat height increases, the particle distribution becomes sharp, and the mean particle velocity decreases along the transverse direction, 3. As the powder injector height increases, the mean particle velocity increases.

M Grujicic [24] used the one-dimensional isentropic model to analyze the dynamics of dilute two-phase flow during the cold spray process. His obtained results show that there is a particle velocity dependent, carrier gas invariant optimal value of the relative gas or particle Mach number that maximizes the drag force acting on feed powder particles and, hence, maximizes the particle acceleration. He found that to increase the average velocity of the particles at the nozzle exit; the gas dynamic cold spray nozzle is designed in such a way that at each axial location, the acceleration of the particles is maximized. He showed

that the exit velocity of particles could be substantially increased when helium is used as the carrier gas.

Muhammad Faizan Ur Rab [25] developed a three dimensional CFD multicomponent model to estimate cold spray gas conditions involving both nitrogen and air. He claimed that the developed holistic model is useful in determining the state of gas and particles from injection point to the substrate surface with the advantage of optimizing very rapid cold spray deposition in nanoseconds. He utilized the two equation k- ε model for developing the three-dimensional numerical model. The model was tested and validated with temperature parameter measured experimentally for a titanium substrate. He showed that the multicomponent model could be identified as a realistic model for cold spray process revealing the information about the complex thermos-mechanical events concerning gas temperature, velocity and turbulence kinetic energy from gas inlet to the location, at which the supersonic jet impinges onto the substrate.

R.Lupoi [26] presented deposition efficiency (DE) results from for different supersonic nozzles when using titanium as the feedstock material. He carried out a theoretical analysis through computational fluid dynamics to compare numerical results against experimental findings. For running CFD simulations, he used Fluent v14.0 solver. He manufactured four nozzles with different internal profiles and tested them using the same processing conditions with titanium powder. His results have suggested that current commercial codes cannot accurately predict the acceleration process under realistic working conditions.

Chang-Jiu Li [27] theoretically examined the deposition behavior of a spray particle stream with a particle size distribution regarding deposition efficiency as a function of spray angle and parameters of the particle. He conducted few experiments where has he measured the

deposition efficiency at different driving gas conditions and spray angles using copper powder. His analysis revealed that the particle velocity distribution resulting from particle size distribution significantly influences the deposition efficiency in cold spraying. He proposed a formula to calculate the deposition efficiency using the modified Rosin-Rammler model of particle size distribution and the relation between the size and velocity of the particle. His works established a theoretical relationship between the deposition efficiency and spray angle to explain the effect of off-normal spray angle on the deposition efficiency in cold spraying when the impact of the tangential component of the velocity on particle deposition was neglected.

Research Objective

Notwithstanding these critical findings, several vital problems still need to be further studied. In actual application, many industries use step drilled nozzle for its cheaper design and manufacturing cost. There are no research studies performed on determining the effects of step drilled nozzle numerically. In this study, as a first approximation, a numerical investigation is conducted on a step drilled nozzle design and a couple of other models (conical and curved shaped divergent sections) with the same operating parameters except the divergent cross-section shape. The main aim is to clarify the effect of nozzle cross-section shape on gas flow, numerically expose the losses of step-nozzle design and determine preferable nozzle shape.

CHAPTER 3: METHOD AND APPROACH

Methods and techniques used in the modeling and simulation of various cold spray nozzle CAD models and CFD analysis are discussed in this chapter.

Methodology

- Problem Statement
- Geometry
- Cad Model Generation
- Discretization
- Physics
- Solution
- Visualization
- Validation

Problem statement

The problem addressed in this research is:

How the supersonic jet characteristics differ in cold spray deposition system when Step Drilled nozzle, Conical nozzle, and curved nozzle are used with the same operating conditions?

Geometry

Nozzle 1 (Step Drilled)

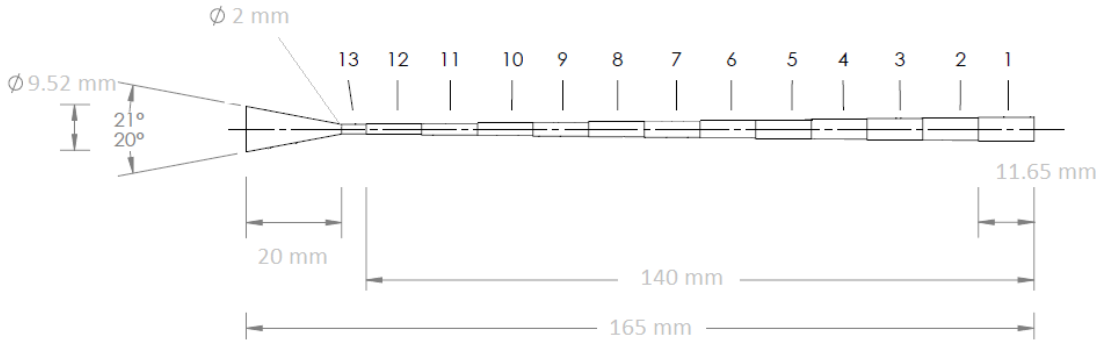

Figure 7: Step Drilled Nozzle Geometry

	Diameter (mm)	**Step length (mm)**
Step 1	4.97	11.65
Step 2	4.69	11.65
Step 3	4.49	11.65
Step 4	4.21	11.65
Step 5	3.98	11.65
Step 6	3.73	11.65
Step 7	3.45	11.65
Step 8	3.25	11.65
Step 9	2.94	11.65
Step 10	2.69	11.65
Step 11	2.43	11.65
Step 12	2.18	11.65
Step 13	2	Remainder

Table 1: Step Drilled Nozzle Step Dimensions

Nozzle 2 (Conical)

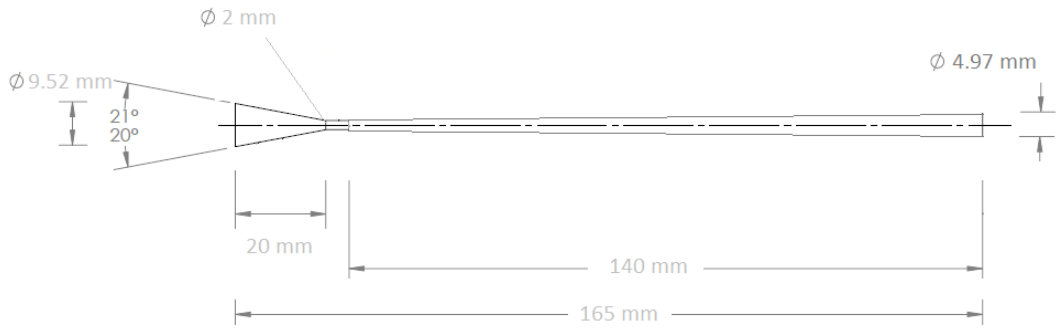

Figure 8: Conical Shaped Nozzle Geometry

Nozzle 3 (De-Laval or Curved)

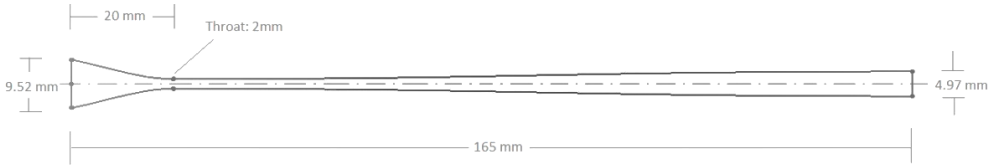

Figure 9: Curved Nozzle Geometry

Summary of the Geometrical Dimensions

	Nozzle 1	**Nozzle 2**	**Nozzle 3**
Inlet Diameter (mm)	9.52	9.52	9.52
Outlet Diameter (mm)	4.97	4.97	4.97
Throat (mm)	2	2	2
Convergent Length (mm)	20	20	20
Divergent Length (mm)	145	145	145
Divergent Profile (mm)	Stepped	Conical	Curved
Stand Off Distance (mm)	20	20	20

Table 2: Summary of Nozzle Dimensions

CAD Model Generation

CAD Models of the Geometries provided in the Geometry section are generated using the StarCCM+ software. The operational procedure for CAD Modeling in StarCCM+ is briefly discussed in the Appendix section.

Nozzle 1 (Step Drilled)

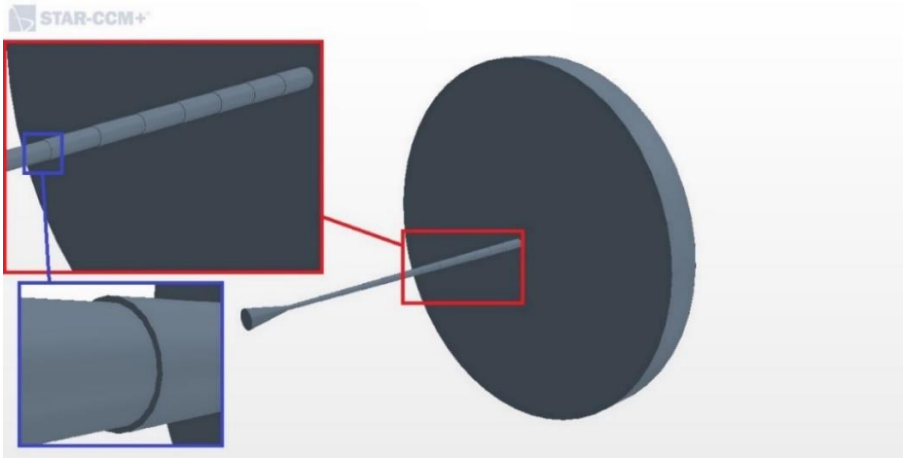

Figure 10: Step Drilled Nozzle CAD Model

Nozzle 2 (Conical)

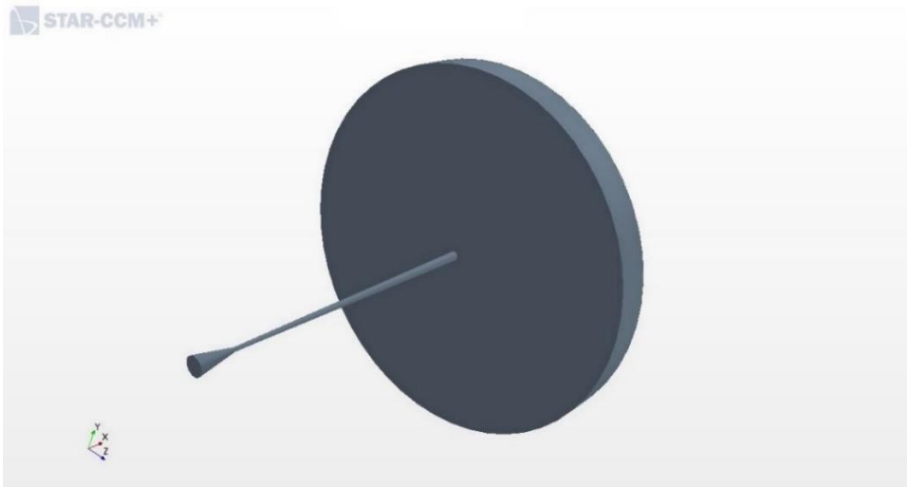

Figure 11: Conical Nozzle CAD Model

Nozzle 3 (Curved)

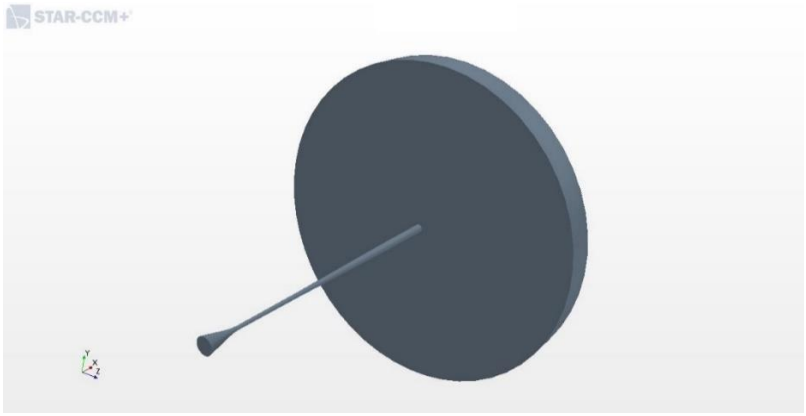

Figure 12: Curved Nozzle CAD Model

Discretization

There are numerous methods of discretization, which can broadly have classified into a mesh (grid) methods and mesh-free methods. Mesh methods are more widely used. In the Meshing process, the region is divided into smaller areas. These smaller regions may be of different shapes like triangles, rectangles in case of 2D geometry, hexahedrons, tetrahedrons in case of 3D geometry. Then, the governing equations are discretized over the mesh. Finite Difference Method, Finite Element Method, and Finite Volume Method are very popular methods of discretization in Computational Fluid Dynamics.

Meshing models used for the simulation

- Extruder
- Advanced Layer Mesher
- Surface Wrapper
- Surface Remesher

Instructions for setting up the meshing in Starccm+ is provided in the Appendix section.

Nozzle 1 (Stepped Nozzle)

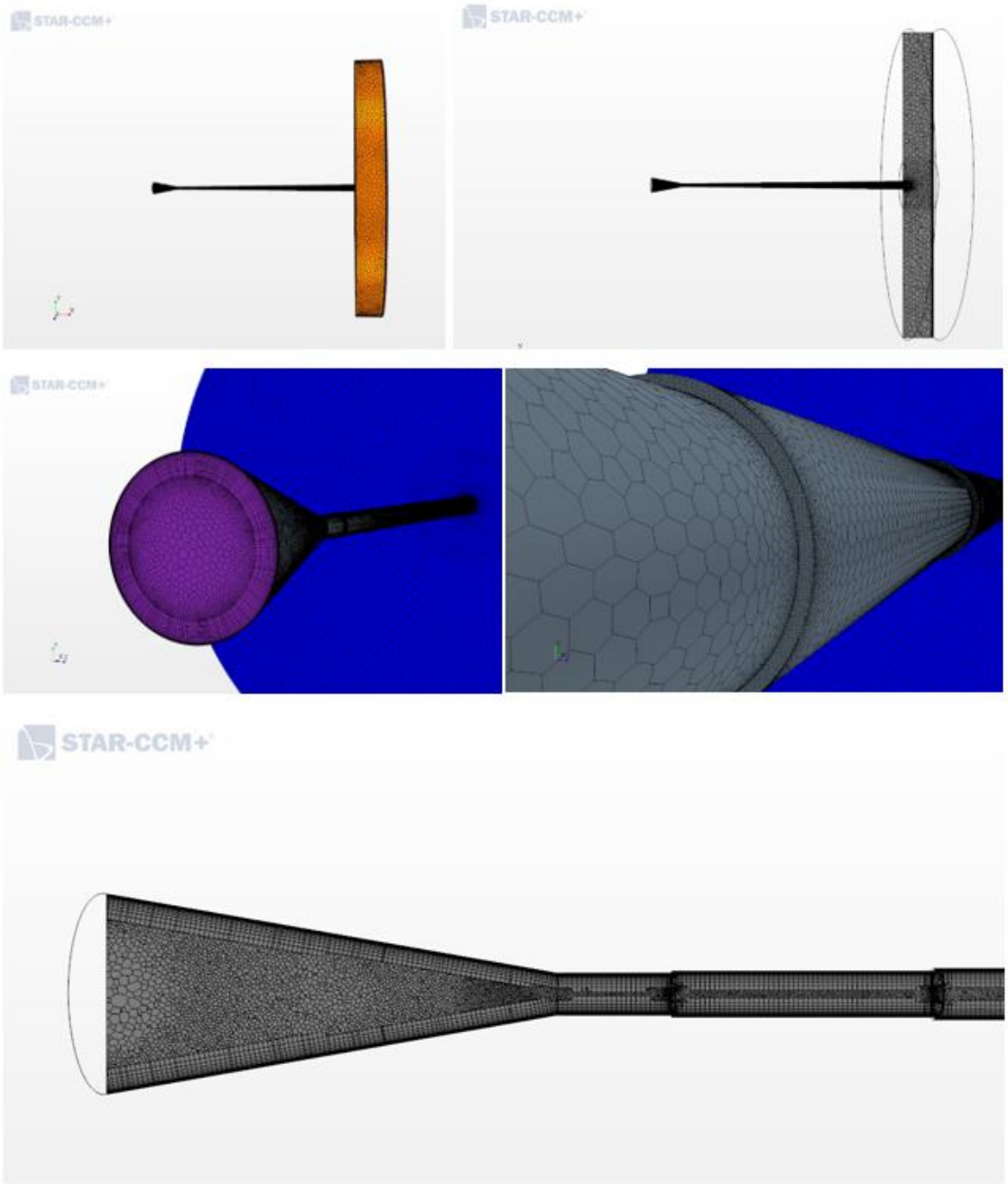

Figure 13: Step Drilled Nozzle Mesh

Number of Cells: 3033421 Number of Face: 7668366

Nozzle 2 (Conical Nozzle)

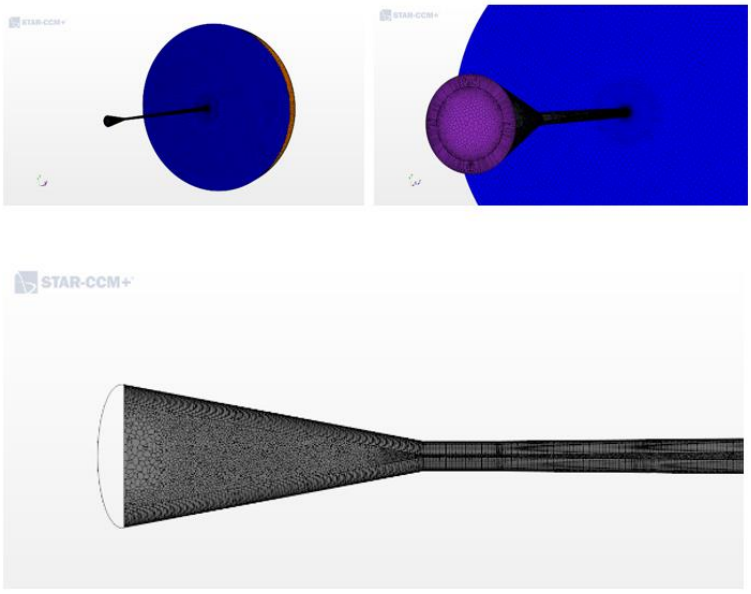

Figure 14: Conical Nozzle Mesh

Number of Cells: 1686663 Number of Face: 7778737

Nozzle 3 (Curved Nozzle)

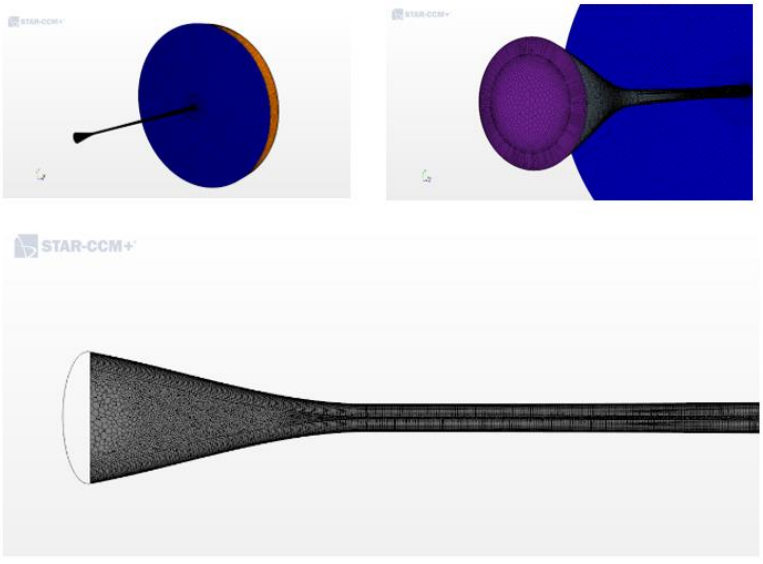

Figure 15: Curved Nozzle Mesh

Number of Cells: 1657432 Number of Face: 7610608

Physics

Nozzle throat is referred to the smaller cross-section area of the converging/diverging nozzle. The gas temperature at nozzle throat (T^*) is defined as

$$\frac{T_0}{T^*} = 1 + \frac{\gamma - 1}{2}$$

$$T^* = \frac{T_0}{1 + \frac{\gamma - 1}{2}}$$

Gas velocity at nozzle throat (V^*) is defined as

$$V^* = \sqrt{\gamma R T^*}$$

The mass flow rate ($\dot{m}$) of the sonic gas can be defined by

$$\rho^* = \frac{\dot{m}}{V^* A^*}$$

The gas pressure at the nozzle throat can be determined using the ideal gas law:

$$P^* = \rho^* R T^*$$

The stagnation pressure at the nozzle throat can be defined using the isentropic relations

$$\frac{P_o}{P^*} = \left(\frac{T_0}{T^*}\right)^{\frac{\gamma}{\gamma-1}}$$

$$\frac{P_o}{P^*} = \left(1 + \frac{\gamma - 1}{2}\right)^{\frac{\gamma}{\gamma-1}}$$

$$P_0 = P^* \left(1 + \frac{\gamma - 1}{2}\right)^{\frac{\gamma}{\gamma-1}}$$

Once the parameters at the throat are defined, it is possible to determine these quantities along the diverging section of the nozzle. When the variation of the nozzle cross-sectional area is specified, the corresponding Mach number (M) can be determined using the following equation

$$\frac{A}{A^*} = \left(\frac{1}{M}\right)\left[\left(\frac{2}{\gamma+1}\right)\left(1 + M^2\frac{\gamma-1}{2}\right)\right]^{\frac{\gamma+1}{[2(\gamma-1)]}}$$

Once the Mach number is obtained at a given cross-sectional area of the diverging nozzle section, the remaining corresponding values can be determined by using the following isentropic relations

$$\frac{P}{P^*} = \left(\frac{\gamma+1}{2+(\gamma-1)M^2}\right)^{\frac{\gamma}{\gamma-1}}$$

$$P = P^*\left(\frac{\gamma+1}{2+(\gamma-1)M^2}\right)^{\frac{\gamma}{\gamma-1}}$$

$$\frac{T_o}{T} = 1 + \frac{\gamma-1}{2}M^2$$

$$T = \frac{T_o}{1 + \frac{\gamma-1}{2}M^2}$$

$$\frac{\rho_o}{\rho} = \left(1 + \frac{\gamma-1}{2}M^2\right)^{\frac{1}{(\gamma-1)}}$$

$$\rho = \frac{\rho_o}{\left(1 + \frac{\gamma-1}{2}M^2\right)^{\frac{1}{(\gamma-1)}}}$$

Governing equations

The flow in cold spray is considered as steady-state supersonic turbulent flow with heat transfer during the process.

The governing equations are

- Continuity equation,
- Momentum equation, and
- Energy equation

Continuity equation:

$$\frac{\partial \rho}{\partial t} + \frac{\partial}{\partial x_i}(\rho u_j) = 0$$

Momentum Equation:

$$-\frac{\partial(\rho u_i)}{\partial t} + \frac{\partial(\rho u_i u_j)}{\partial x_j} = -\frac{\partial P}{\partial x_i} + \left[\frac{\partial \tau_{ij}}{\partial x_j}\right]$$

$$\tau_{ij} = \mu\left[\frac{\partial u_i}{\partial x_j} + \frac{\partial u_j}{\partial x_j} - \frac{2}{3}\frac{\partial u_k}{\partial x_k}\delta_{ij}\right]$$

Energy Equation:

$$\frac{\partial \rho E}{\partial t} + \frac{\partial}{\partial t}(\rho E + P) = \frac{\partial \tau_{ij}}{\partial x_j} u_i + \frac{\partial}{\partial x_j}\left(k\frac{\partial T}{\partial x_j}\right)$$

Solver Settings

Fluid motion equations are generally very complex and mostly require computational ways to solve. The CFD program solves the Navier-Stokes equations for compressible flow. In this study, CFD simulations were performed using STARCCM+ to predict the gas flow field.

Selected Physics Models for the simulation

- Three Dimensional
- Steady State
- Fluid: Gas (Helium)
- Ideal Gas
- Reynolds Averaged Navier Stokes
- Coupled Flow
- Coupled Energy
- Turbulent Flow
- SST K – Omega
- Turbulence Suppression
- Transition Boundary Distance
- All y+ Wall Treatment
- Exact Wall Distance
- Gradients

Setting up physics models with Starccm+ is briefly discussed in Appendix.

Primary Input variables

- Carrier gas Inlet Pressure: 3103000 Pa
- Carrier gas Inlet Temperature: 523K
- Carrier gas type: Helium

Boundary Conditions

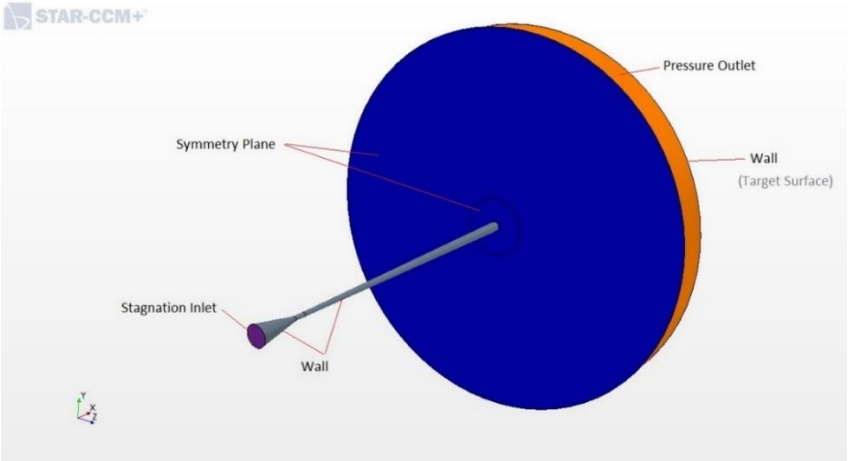

Figure 16: Model Showing Boundary Conditions

Summary of Boundary Conditions used for various nozzles

	Nozzle 1	***Nozzle 2***	***Nozzle 3***
Stagnation Inlet	Nozzle Inlet	Nozzle Inlet	Nozzle Inlet
Pressure Outlet	Radial Outlet	Radial Outlet	Radial Outlet
Symmetry Plane	Top1, Top2	Top1, Top2	Top1, Top2
Wall	Convergent, Divergent	Convergent, Divergent	Convergent, Divergent

Table 3: Summary of Boundary Conditions used for the Nozzles

CHAPTER 4: RESULTS AND DISCUSSION

In this chapter, the calculated results obtained from the numerical simulations are visualized, and the results are validated. For visualization, a scalar cross-section view along with an XY plot at the center axis with various scalar fields are provided. Then the data obtained by multiple nozzles is compared with the help of a line plot derived from a MATLAB code and bar charts from MS Excel.

Visualization

Nozzle 1 (Stepped Nozzle) - Absolute pressure

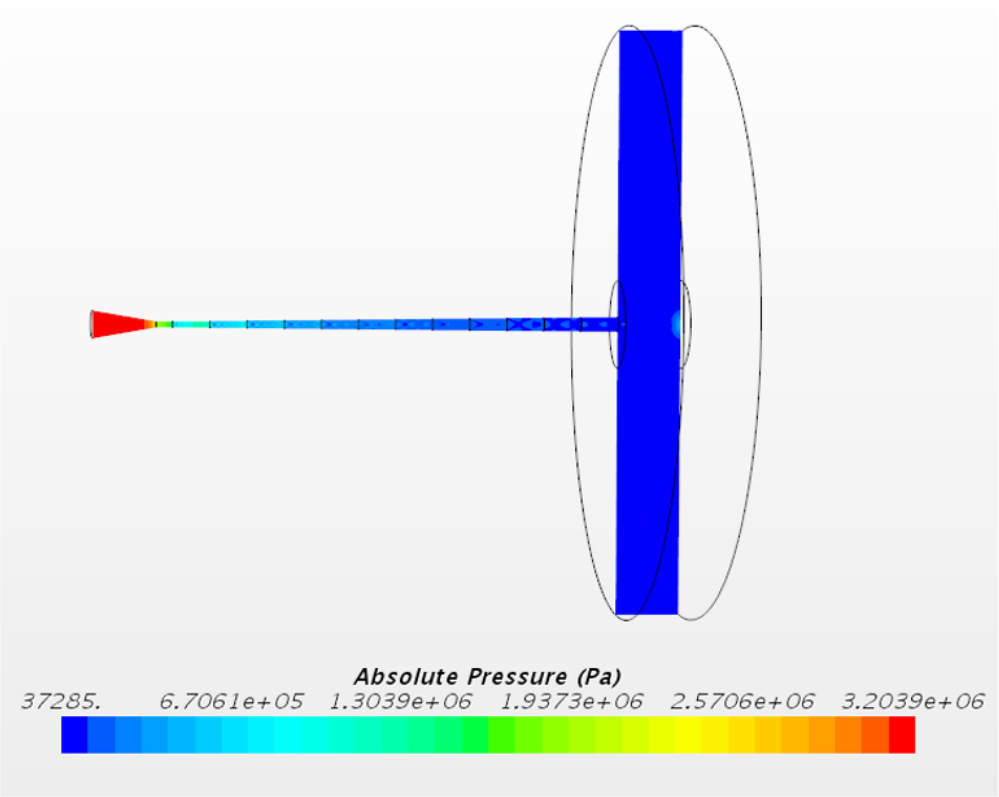

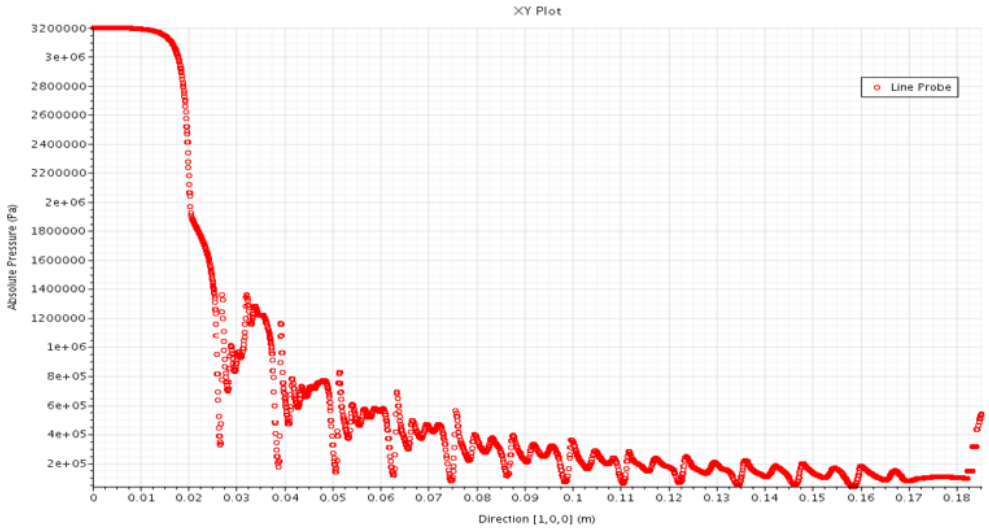

Figure 17: Visualization of Absolute Pressure in Step Drilled Nozzle

Nozzle 2 (Conical Nozzle) - Absolute pressure

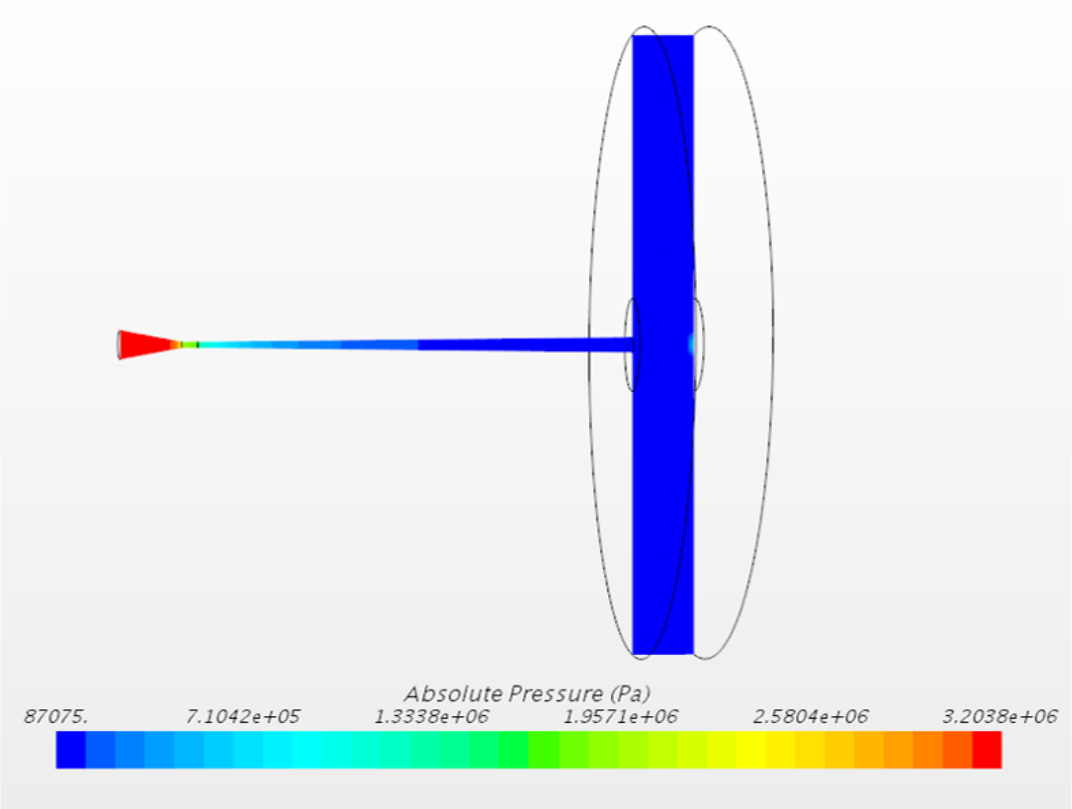

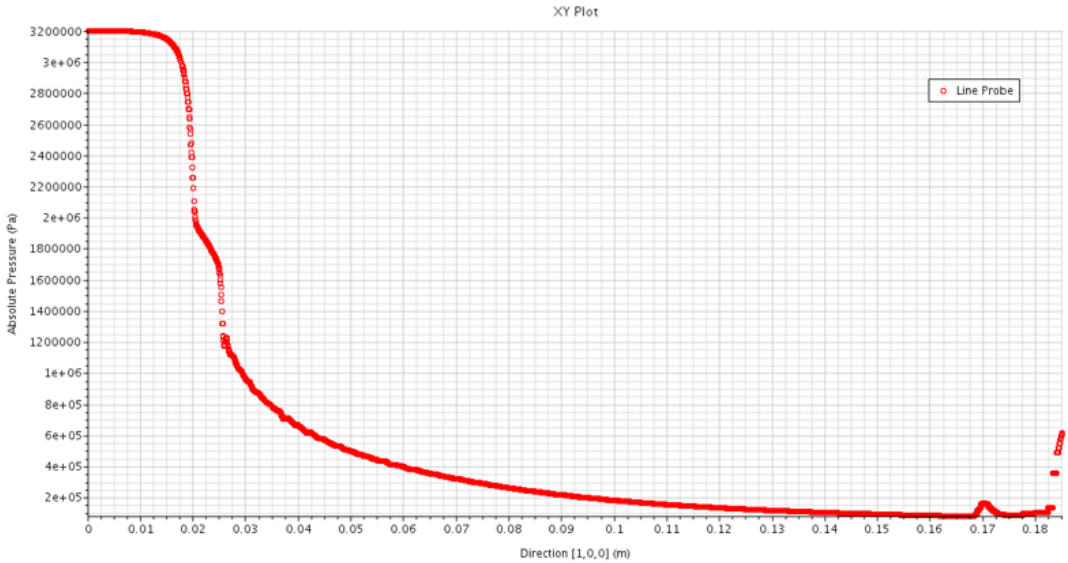

Figure 18: Visualization of Absolute Pressure in Conical Nozzle

Nozzle 3 (Curved Nozzle) - Absolute pressure

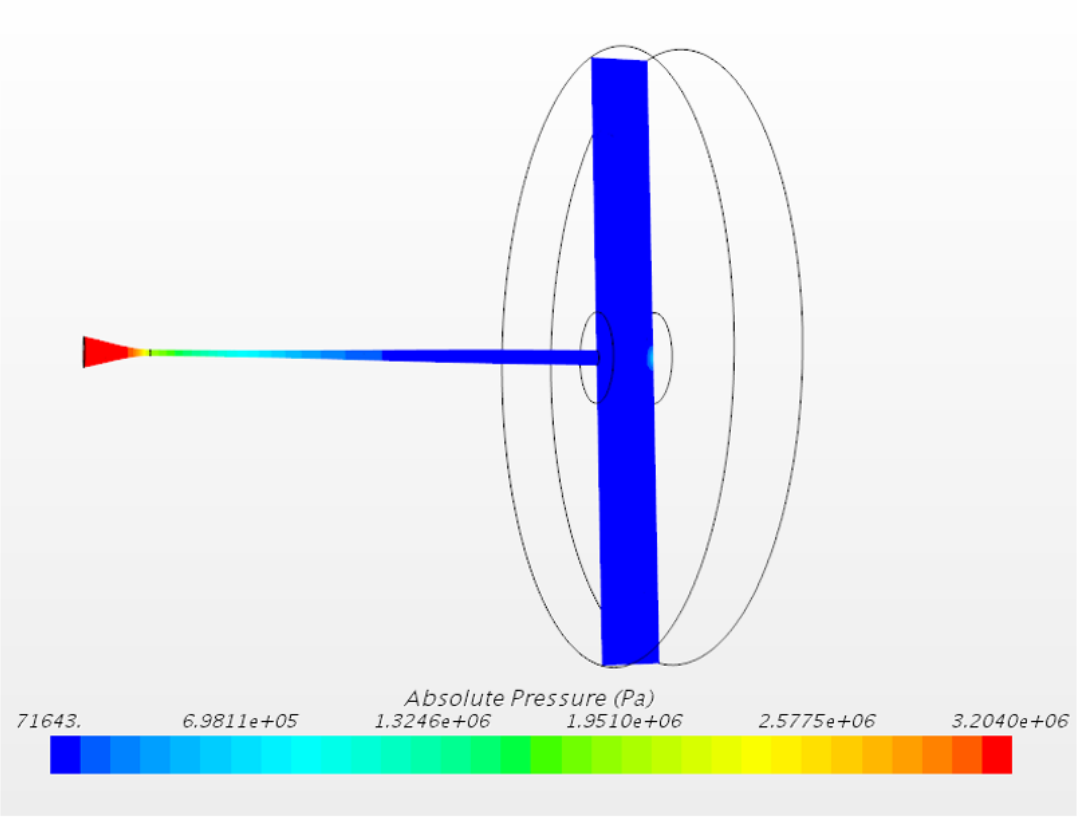

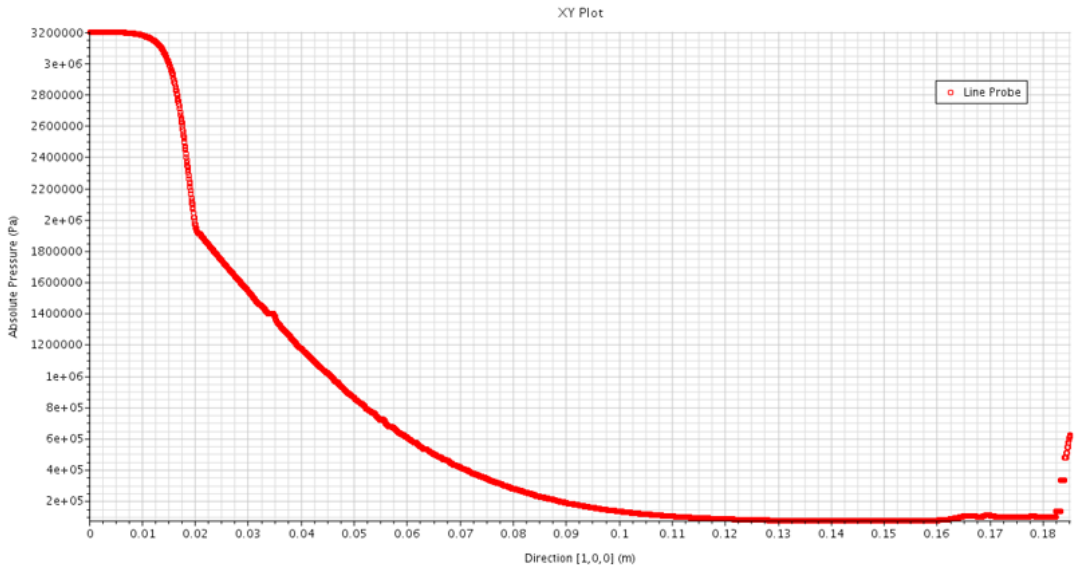

Figure 19: Visualization of Absolute Pressure in Curved Nozzle

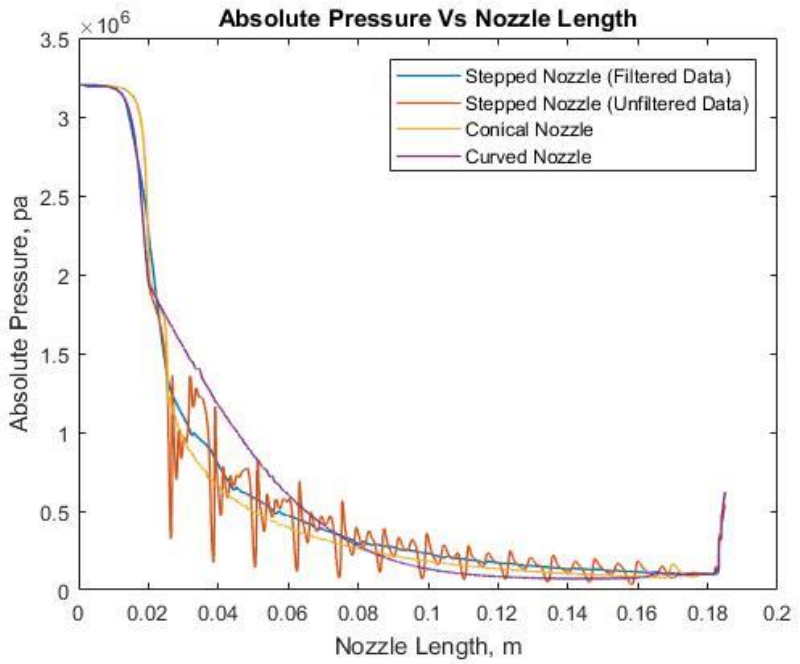

Figure 20: Absolute Pressure comparison among various Nozzles using Line Graph

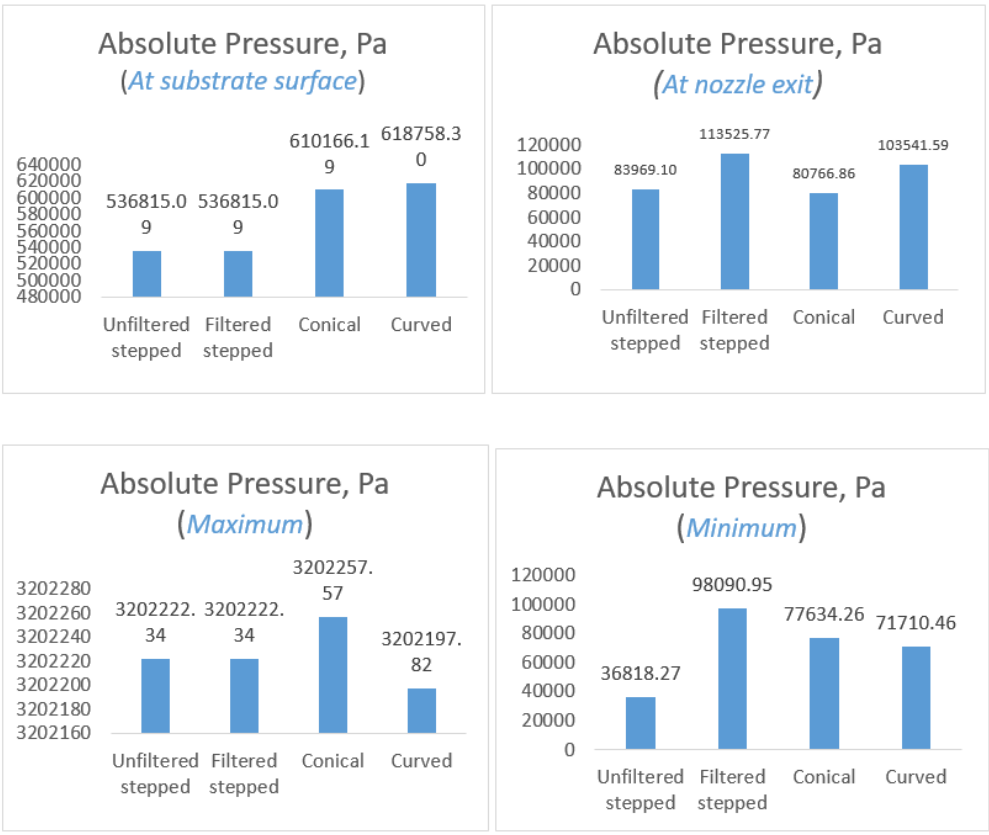

Figure 21: Absolute Pressure Bar Graphs

Nozzle 1 (Stepped Nozzle) -Density

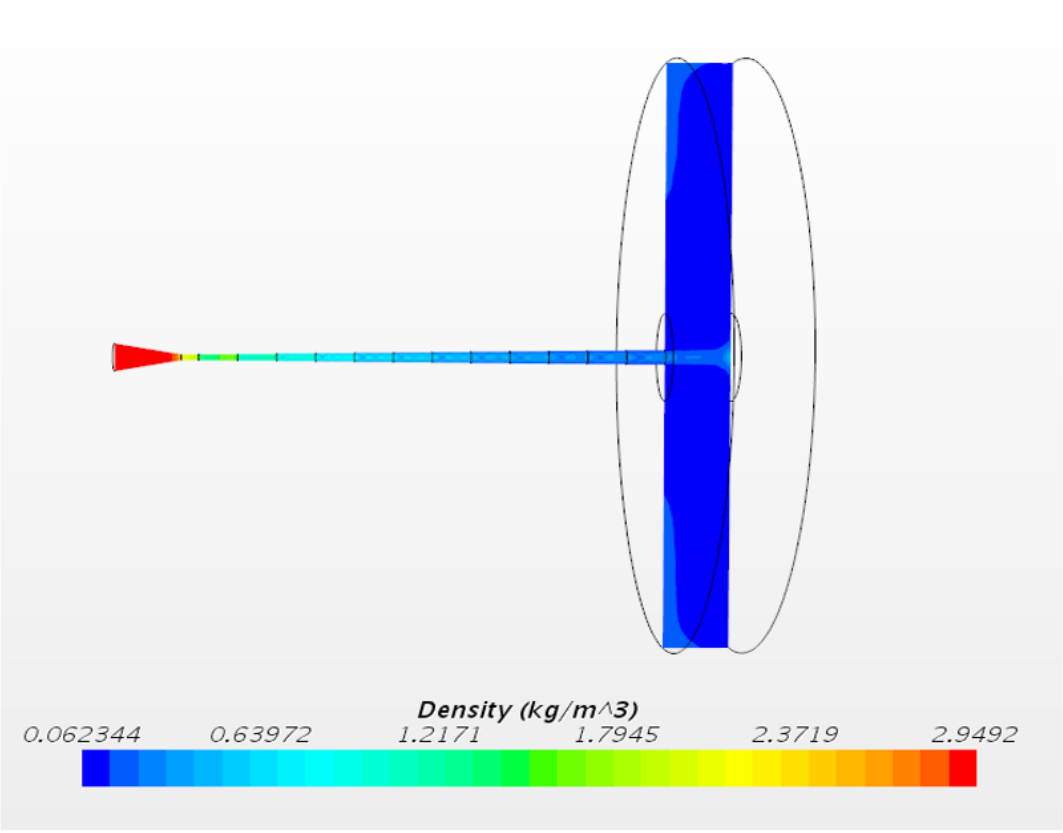

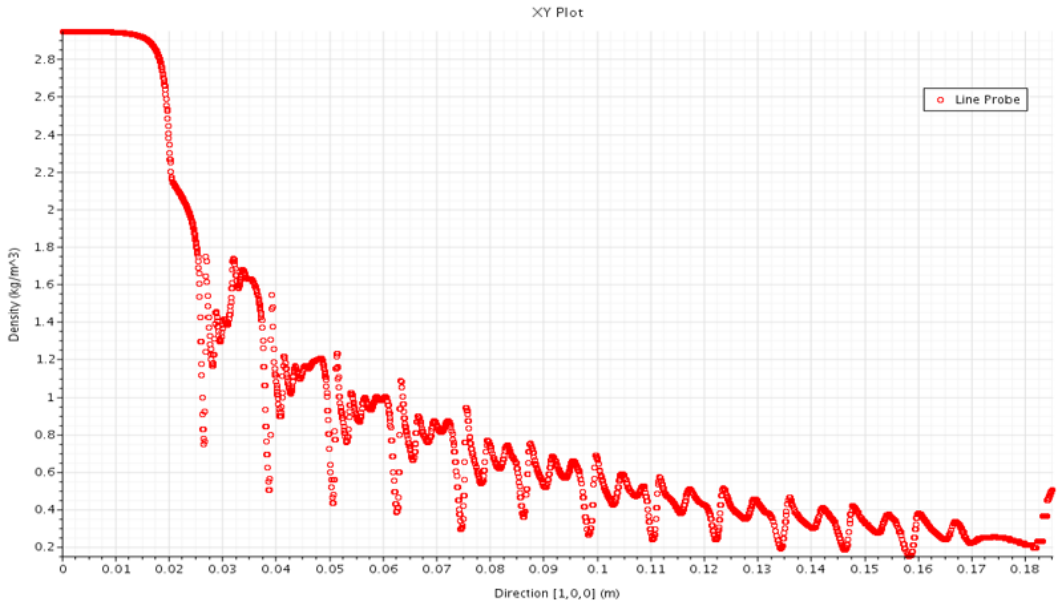

Figure 22: Visualization of Density in Step Drilled Nozzle

Nozzle 2 (Conical Nozzle) - Density

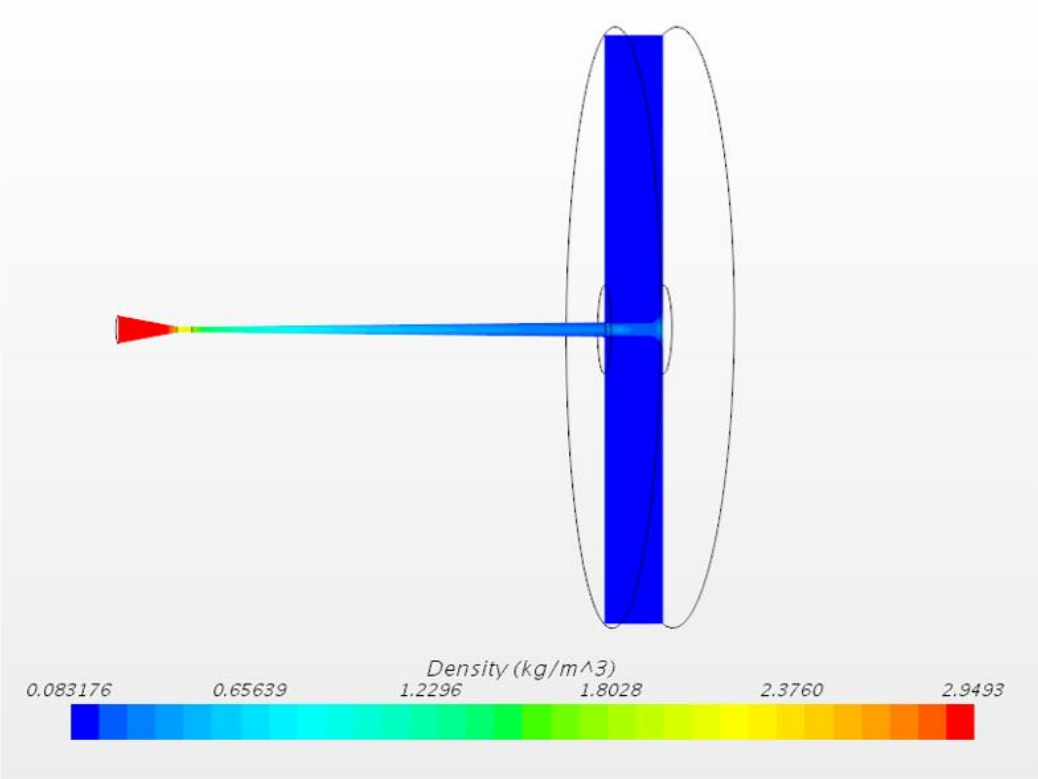

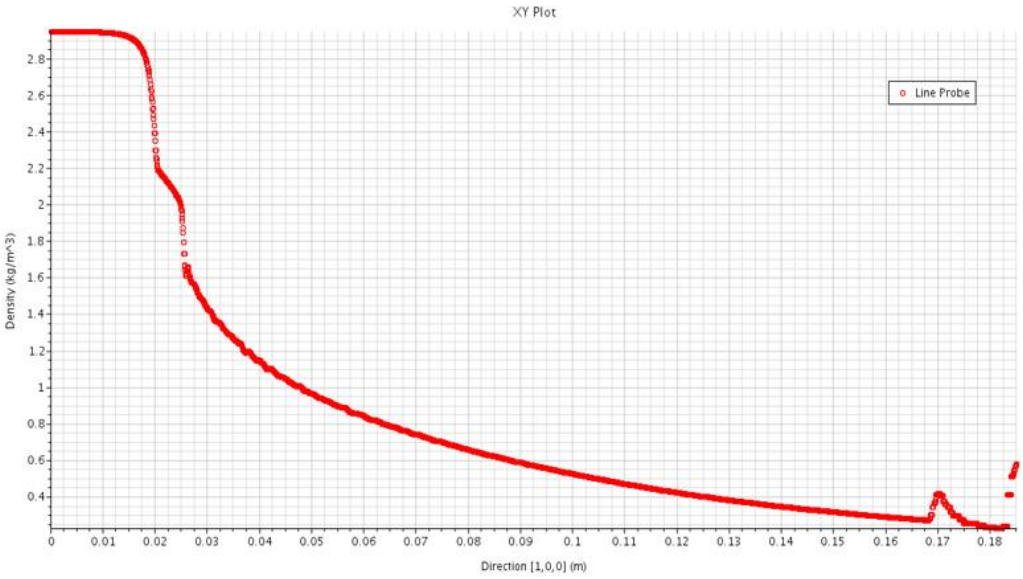

Figure 23: Visualization of Density in Conical Nozzle

Nozzle 3 (Curved Nozzle) - Density

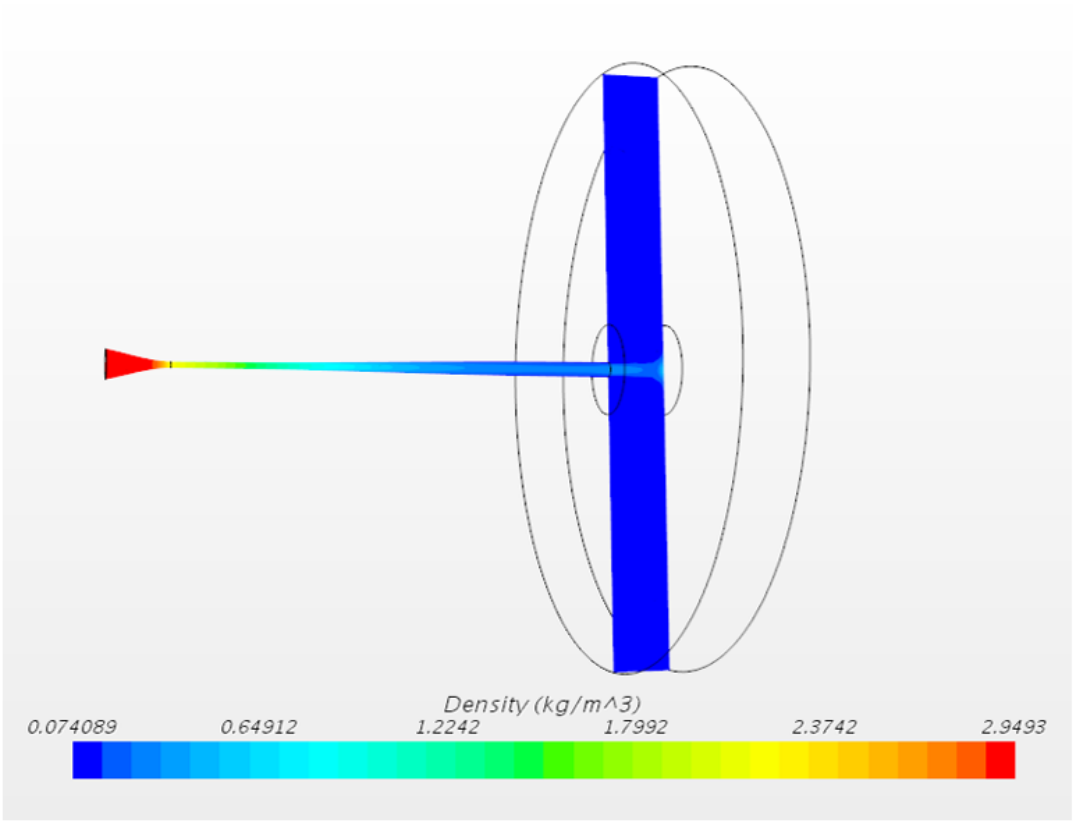

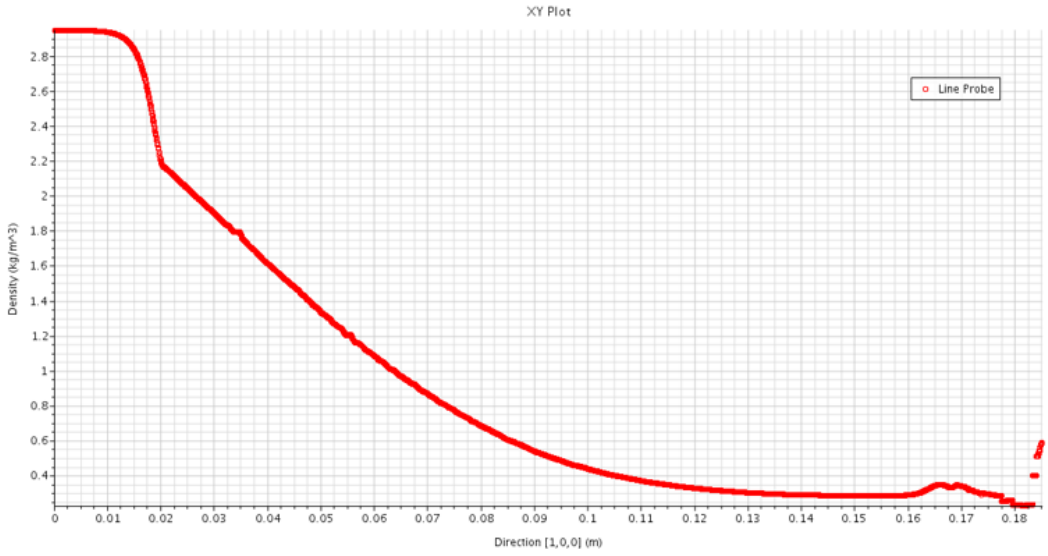

Figure 24: Visualization of Density in Curved Nozzle

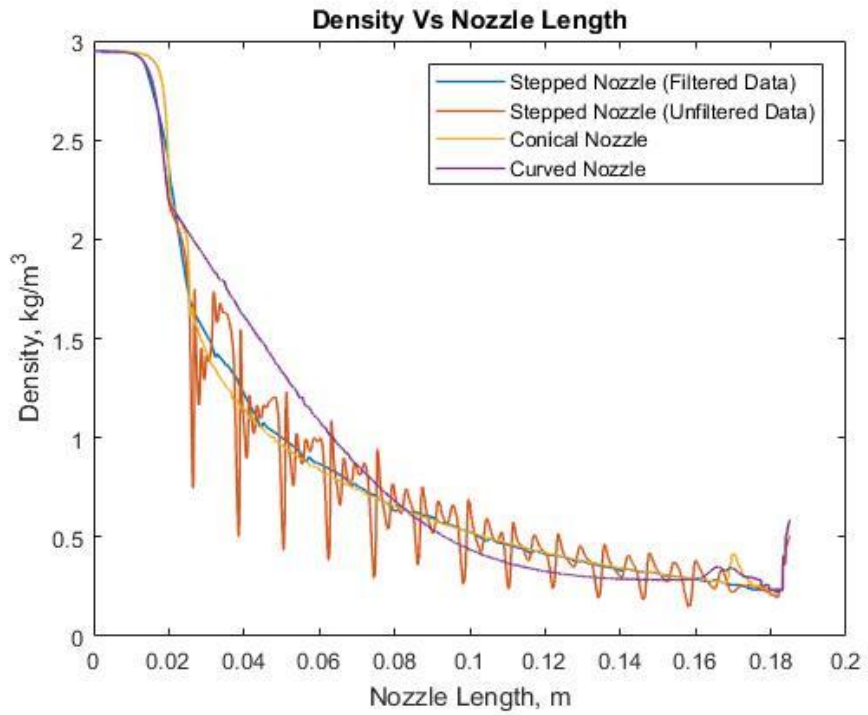

Figure 25: Density comparison among various Nozzles using Line Graph

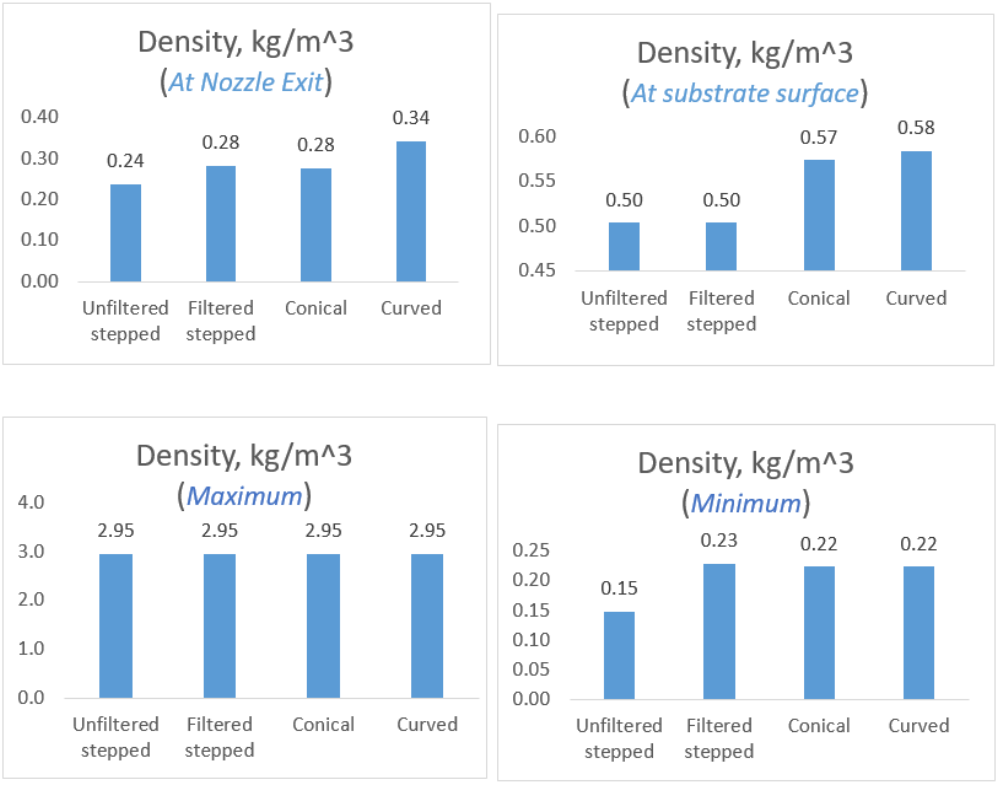

Figure 26: Density Bar Graphs

Nozzle 1 (Stepped Nozzle) - Mach

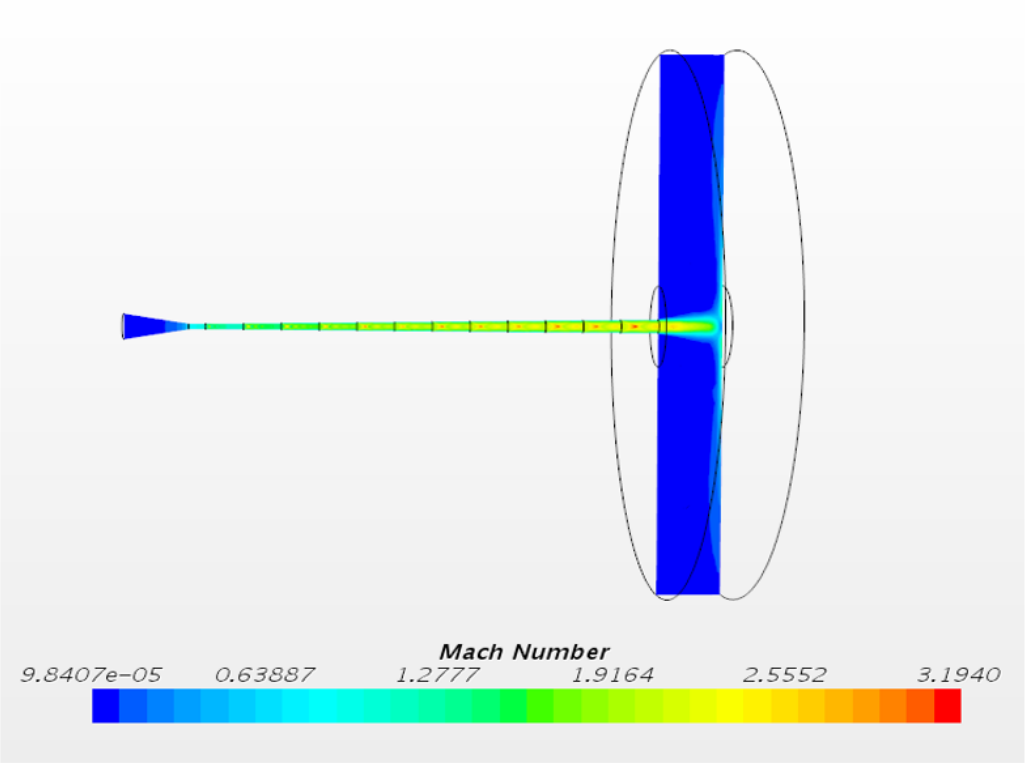

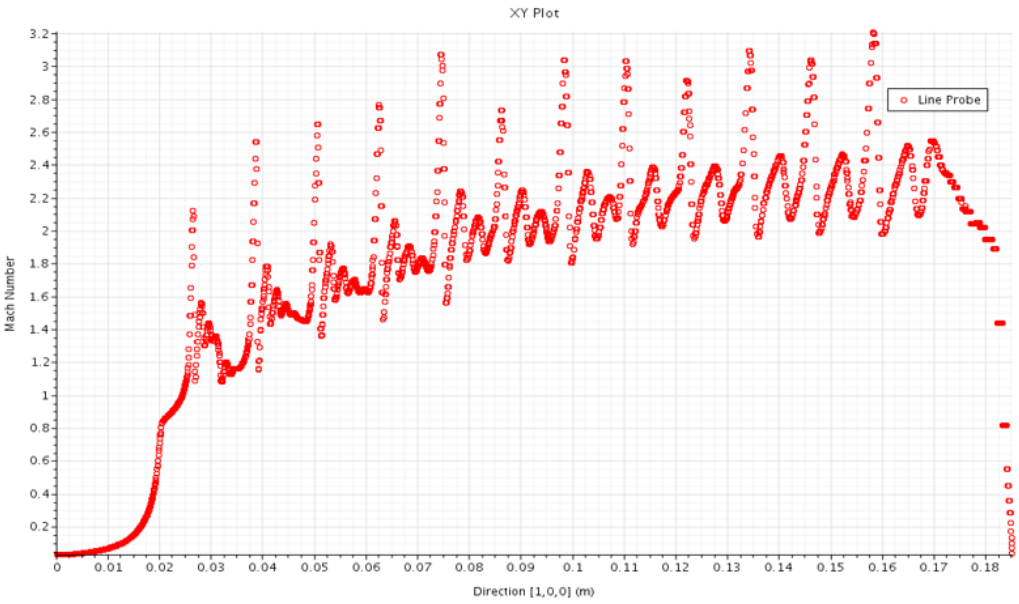

Figure 27: Visualization of Mach in Step Drilled Nozzle

Nozzle 2 (Conical Nozzle) - Mach

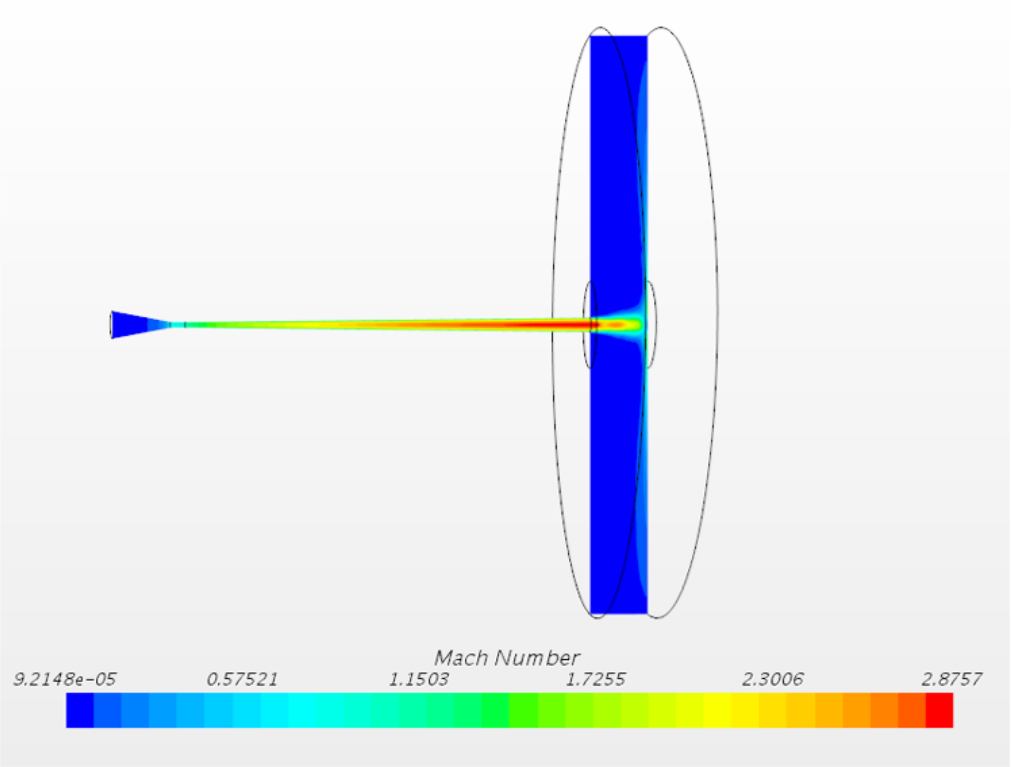

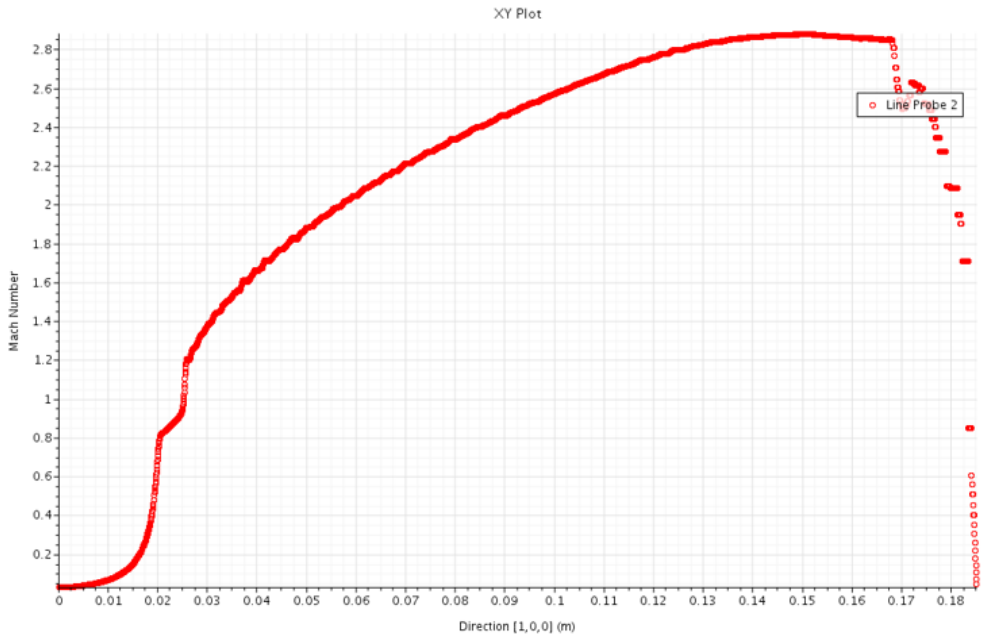

Figure 28: Visualization of Mach in Conical Nozzle

Nozzle 3 (Curved Nozzle) - Mach

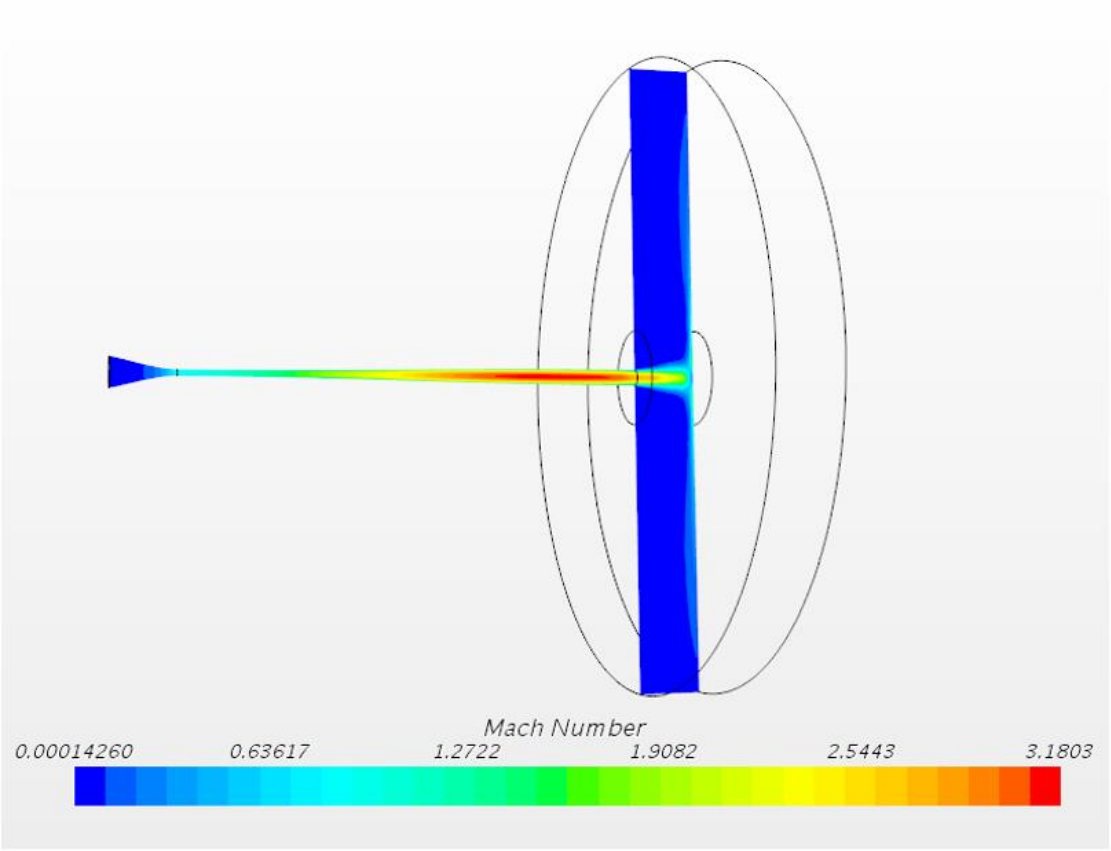

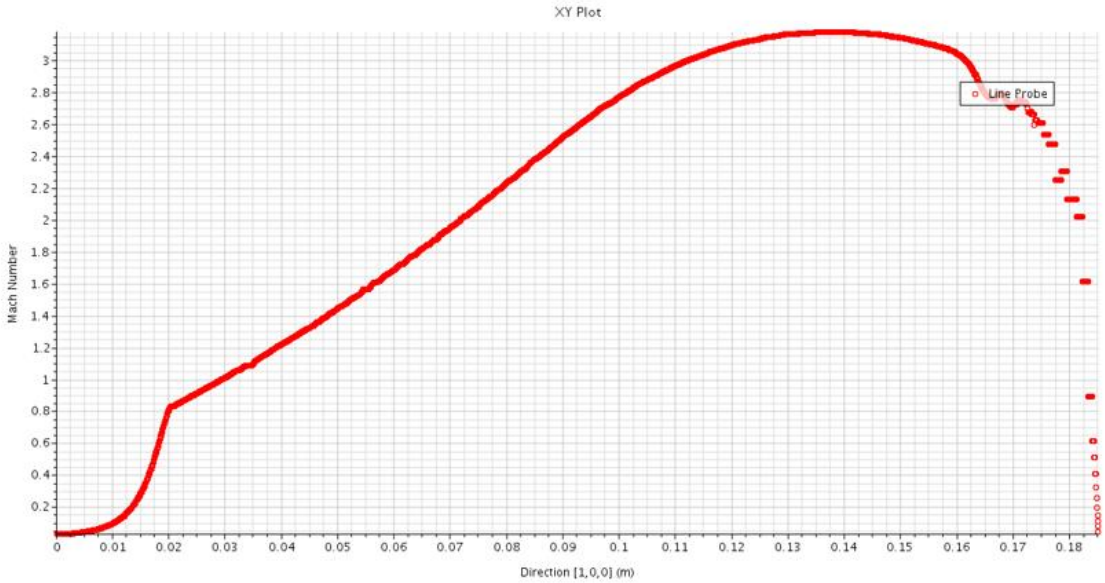

Figure 29: Visualization of Mach in Curved Nozzle

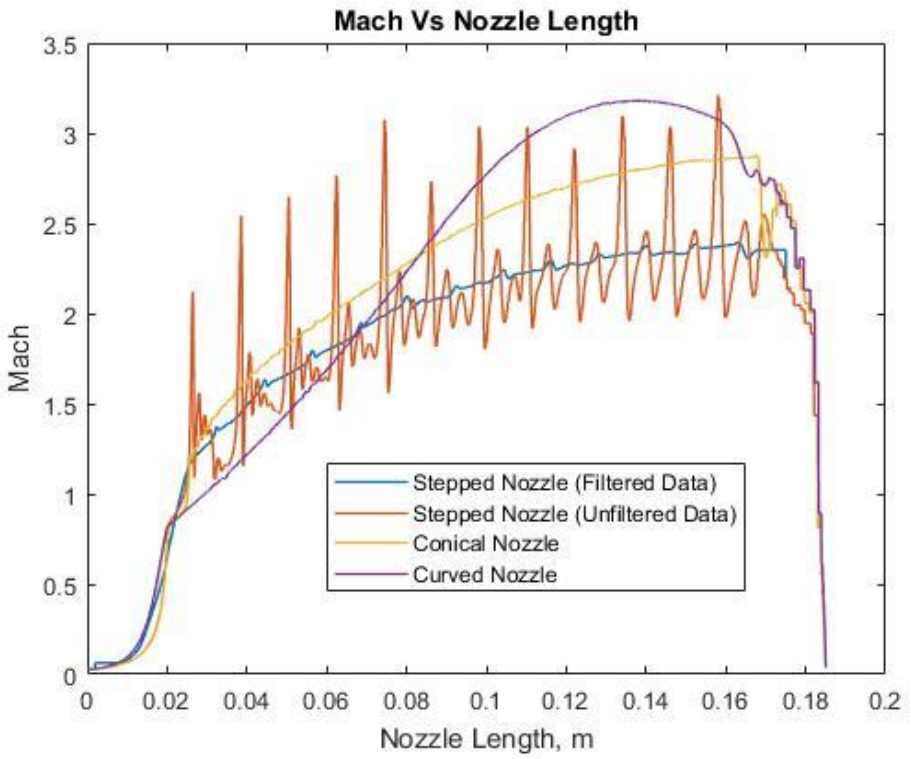

Figure 30: Mach comparison among various Nozzles using Line Graph

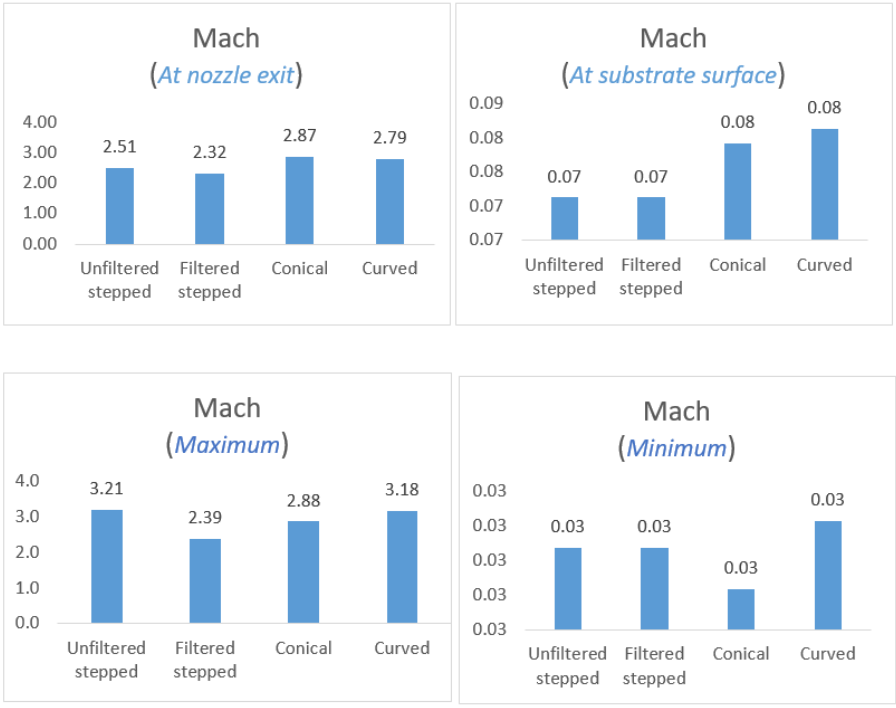

Figure 31: Mach Bar Graphs

Nozzle 1 (Stepped Nozzle)- Pressure

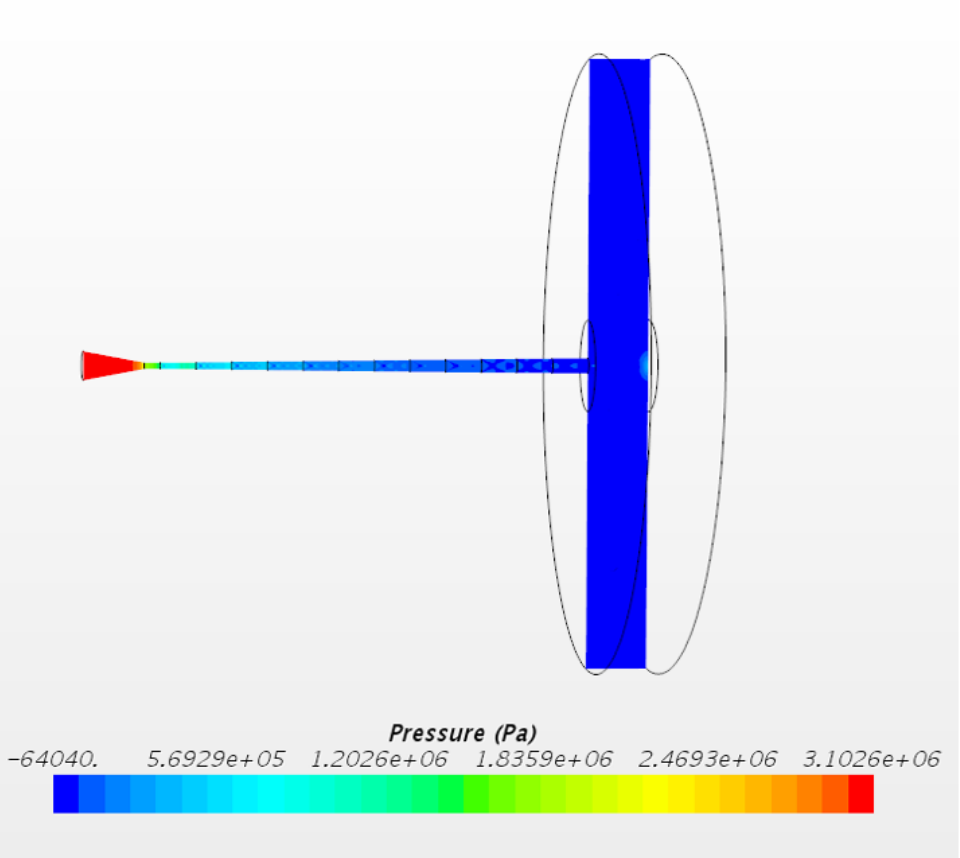

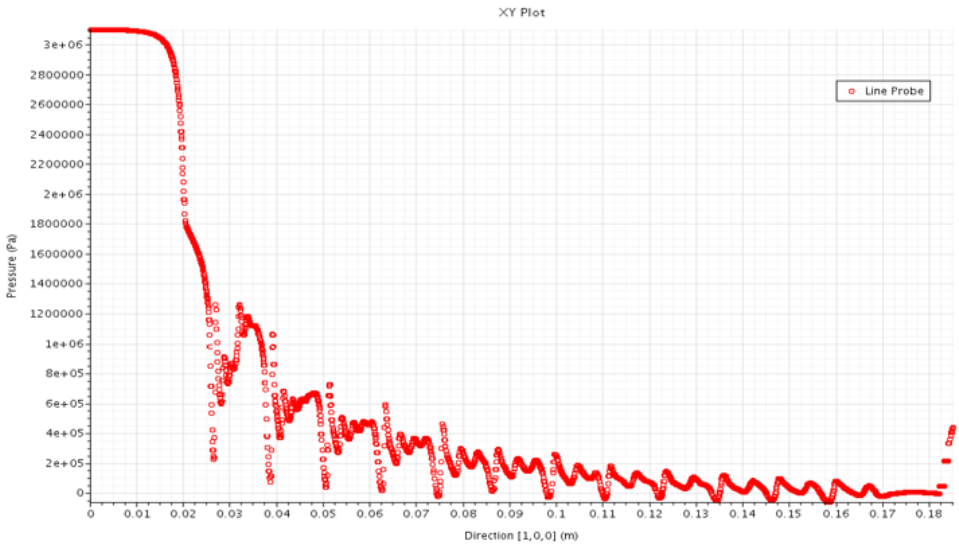

Figure 32: Visualization of Pressure in Step Drilled Nozzle

Nozzle 2 (Conical Nozzle) - Pressure

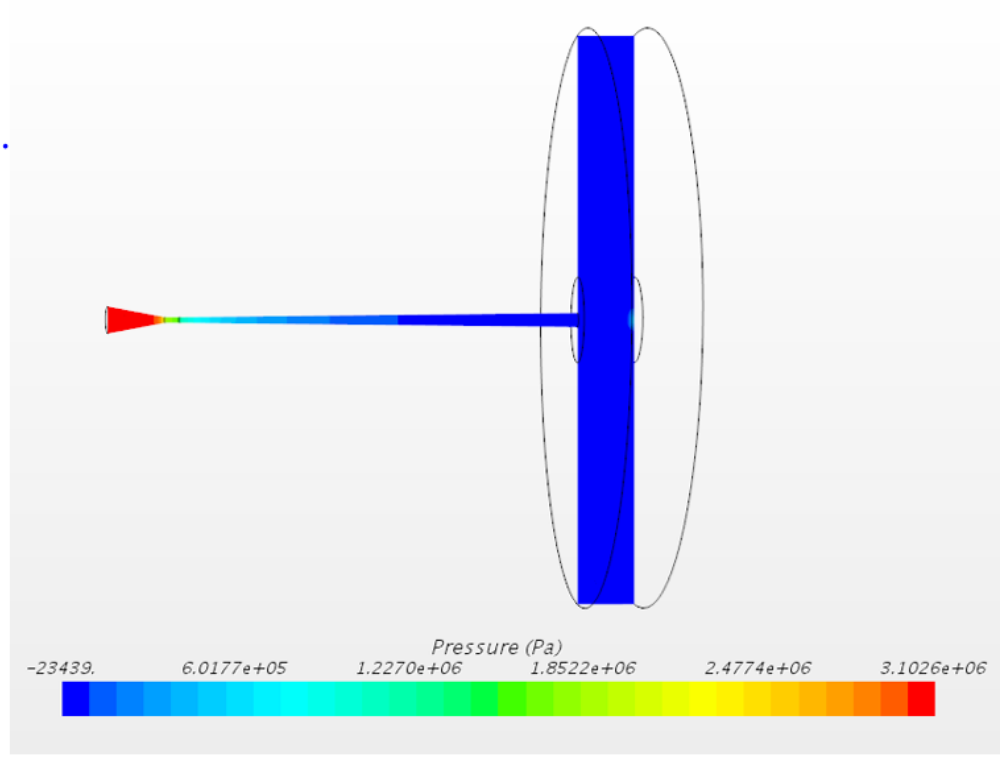

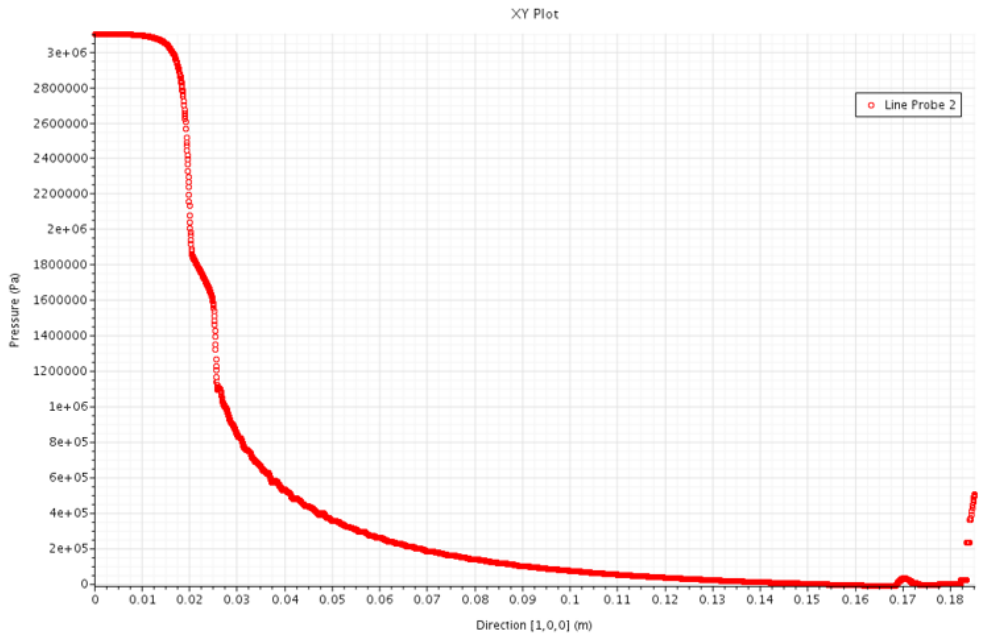

Figure 33: Visualization of Pressure in Conical Nozzle

Nozzle 3 (Curved Nozzle) - Pressure

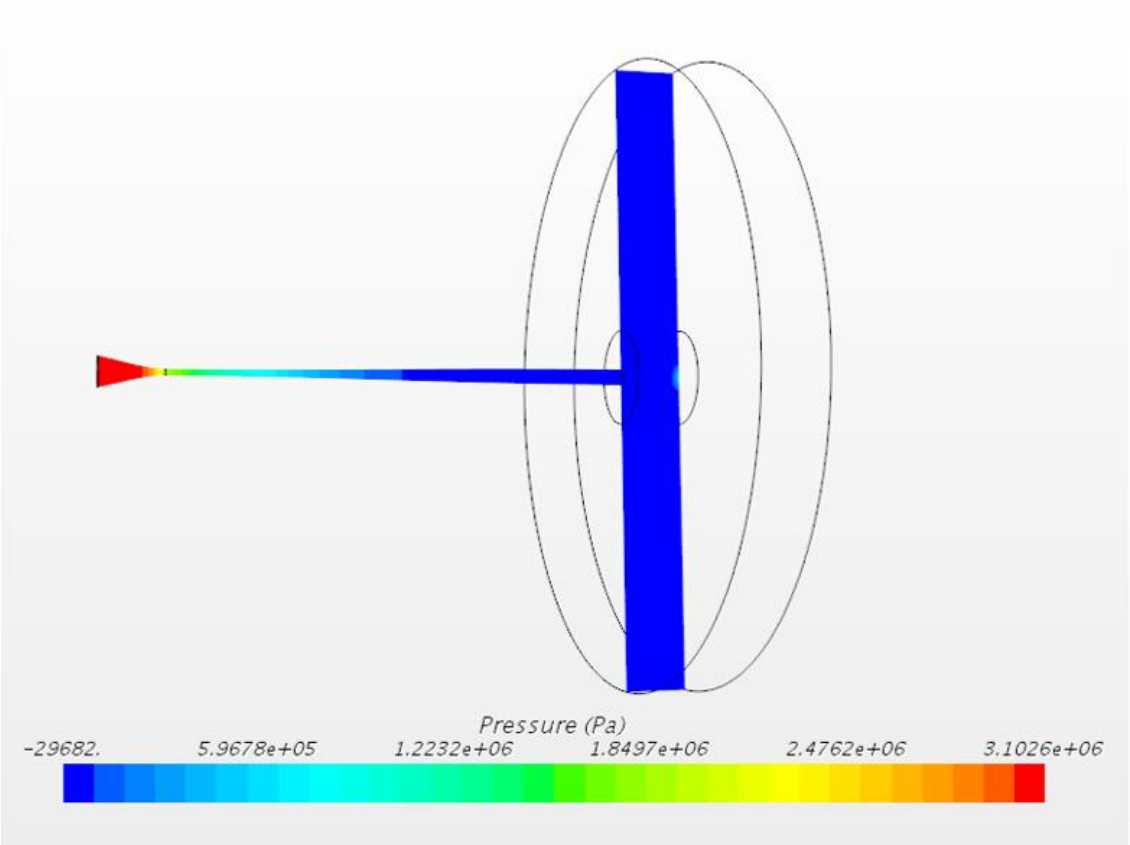

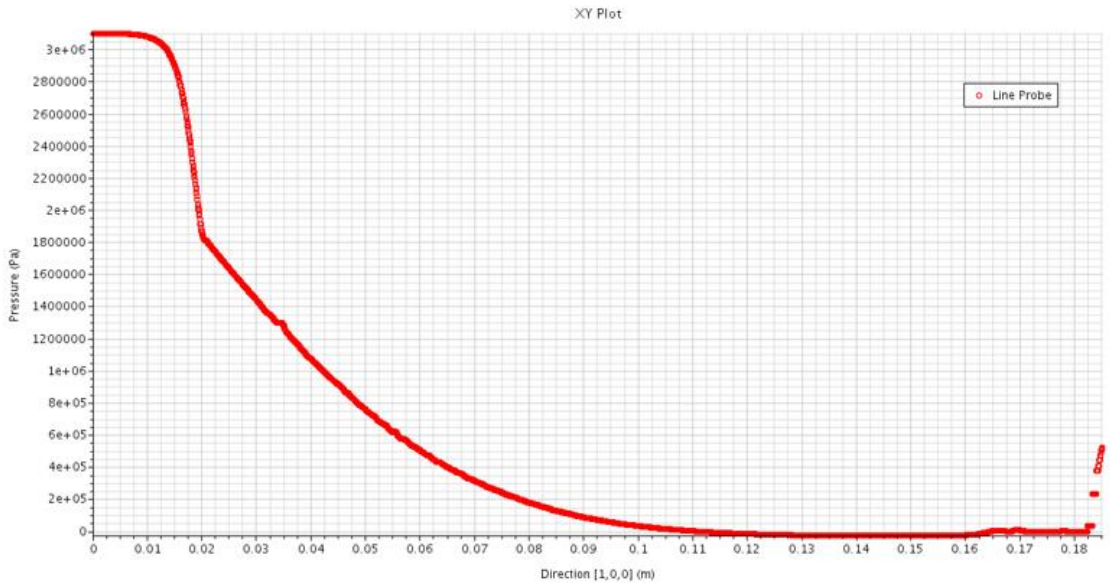

Figure 34: Visualization of Pressure in Curved Nozzle

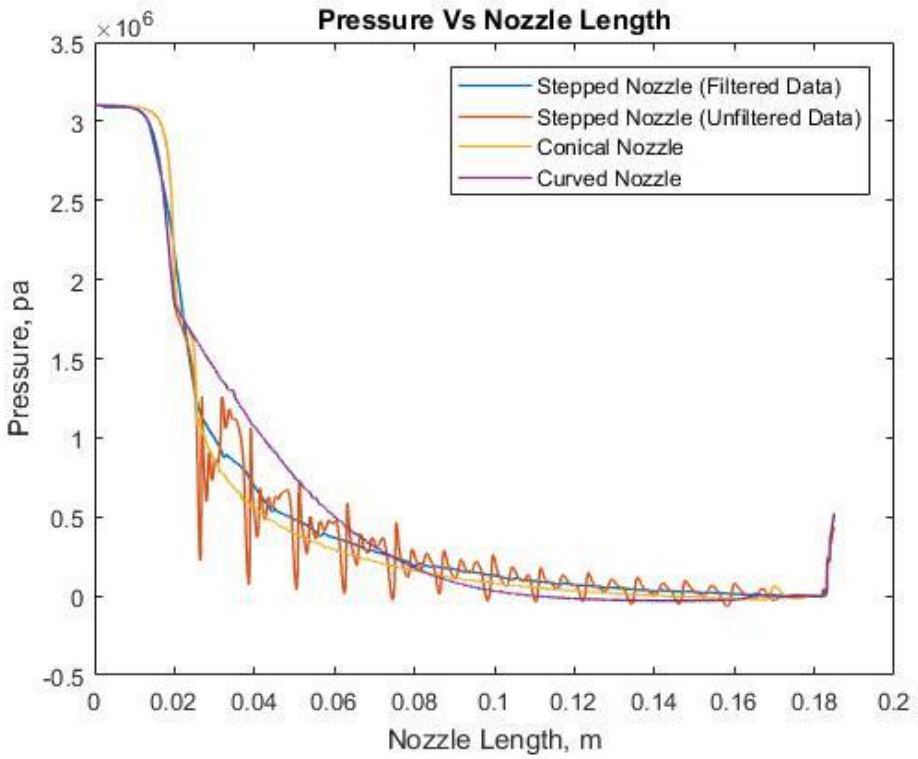

Figure 35: Pressure comparison among various Nozzles using Line Graph

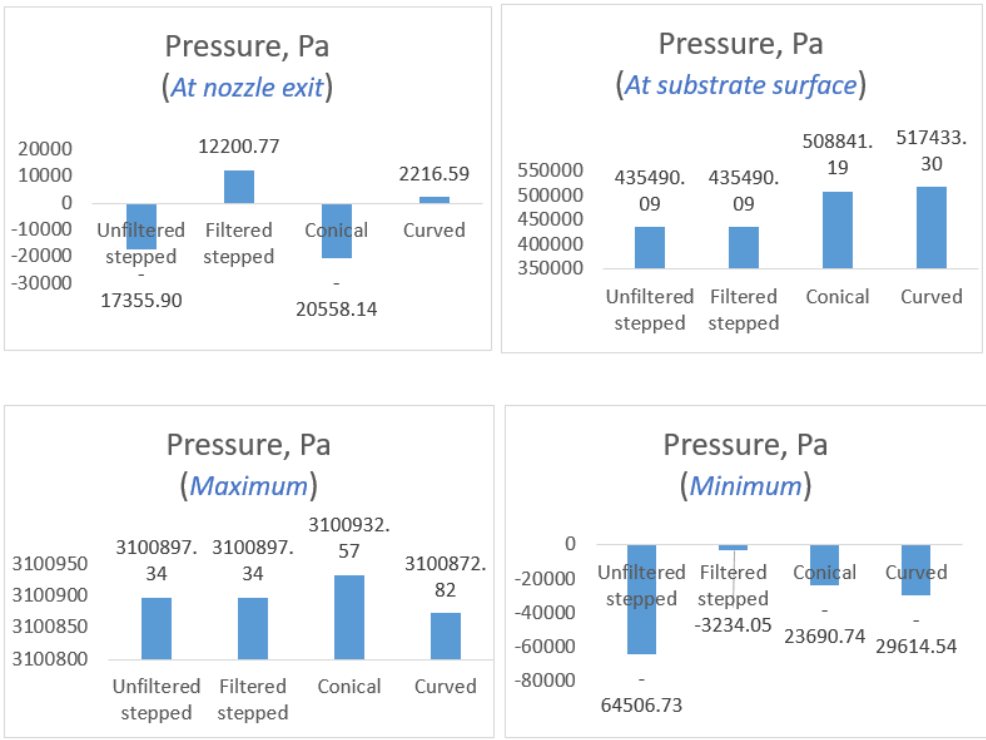

Figure 36: Pressure Bar Graphs

Nozzle 1 (Stepped Nozzle) - Total Pressure

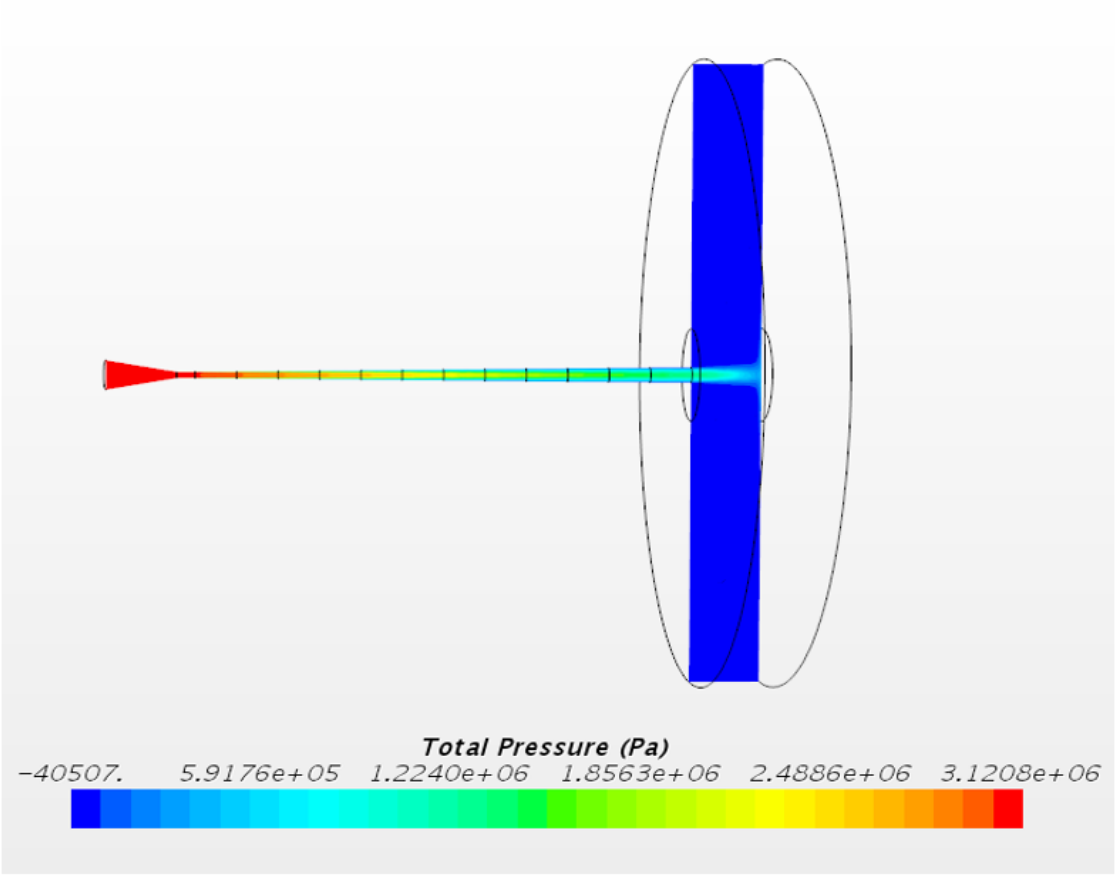

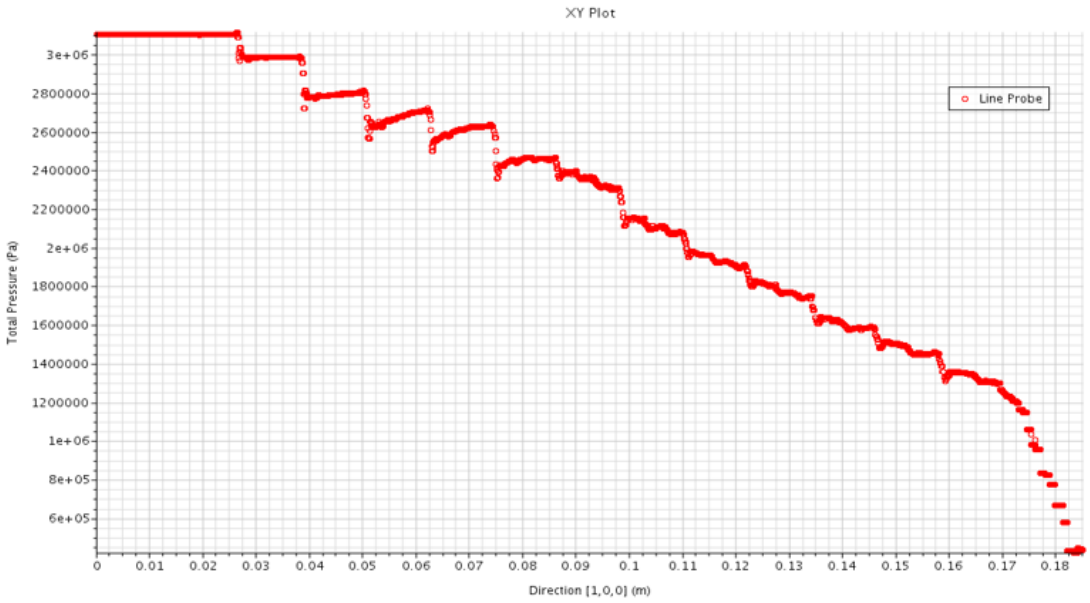

Figure 37: Visualization of Total Pressure in Step Drilled Nozzle

Nozzle 2 (Conical Nozzle) - Total Pressure

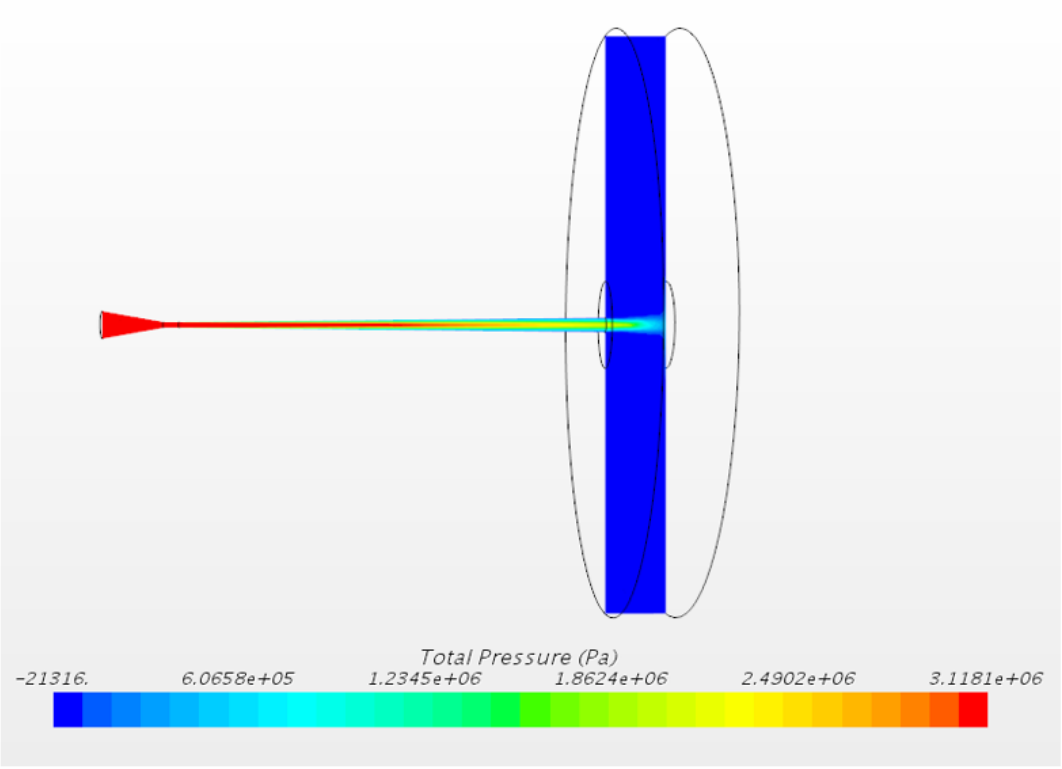

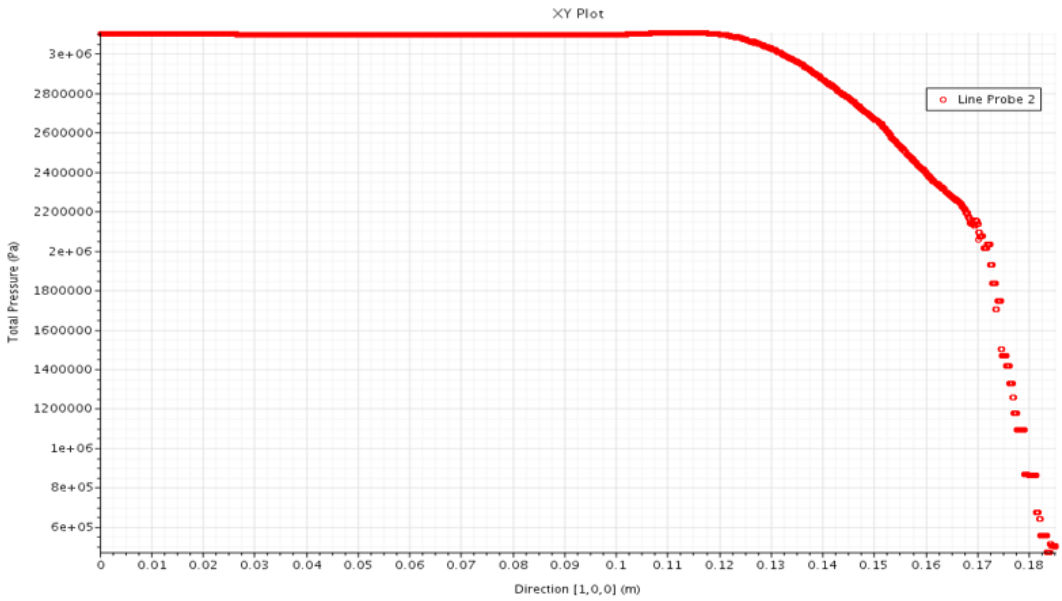

Figure 38: Visualization of Total Pressure in Conical Nozzle

Nozzle 3 (Curved Nozzle) - Total Pressure

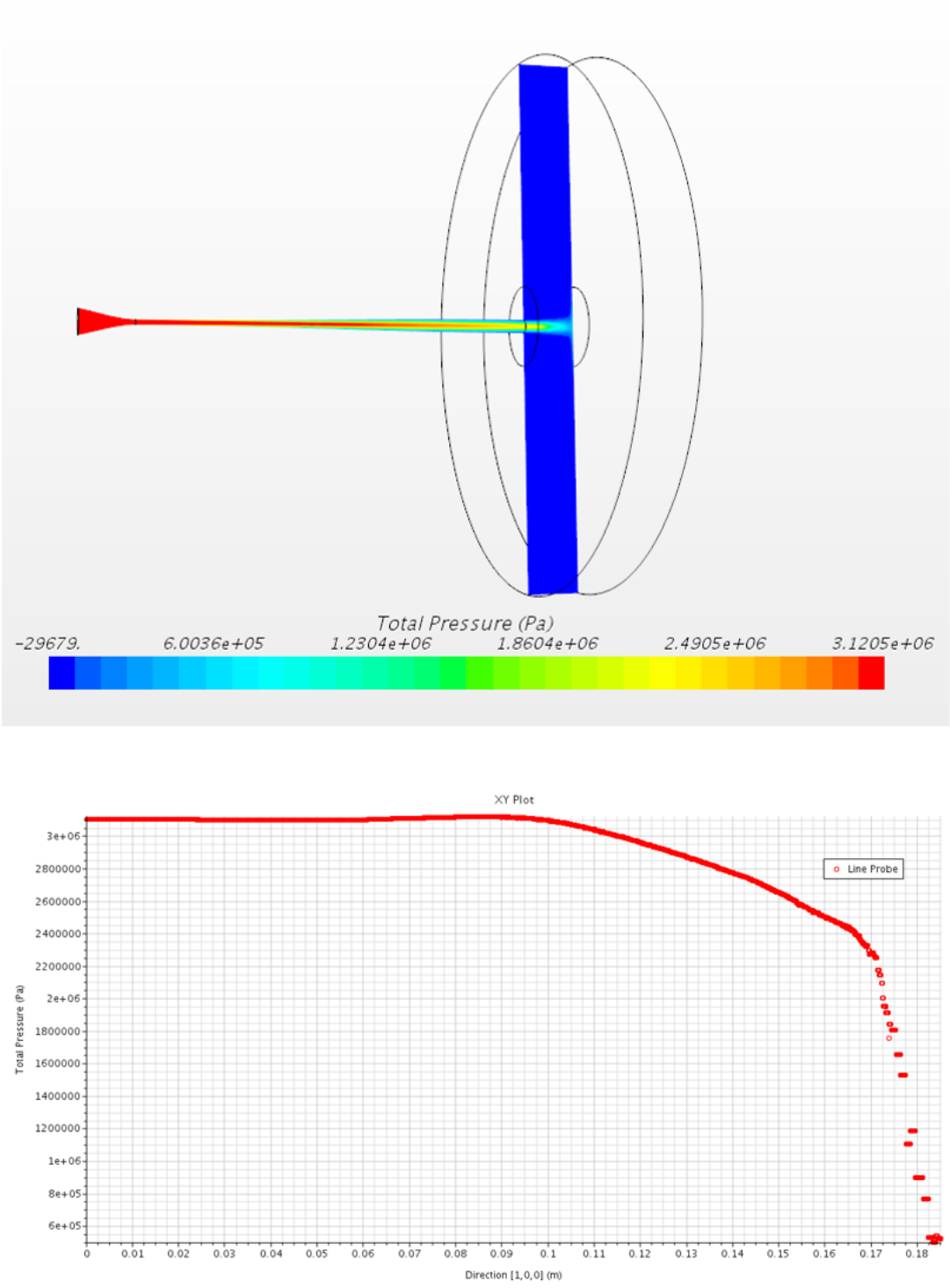

Figure 39: Visualization of Total Pressure in Curved Nozzle

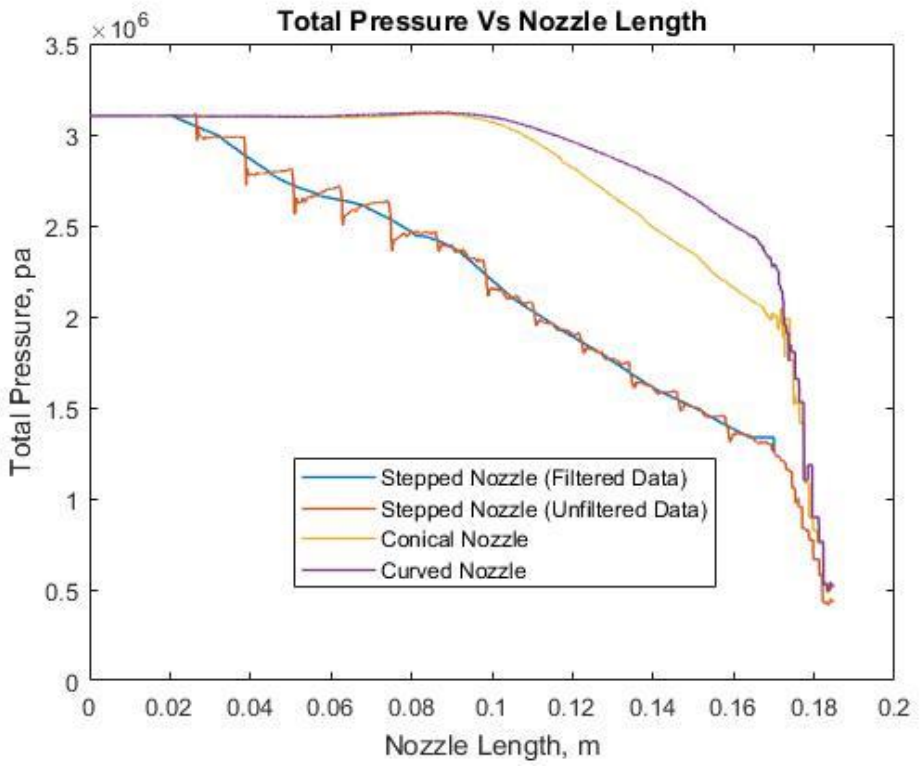

Figure 40: Total Pressure comparison among various Nozzles using Line Graph

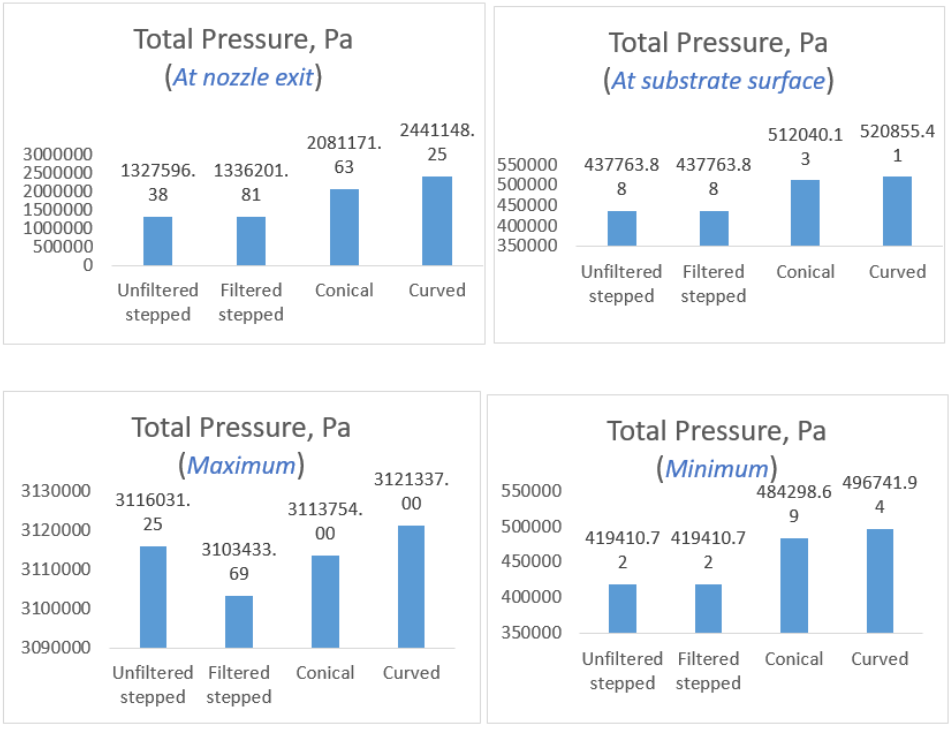

Figure 41: Total Pressure Bar Graphs

Nozzle 1 (Stepped Nozzle) - Temperature (nozzle, substrate)

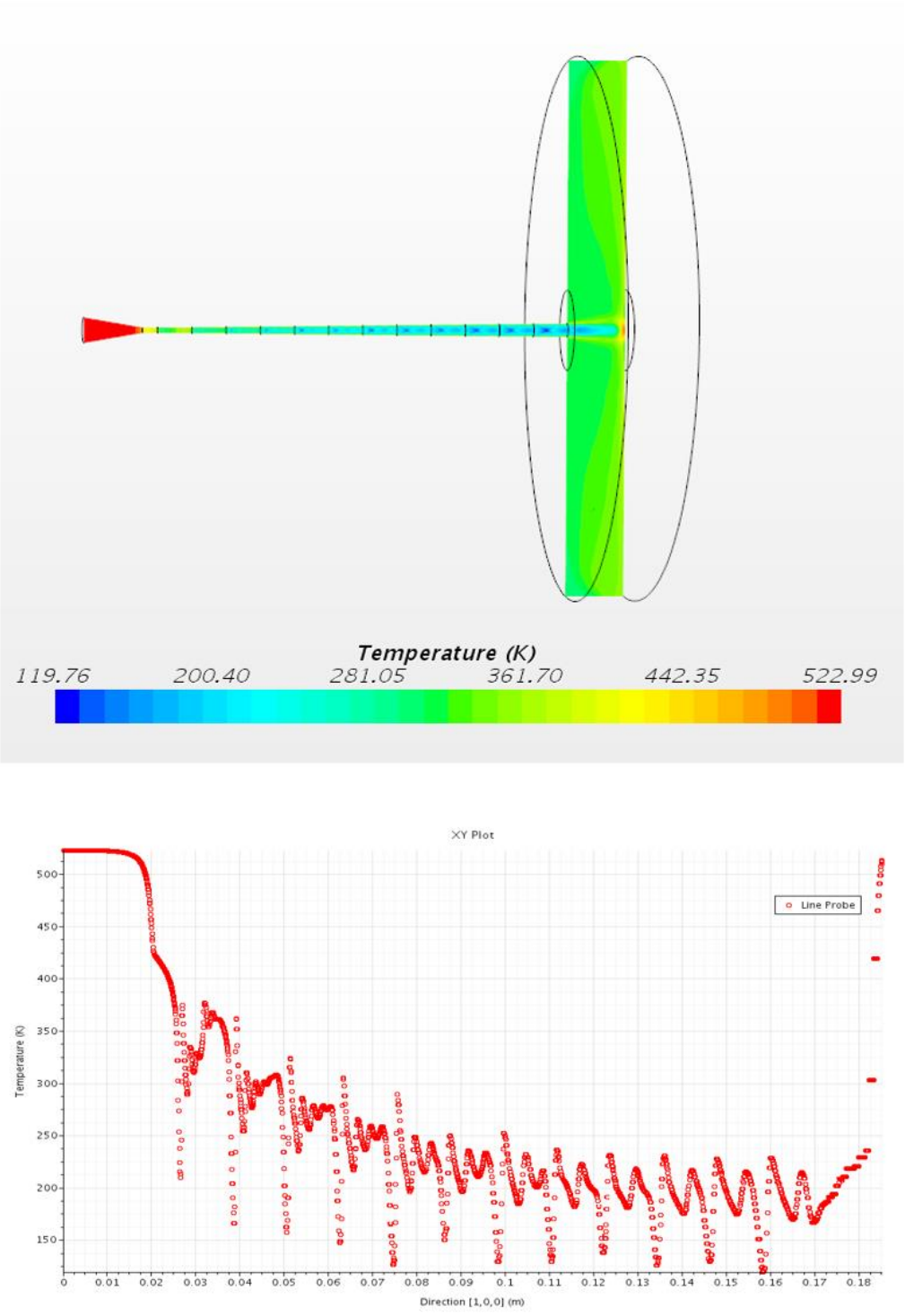

Figure 42: Visualization of Temperature in Step Drilled Nozzle

Nozzle 2 (Conical Nozzle) - Temperature (nozzle, substrate)

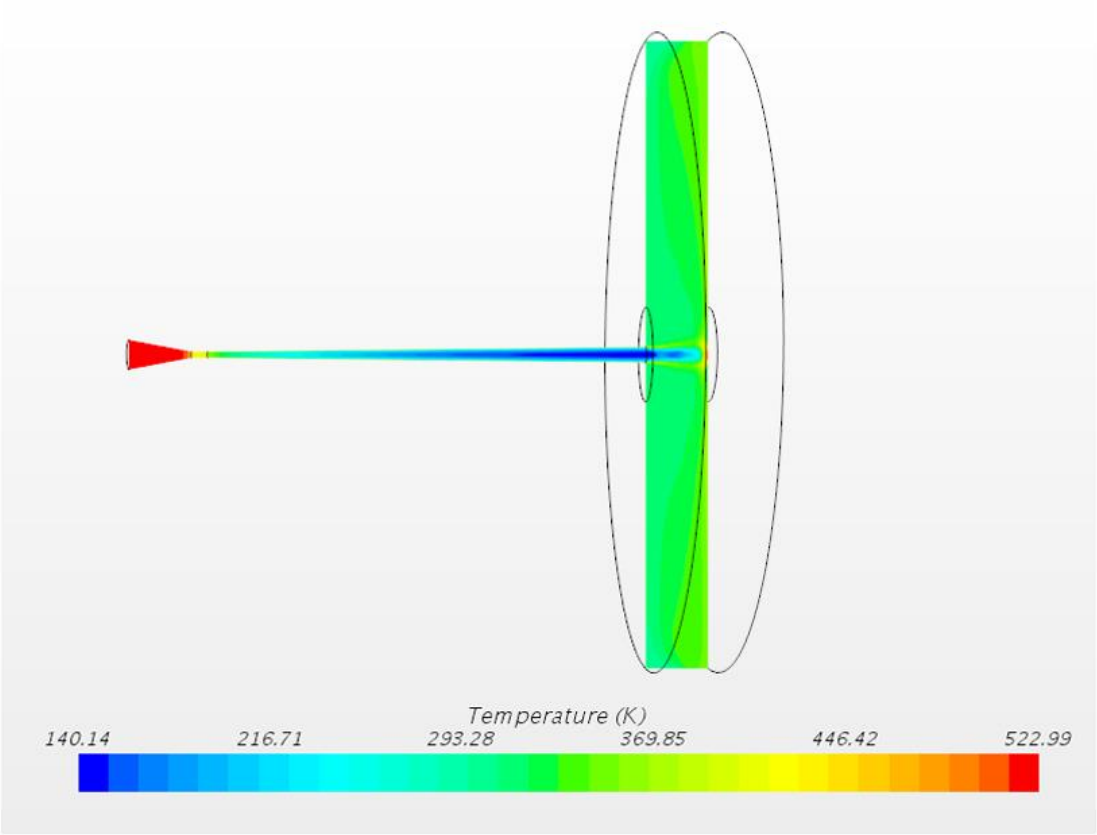

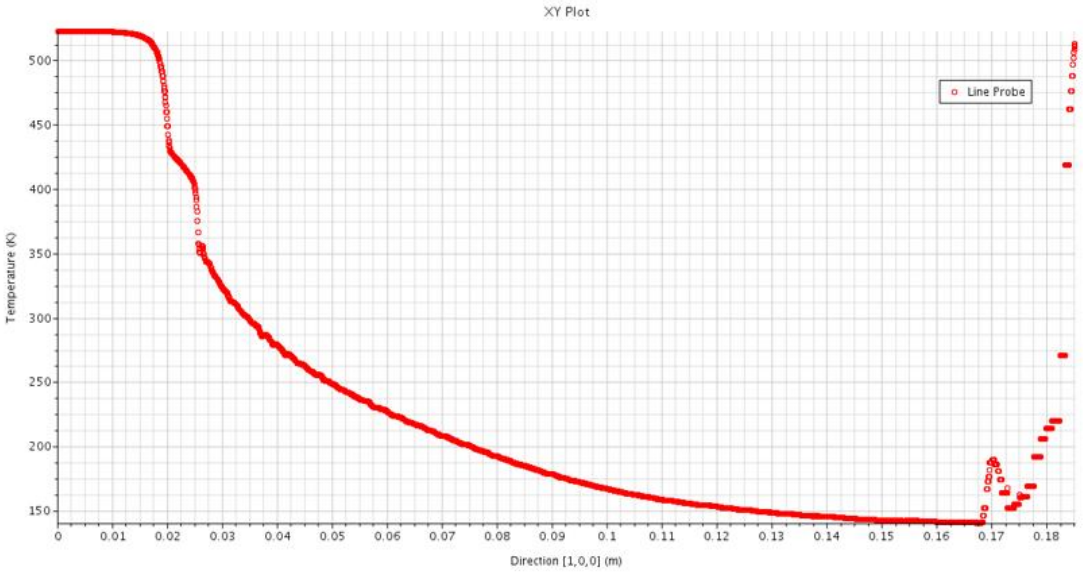

Figure 43: Visualization of Temperature in Conical Nozzle

Nozzle 3 (Curved Nozzle) - Temperature (nozzle, substrate)

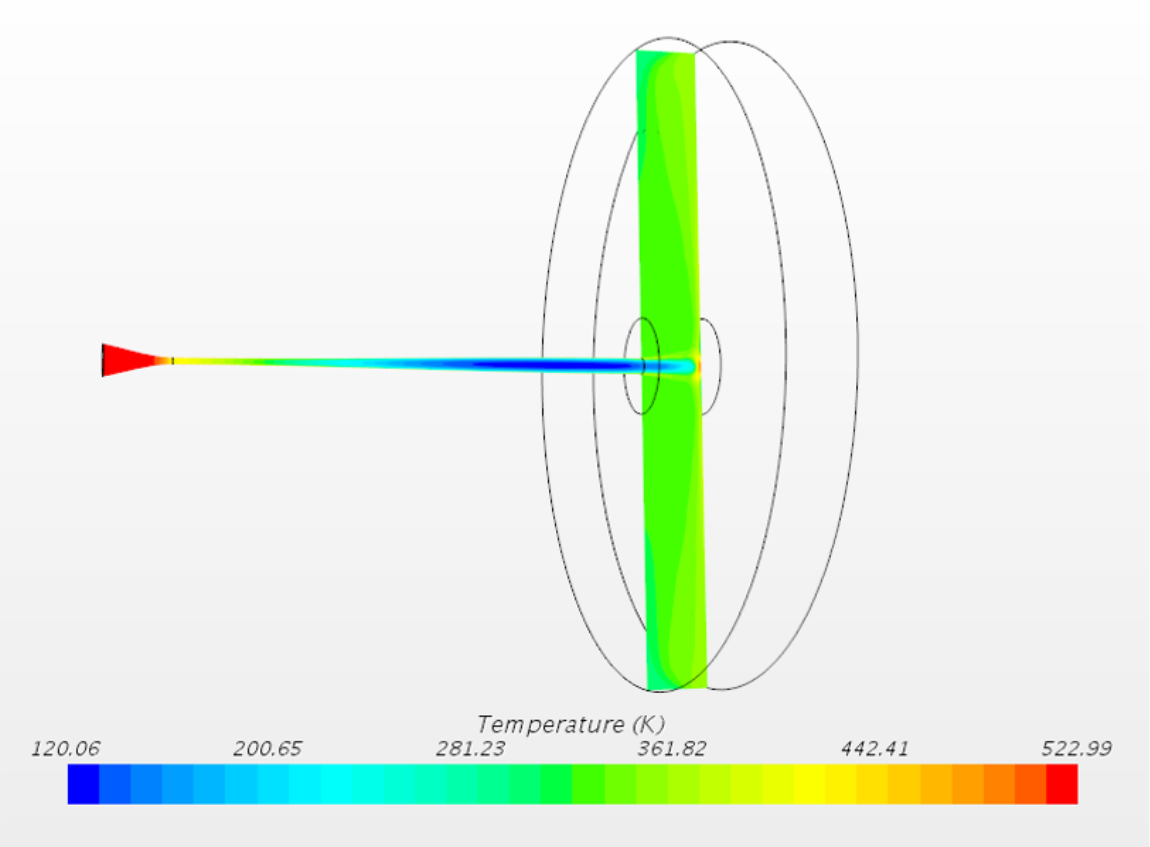

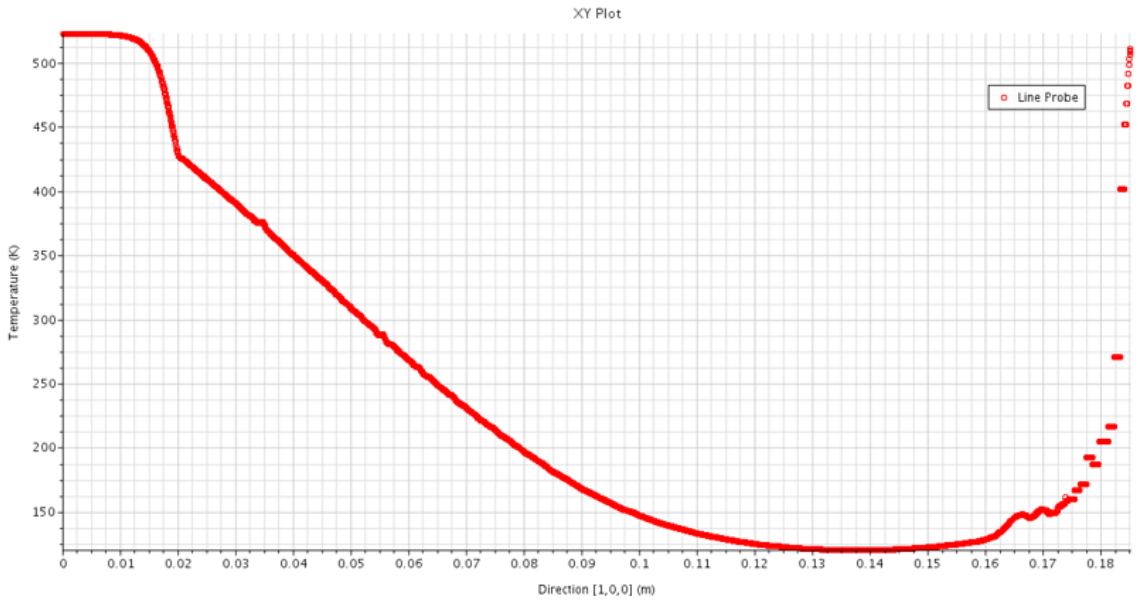

Figure 44: Visualization of Temperature in Curved Nozzle

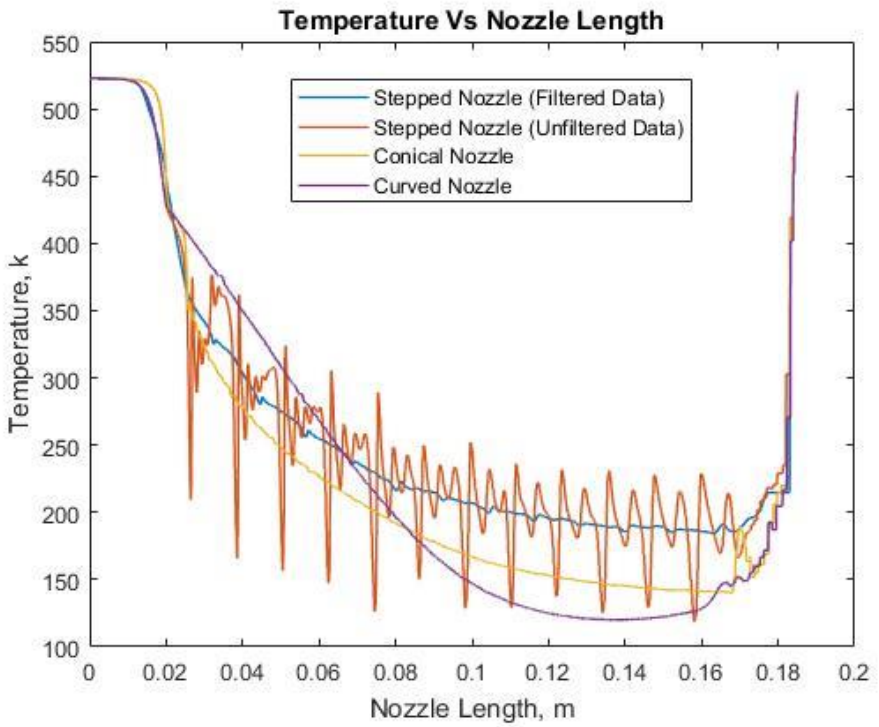

Figure 45: Temperature comparison among various Nozzles using Line Graph

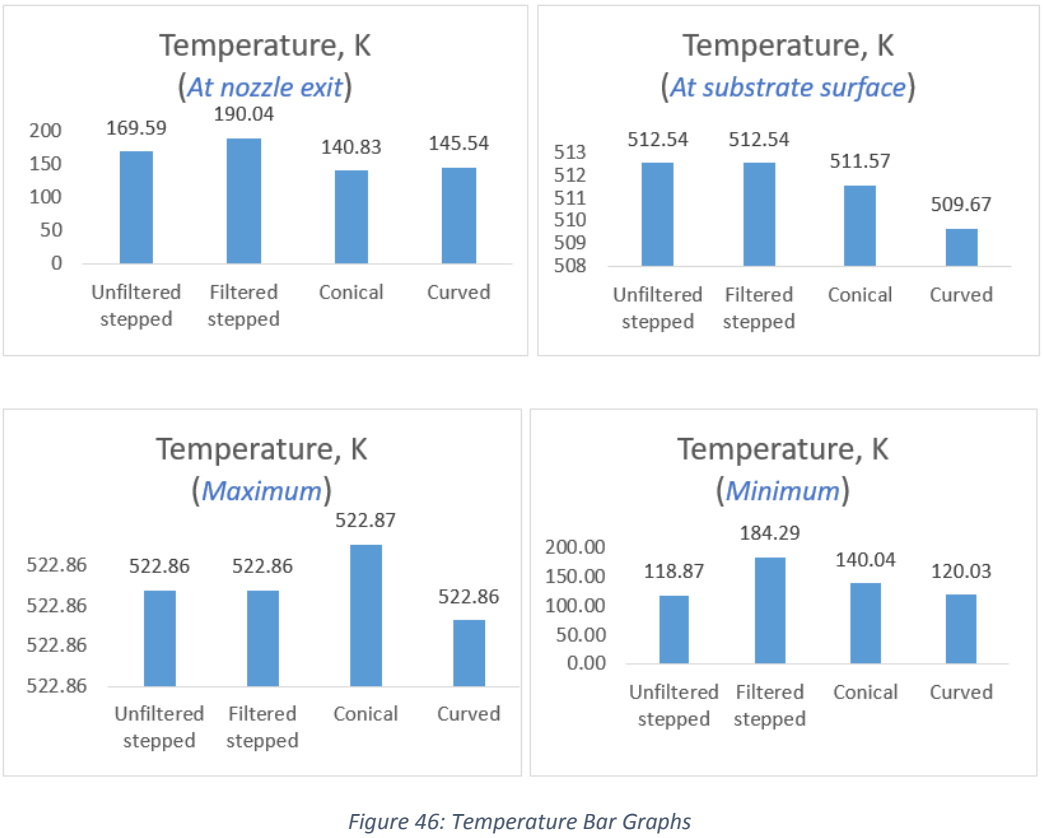

Figure 46: Temperature Bar Graphs

Nozzle 1 (Stepped Nozzle) - TKE

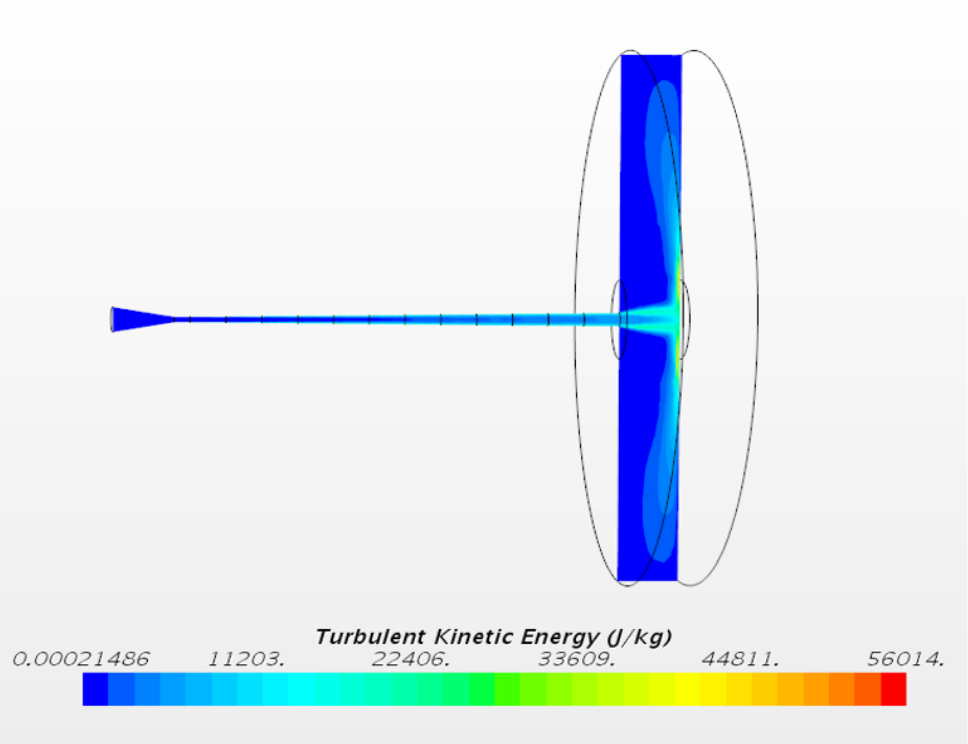

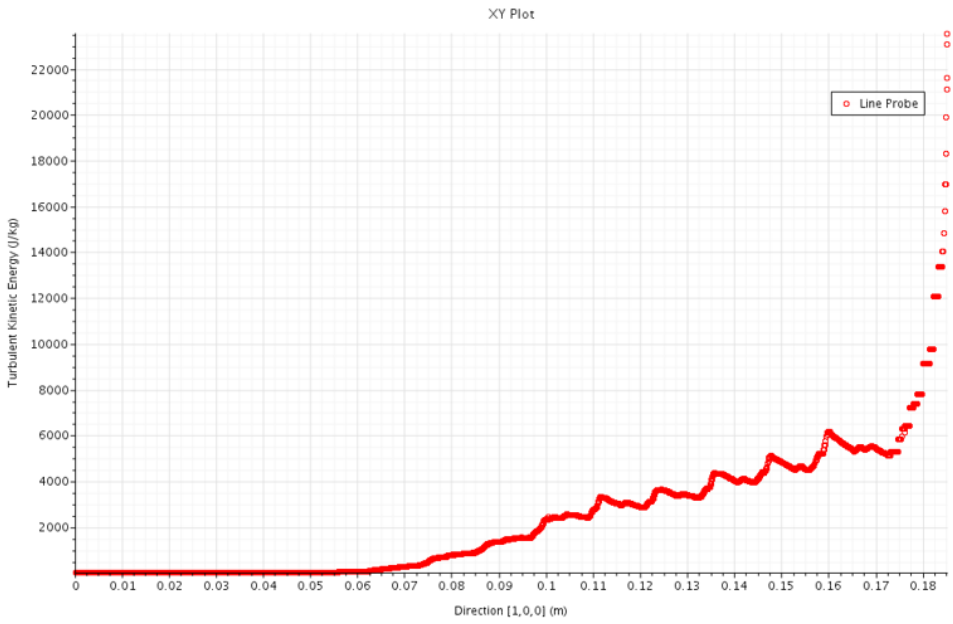

Figure 47: Visualization of Turbulent Kinetic Energy in Step Drilled Nozzle

Nozzle 2 (Conical Nozzle) - TKE

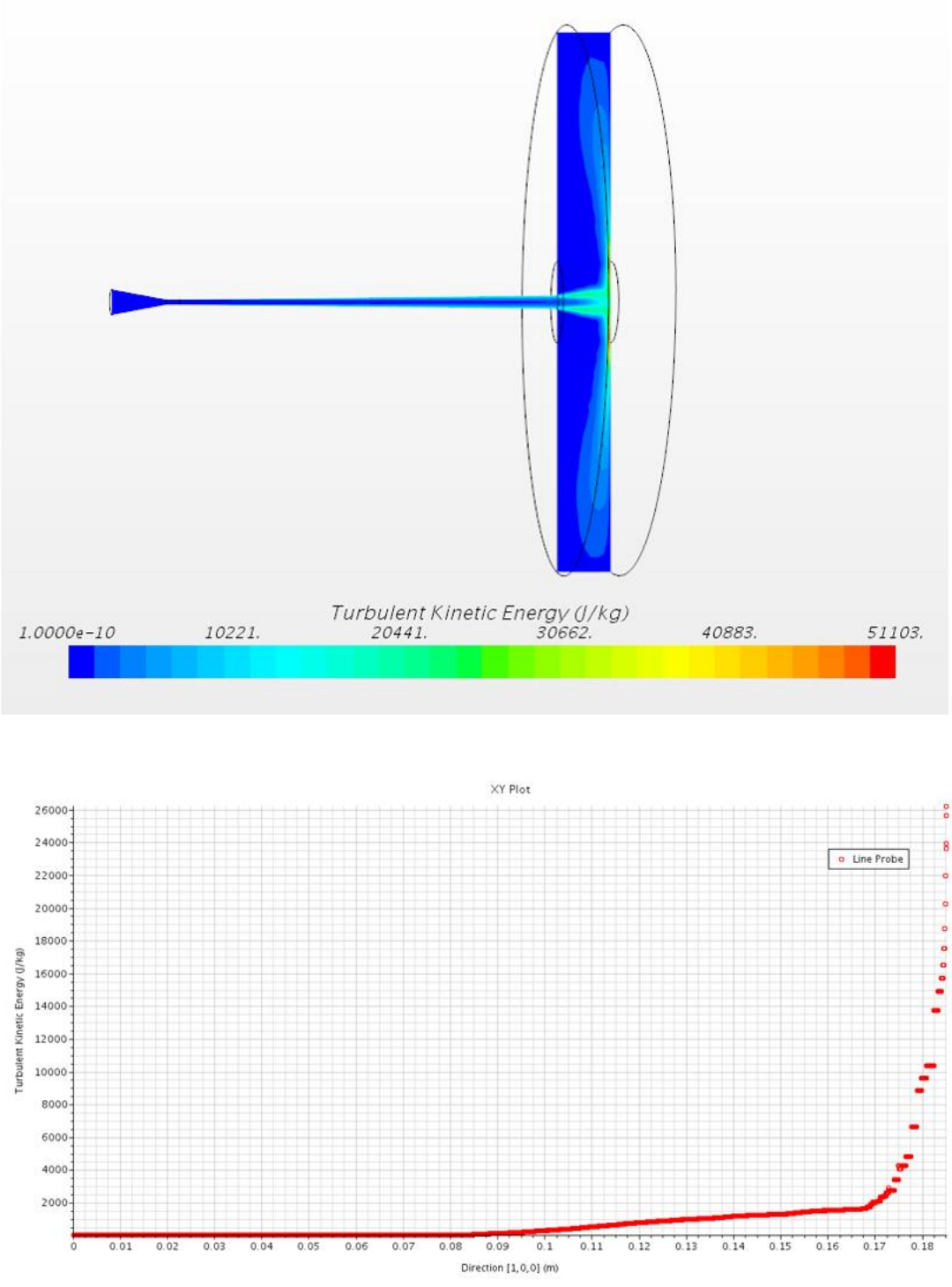

Figure 48: Visualization of Turbulent Kinetic Energy in Conical Nozzle

Nozzle 3 (Curved Nozzle) - TKE

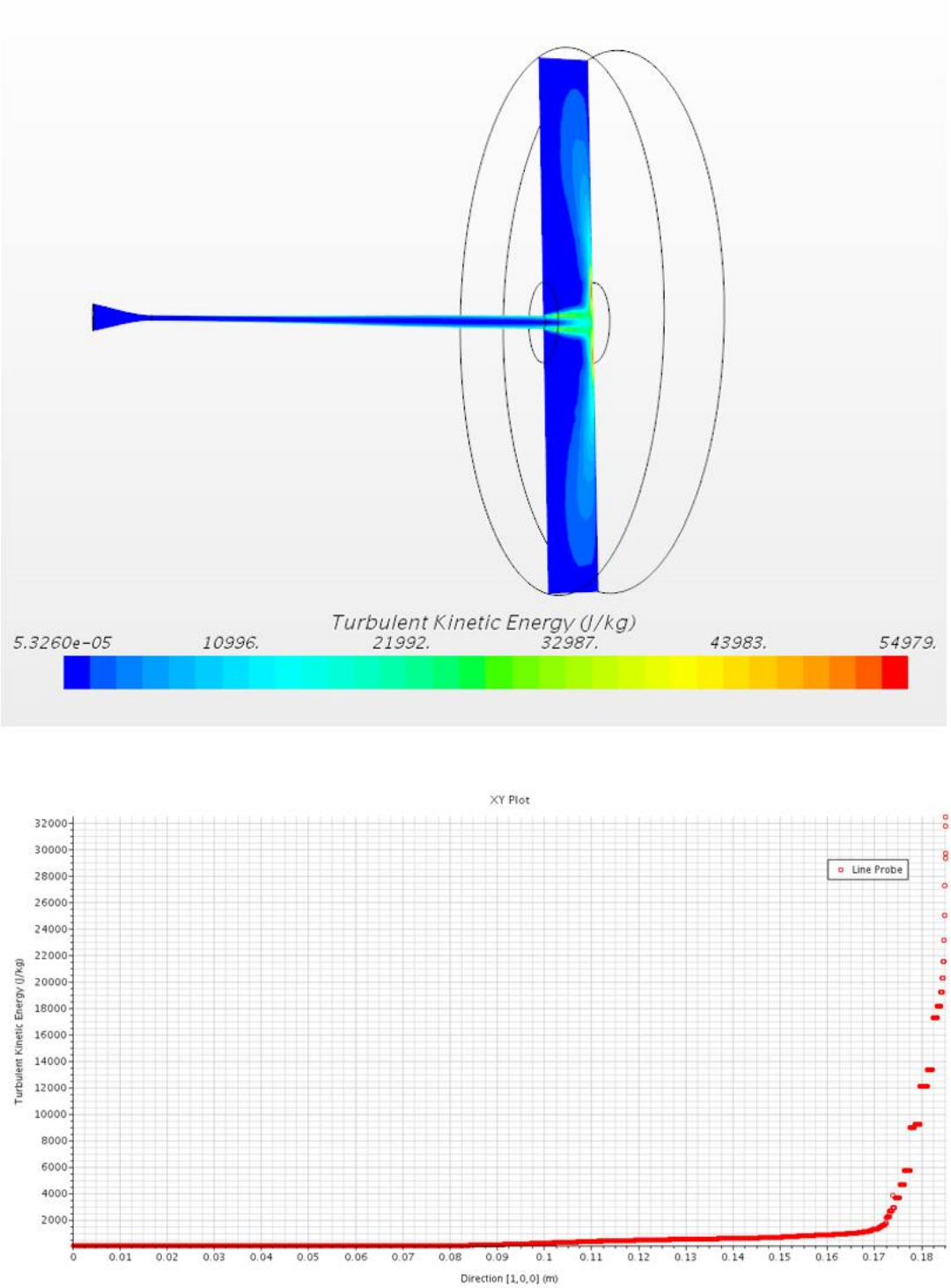

Figure 49: Visualization of Turbulent Kinetic Energy in Curved Nozzle

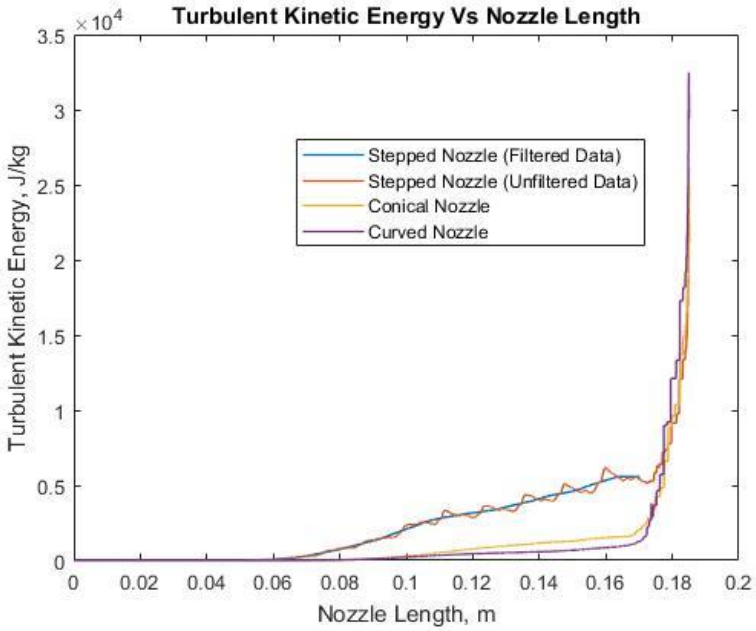

Figure 50: Turbulent Kinetic Energy comparison among various Nozzles using Line Graph

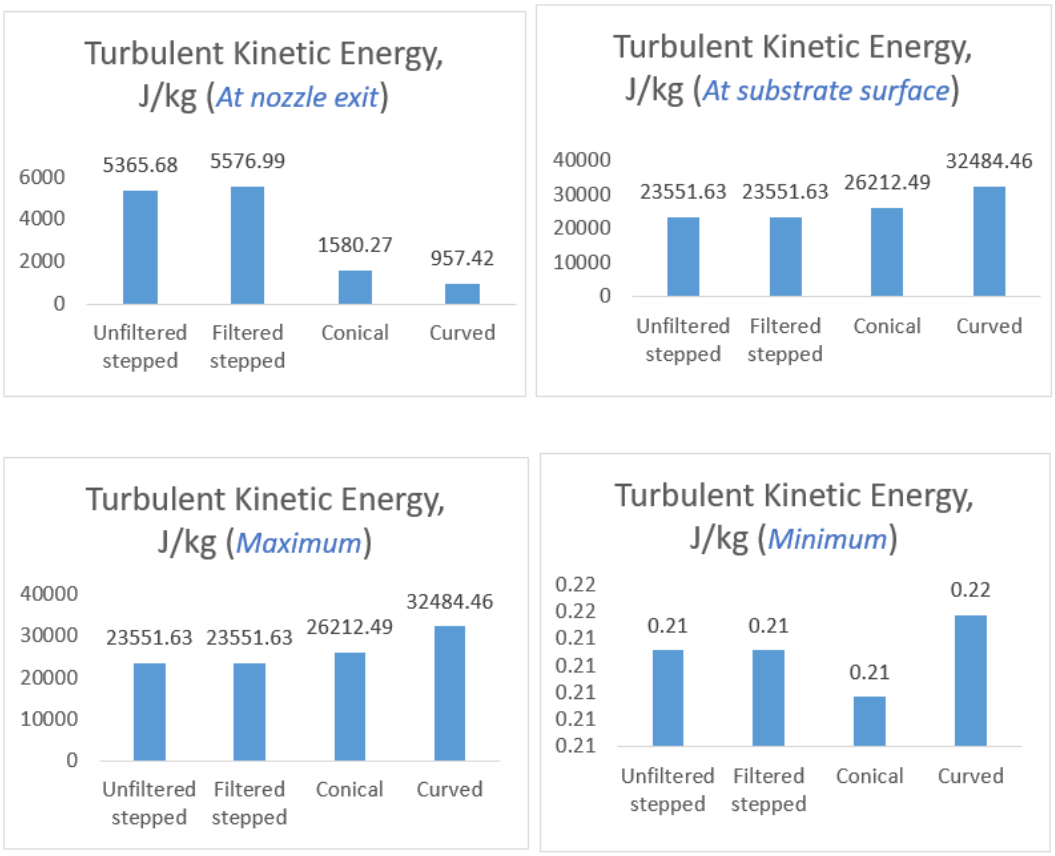

Figure 51: Turbulent Kinetic Energy Bar Graphs

Nozzle 1 (Stepped Nozzle) - Velocity

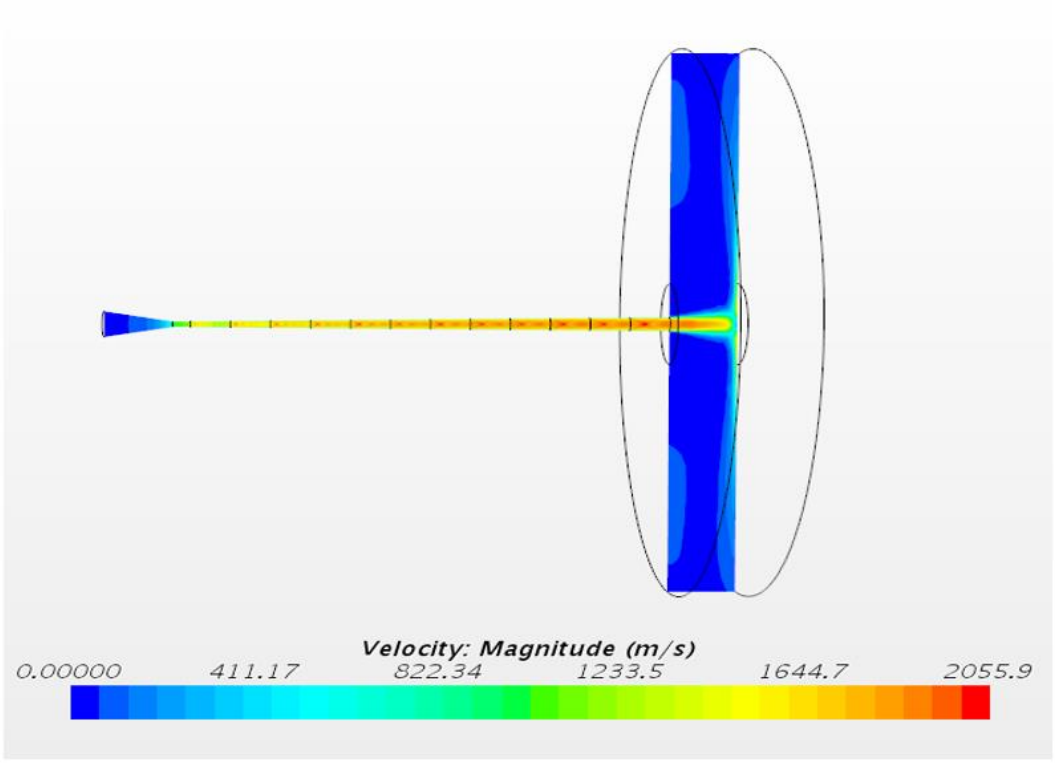

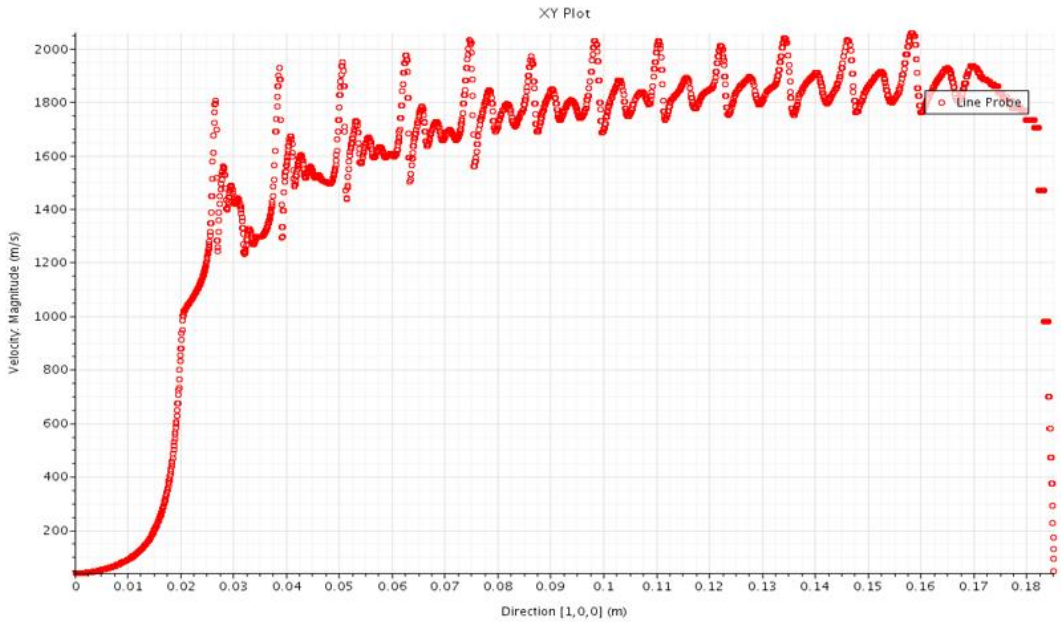

Figure 52: Visualization of Velocity in Step Drilled Nozzle

Nozzle 2 (Conical Nozzle) - Velocity

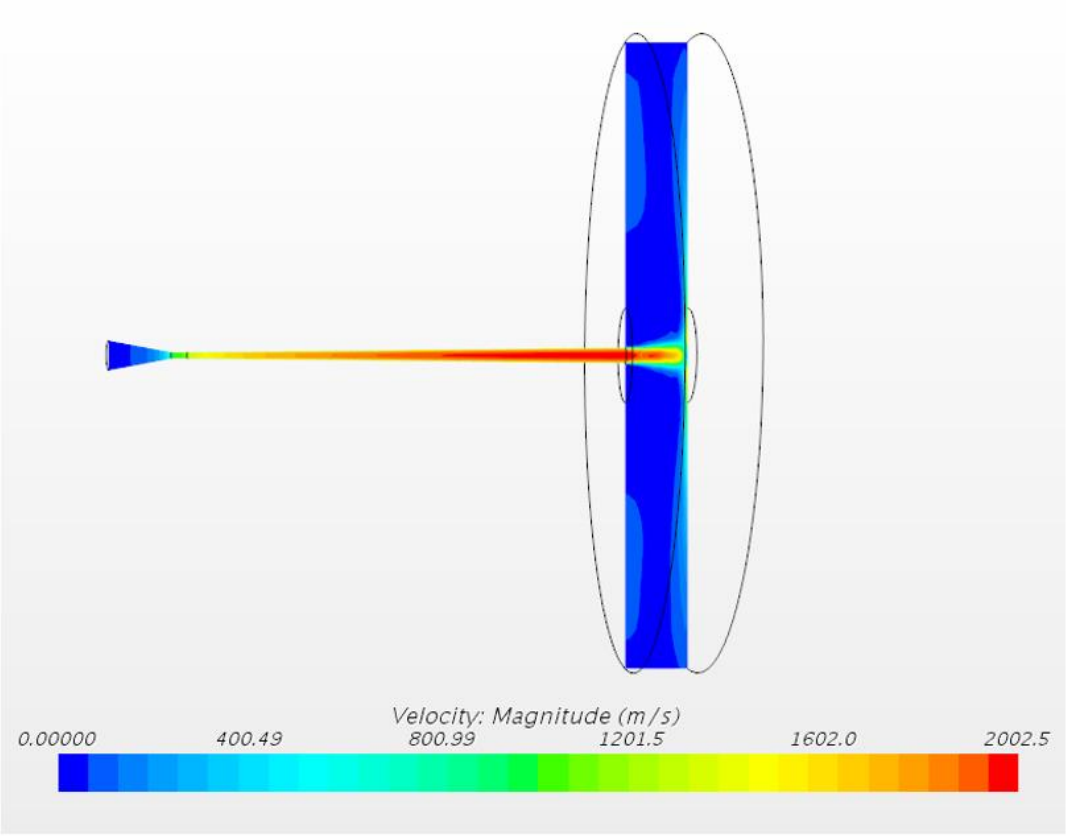

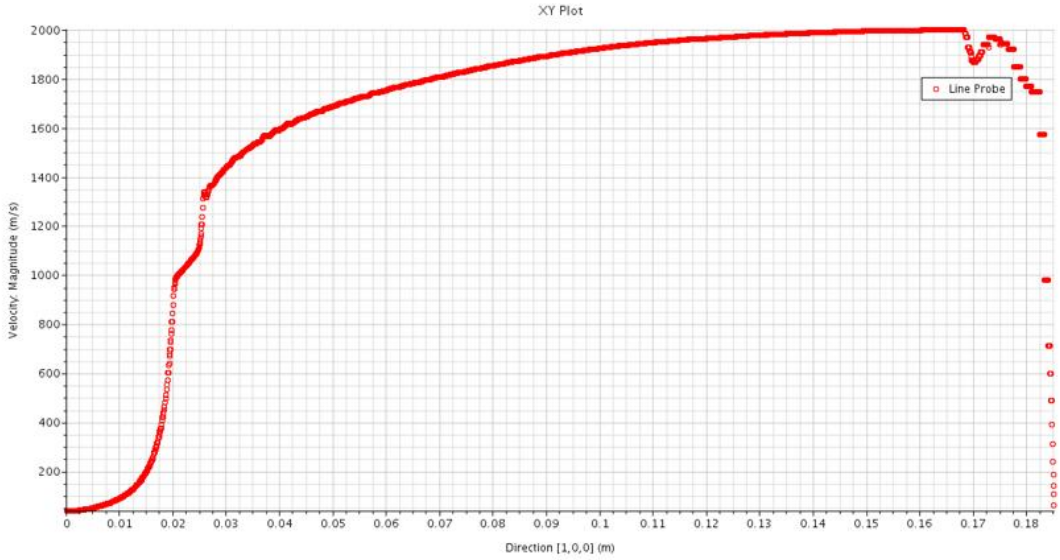

Figure 53: Visualization of Velocity in Conical Nozzle

Nozzle 3 (Curved Nozzle) - Velocity

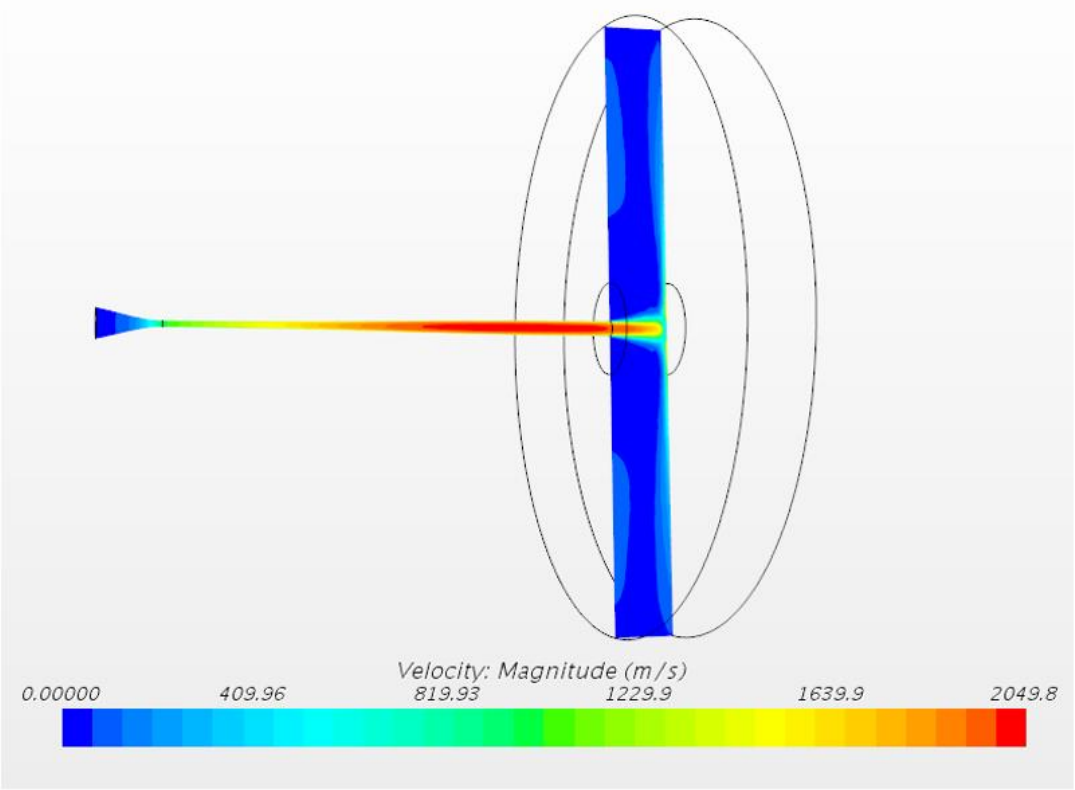

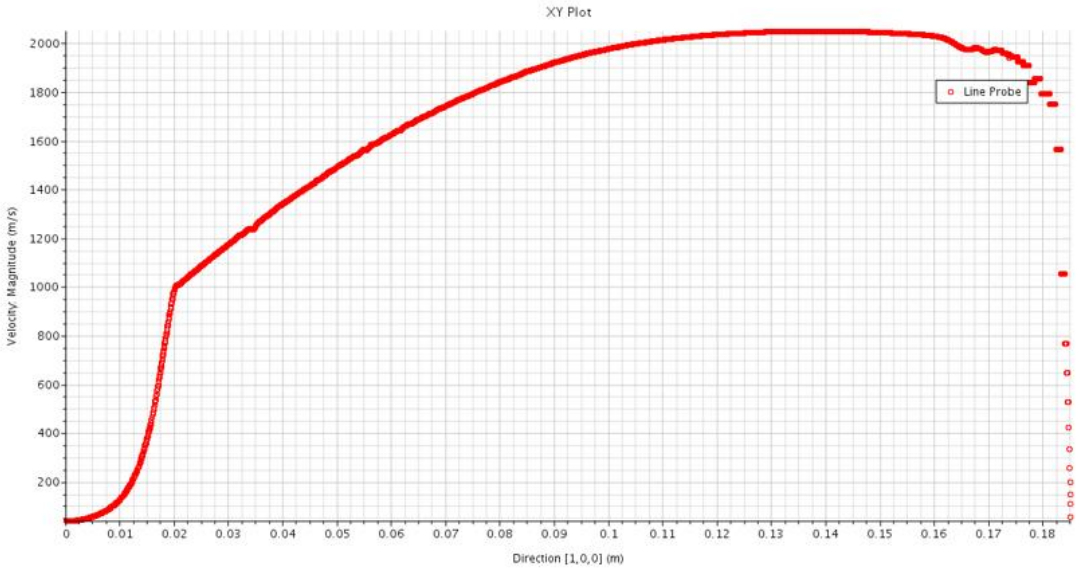

Figure 54: Visualization of Velocity in Curved Nozzle

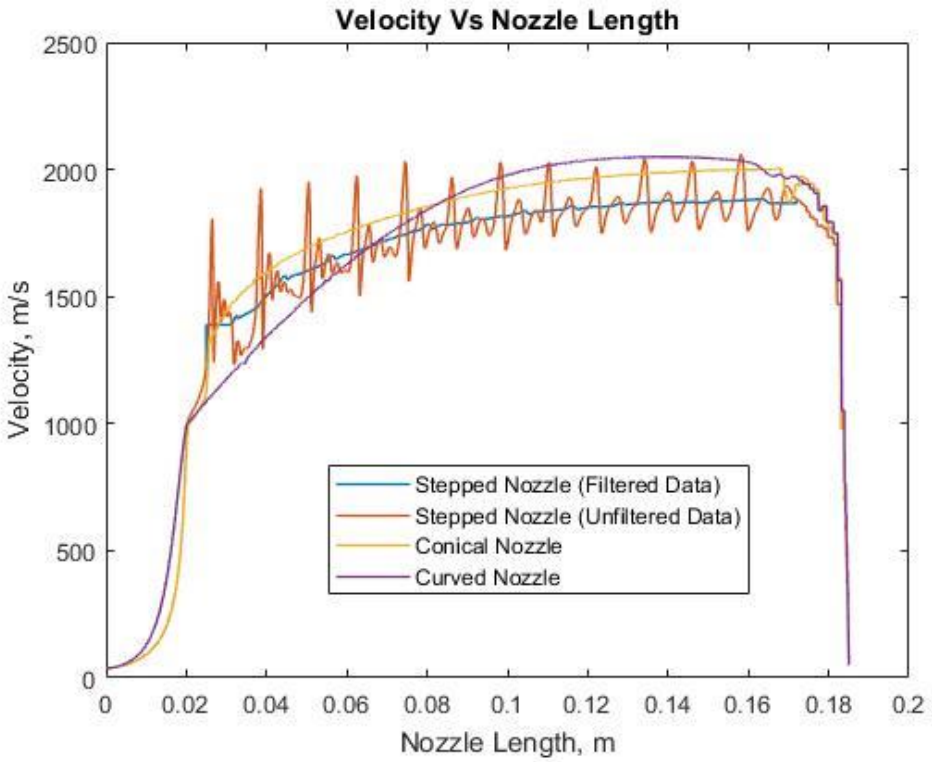

Figure 55: Velocity comparison among various Nozzles using Line Graph

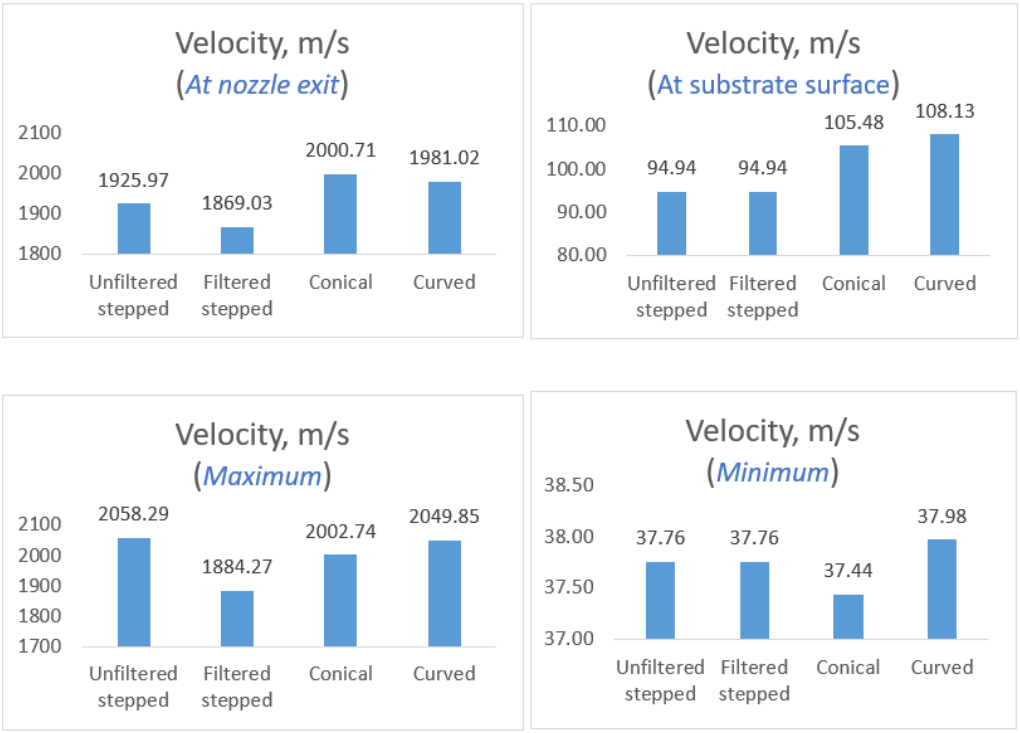

Figure 56: Velocity Bar Graphs

Summary of the Results

To best display the results of the nozzle shape, a typical operating condition was chosen: 3.2 bar, 523 K. The absolute pressure plots show that the step drilled nozzle exhibits 40.5% higher than conical and 9.64% higher than the curved nozzle which means the conversion of pressure to kinetic energy is lowest among other two nozzles. Density among three nozzles does not differ much, but step drilled nozzle achieved 13.79% and 12.28% lesser density than curved and conical nozzle simultaneously. The temperature at the nozzle exit is highest in case of step drilled nozzle (34.94% higher than conical, 30.57% higher than curved). Turbulent Kinetic Energy at nozzle exit in case of step drilled nozzle is 2.59 times higher than conical and 4.82 times higher than the curved nozzle. In case of achieving maximum velocity, step drilled nozzle attained the least (6% lesser than conical, 8% lower than curved nozzle).

Considerable losses happen when shock formation happen inside the nozzle. From velocity scalar field image, one can see the shock formation inside the step drilled nozzle. The main reason for that is because of the presence of steps in the divergent section which creates a low-pressure region the corners and affects the flow from being laminar. On the other hand, the curved nozzle showed the best performance since its design supports better gas expansion.

Summary of Scalar field values at the Nozzle Exit

At Nozzle Exit				
Scalar Function	***Unfiltered stepped***	***Filtered stepped***	***Conical***	***Curved***
Absolute Pressure, Pa	83969.10	113525.77	80766.86	103541.59
Density, kg/m^3	0.24	0.28	0.28	0.34
Mach	2.51	2.32	2.87	2.79
Pressure, Pa	-17355.90	12200.77	-20558.14	2216.59
Temperature, K	169.59	190.04	140.83	145.54
Turbulent Kinetic Energy, J/kg	5365.68	5576.99	1580.27	957.42
Total Pressure, Pa	1327596.38	1336201.81	2081171.63	2441148.25
Velocity, m/s	1925.97	1869.03	2000.71	1981.02

Table 4: Summary of Scalar field values at the Nozzle Exit

Summary of Scalar field values at the Substrate Surface

At Substrate Surface				
Scalar Function	***Unfiltered stepped***	***Filtered stepped***	***Conical***	***Curved***
Absolute Pressure, Pa	536815.09	536815.09	610166.19	618758.30
Density, kg/m^3	0.50	0.50	0.57	0.58
Mach	0.07	0.07	0.08	0.08
Pressure, Pa	435490.09	435490.09	508841.19	517433.30
Temperature, K	512.54	512.54	511.57	509.67
Turbulent Kinetic Energy, J/kg	23551.63	23551.63	26212.49	32484.46
Total Pressure, Pa	437763.88	437763.88	512040.13	520855.41
Velocity, m/s	94.94	94.94	105.48	108.13

Table 5: Summary of Scalar field values at the Substrate Surface

Scalar Function	*Unfiltered stepped*	*Location (mm)*	*Filtered stepped*	*Location (mm)*	*Conical*	*Location (mm)*	*Curved*	*Location (mm)*
Absolute Pressure, Pa	3202222.34	0	3202222.34	0	3202257.57	0	3202197.82	0
Density, kg/m^3	2.95	0	2.95	0	2.95	0	2.95	0
Mach	3.21	158	2.39	163.05	2.88	167.3	3.18	137.8
Pressure, Pa	3100897.34	0	3100897.34	0	3100932.57	0	3100872.82	0
Temperature, K	522.86	0	522.86	0	522.87	0	522.86	0
Turbulent Kinetic Energy, J/kg	23551.63	185	23551.63	185	26212.49	185	32484.46	185
Total Pressure, Pa	3116031.25	26.2	3103433.69	20.2	3113754	85.5	3121337	87.5
Velocity, m/s	2058.29	158	1884.27	163.05	2002.74	167.3	2049.85	138.3

Table 6: Summary of maximum scalar field values and their location

Scalar Function	*Unfiltered stepped*	*Location (mm)*	*Filtered stepped*	*Location (mm)*	*Conical*	*Location (mm)*	*Curved*	*Location (mm)*
Absolute Pressure, Pa	36818.27	158.15	98090.95	174.65	77634.26	167.9	71710.46	146.2
Density, kg/m^3	0.15	158.15	0.23	183.05	0.22	180.85	0.22	181.2
Mach	0.03	0	0.03	0	0.03	0	0.03	0
Pressure, Pa	-64506.73	158.15	-3234.05	174.65	-23690.74	167.9	-29614.54	146.2
Temperature, K	118.87	158	184.29	163.05	140.04	167.3	120.03	137.8
Turbulent Kinetic Energy, J/kg	0.21	0.35	0.21	0.35	0.21	0	0.22	0
Total Pressure, Pa	419410.72	183.15	419410.72	183.15	484298.69	183.25	496741.94	183.25
Velocity, m/s	37.76	0	37.76	0	37.44	0	37.98	0

Table 7: Summary of minimum scalar field values and their location

Validation

Validation is performed by comparing the results of Muhammad Faizan Ur Rab's simulation [25] to the results obtained by the conical nozzle in the current study. Figure 57 shows the computed velocity profile concerning the nozzle axis for cold spray supersonic jet at 800C and 3 MPa. Figure 58 shows the calculated velocity profile concerning the nozzle axis for cold spray supersonic jet at 250 C and 3.2 MPa. As it can be seen from the velocity profiles of the validation case and current study, the velocity along the axis on both nozzles exhibits striking similarity in the trend. Both the nozzles witness significant acceleration in velocity when the gas enters to diverging section, a gradual increase in the velocity till the gas exits the nozzle, negative peak during the travel in the stand-off distance and comes down to zero when it the gas impacts the surface of the substrate. Since the process variables vary in both cases, the velocity magnitude varies but not the trend. Table 8 shows the differences in the process variables. Since there are not much research articles published on a step drilled nozzle used for cold spray, further investigation regarding experimentation and modeling will be required in future work for more exact comparison and validation. Therefore, it is sensible to conclude that the simulation results obtained for the current study are validated.

	Current Study	**Validation Case**
Gas Inlet Pressure, MPa	3.2	3
Gas Inlet Temperature, C	250	800
Gas Type	Helium	Nitrogen
Nozzle Throat Diameter, mm	2	2.7

Stand Off Distance, mm	20	35
Convergent Section Length, mm	20	51.2
Divergent Section Length, mm	145	70.3
Divergent Section Profile	Conical	Conical

Table 8: Summary of Process Variables used in validation case and current case

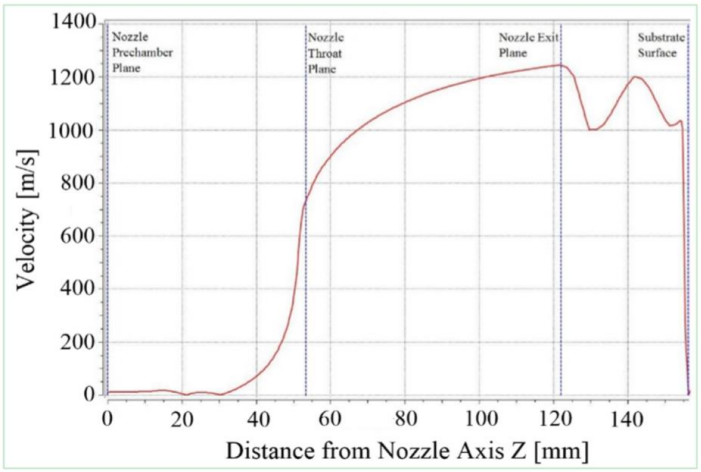

Figure 57: Calculated Velocity profile concerning the nozzle axis for cold spray supersonic jet at 800 C and 3 MPa [Validation Case]

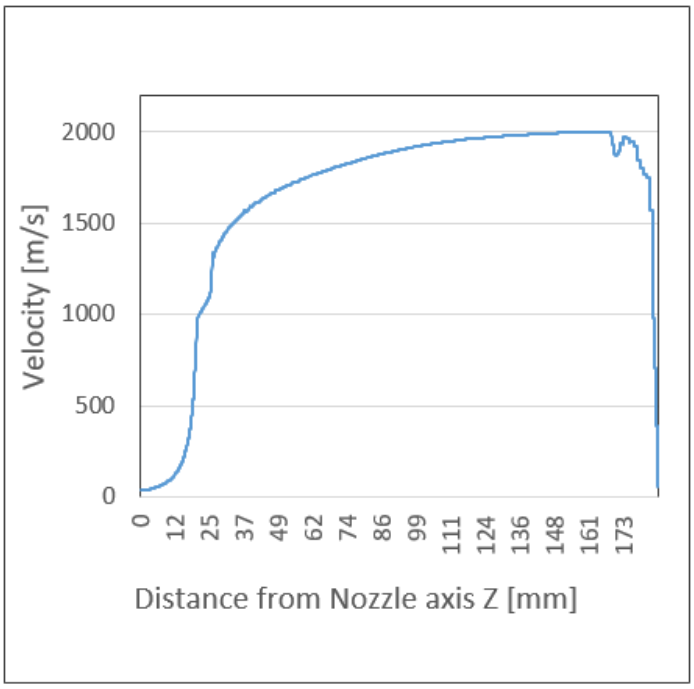

Figure 58: Computed velocity profile in the nozzle axis for cold spray supersonic nozzle jet 250 C and 3.2 MPa [current study]

Research Contribution

For the first time, this research study contributes the numerical analysis performed on the step drilled nozzle. In this study, the effect of step drilled shape on the flow characteristics in the cold spray process is systematically investigated by numerical method. The results are compared with the other two nozzle designs. CFD approach is employed to achieve this objective by solving 3D full Navier-Stokes equations. Based on the numerical results obtained from the simulation, it is found that the shock formation inside the stepped drilled design significantly influences the flow regime and the gas acceleration.

CHAPTER 5: CONCLUSION AND FUTURE WORK

The conclusion of the thesis in this section provides with some suggestions for future work in this area. Comparison of conical, curved and step drilled nozzle designs were performed by numerical simulation using the typical operating parameters. The results obtained are summarized as follows:

- Presence of shock formation inside the divergent section of the step drilled nozzle creating intense fluctuations regarding pressure, temperature, velocity and other scalar fields presented in the study.
- Step drilled nozzle attained the lowest jet velocity in the divergent section as well as at the substrate surface.
- Curved nozzle outperformed other two nozzles because the curved divergent section allows significant gas expansion and its design itself will enable a smooth transition from convergent to divergent avoiding the presence of sharp corners

This thesis has been mainly focused on analyzing the jet characteristics inside the various nozzle, leaving the study of particle behavior in the nozzle outside the scope of the thesis. The following ideas could be tested:

- Inject particles inside multiple nozzles and study their behavior
- Perform Large Eddy simulation for more detailed analysis
- Design De-Laval nozzle using the equations mentioned in the current study
- Perform research study on the shock formation inside the nozzle

REFERENCES

1. "Bonding mechanism in cold gas spraying." Acta Materialia 51(15): 4379-4394.
2. S.H. Thurston, Method of Impacting One Metal Upon Another, US706701, year of priority (issued): 1900 (1902)
3. C.F. Rocheville, Device for Treating the Surface of a Workpiece, US3100724, year of priority (issued): 1958 (1963)
4. Papyrin, V. Kosarev, K.V. Klinkov, A. Alkhimov, and V.M.Fomin, Cold Spray Technology. Elsevier, Oxford, 2006
5. A.I.Kashirin, O.F. Klyuev, and .V. Buzdygar: 'Apparatus for gas-dynamic coating,' US Patent 6402050, 2002.
6. "Cold spray coating: review of material systems and future perspectives." Surface Engineering 30(6): 369-395.
7. "Cold spraying: From process fundamentals towards advanced applications." Surface & Coating Technology, 2014
8. T. H. Van Steenkiste, J. R. Smith, D. W. Gorkiewicz, A. A. Elmoursi, B. A. Gillispie, and N. B. Patel: 'Method of maintaining a non-obstructed interior opening in kinetic spray nozzles,' US Patent 6896933, 2005.
9. A.S.M. Ang, N. Sanpo, M.L. Sesso, S.Y. Kim, C.C. Berndt, J. Thermal Spray Technology 22 (7) (2013) 1170-1183
10. T. Stoltenhoff, H. Kreye, H.J. Richter "An analysis of cold spray process and its coatings." ASM International

11. [A. Arabgol, H. Assadi, T. Schmidt, F. Gartner, and T. Klassen, Analysis of Thermal History and Residual Stress in Cold-Sprayed Coatings, J. Thermal Spray Technology, Vol 23 (No. 1-2), 2014, p 84-90]
12. Shuo Yin, Xiao-fang Wang, Wen-ya Li, “Computational analysis of the effect of nozzle cross-section shape on gas flow and particle acceleration in cold spraying.” Surface & Coatings Technology
13. Masahiro Fukumoto, Hiroki Terada, Masahiro Mashiko, Kazunori Sato, Motohiro Yamada and Eiji Yamaguchi “Deposition of Copper Fine particle by the cold spray process.”
14. "Optimal design of a cold spray nozzle by numerical analysis of particle velocity and experimental validation with 316L stainless steel powder." Materials & Design 28(7): 2129-2137.
15. "Optimal design of a convergent-barrel cold spray nozzle by numerical method." Applied Surface Science 253(2): 708-713.
16. Zheng-Dong, Zhang Guo-qing, Zhou, Zhang Yong, Xu Wen-Yong, “Simulation of Gas Flow Field in Laval Nozzle and Straight Nozzle for Powder Metallurgy and Spray Forming,” Journal of Iron and Steel Research, 2008
17. "Numerical investigations on the effect of total pressure and nozzle divergent length on the flow character and particle impact velocity in cold spraying." Surface and Coatings Technology 232: 290-297.
18. "Design and optimization of rectangular cold spray nozzle: Radial injection angle, expansion ratio and traverse speed." Surface and Coatings Technology 316: 246-254.

19. "An analysis of the particulate flow in cold spray nozzles." Mechanical Sciences 6(2): 127-136.
20. "Significant influence of carrier gas temperature during the cold spray process." Surface Engineering 30(6): 443-450.
21. "Numerical Simulation of the Cold Gas-Dynamic Spray Process." Journal of Thermal Spray Technology 15(4): 518-523.
22. R. Lupoi and O'Neill, "Powder stream characteristics in cold spray nozzles." Surface & Coatings Technology 206 (2011)
23. "Numerical study on the effect of nozzle dimension on particle distribution in cold spraying." Surface and Coatings Technology 220: 107-111.
24. M Grujicic, W S DeRosset, D Helfritch "Flow analysis and nozzle-shape optimization for the cold-gas dynamic-spray process."
25. Muhammad Faizan Ur Rab, Saden Zahiri, Syed H. Masood, Mahnaz Jahedi and Romesh Nagarajah "Development of 3D Multicomponent Model for Cold Spray Process Using Nitrogen and Air."
26. "Current design and performance of cold spray nozzles: experimental and numerical observations on deposition efficiency and particle velocity." Surface Engineering 30(5): 316-322.
27. Chang-Jiu Li, Wen-Ya Li, Yu-Yue Wang, Guan-Jun Yang, H. Fukanuma "A theoretical model for prediction of deposition efficiency in cold spraying."

APPENDIX

Simulation procedure in Starccm+

The instructions with pictures provided below will briefly go through the steps of running the successful CFD simulation in StarCCM+ software.

Step 1: Click Create a file

Select the type of processor and click OK. The file structure will be created.

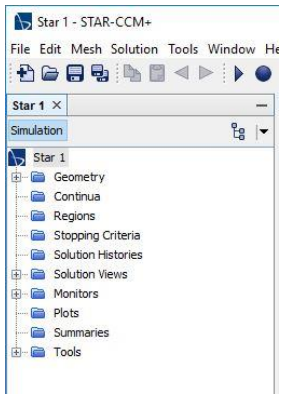

Step 2: Create CAD Geometry

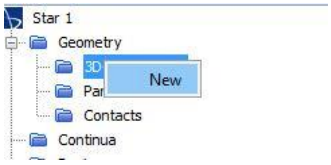

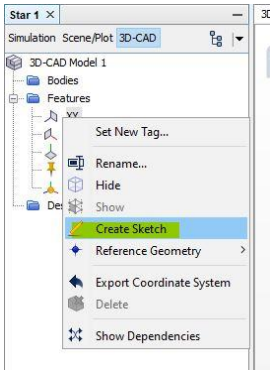

Step 3: After building the 3D CAD model, name the faces of the CAD.

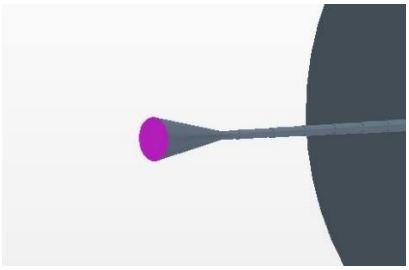

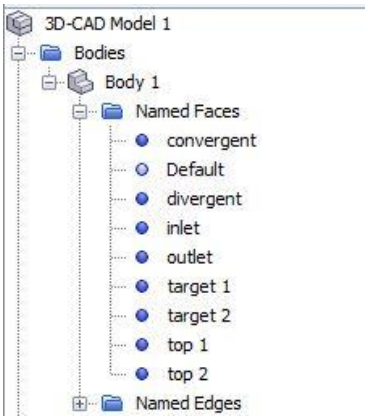

Step 4: Create Regions for the CAD Model

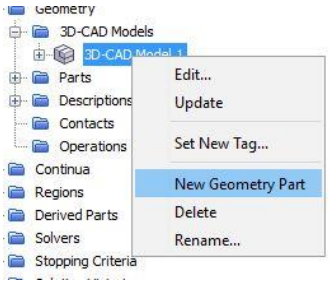

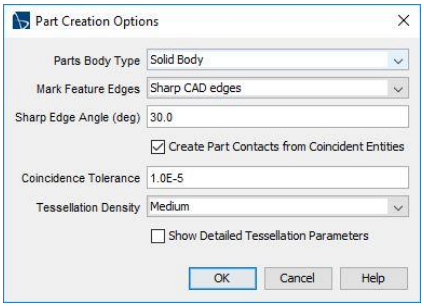

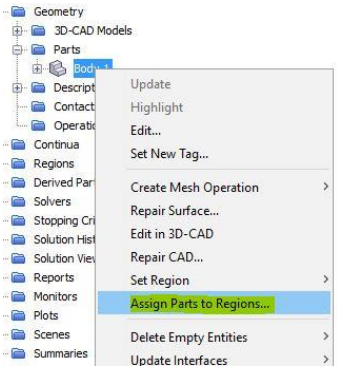

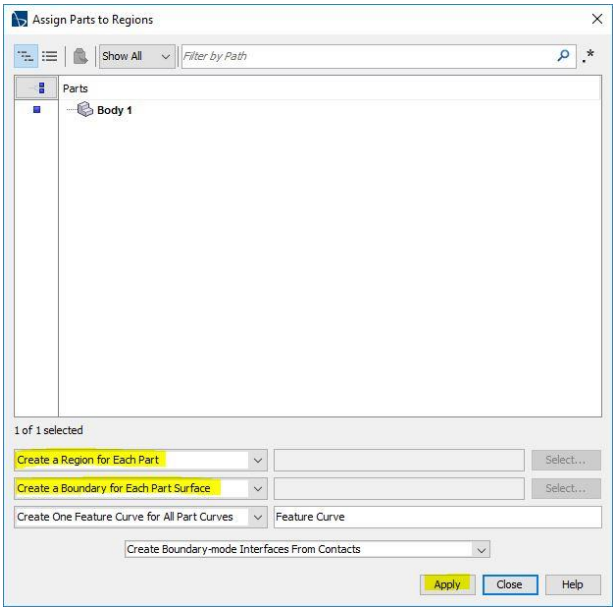

Step 5: Select Meshing Models

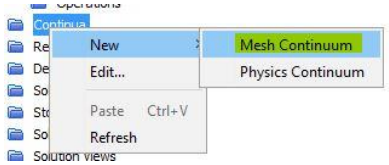

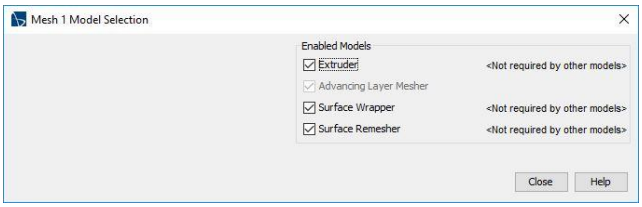

Step 6: Set Mesh control variables properly

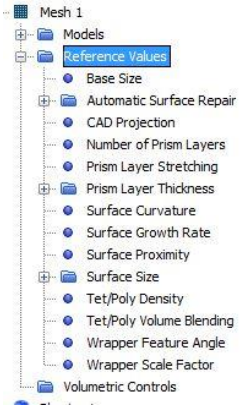

Step 7: Click the ‘Meshed Cube’ to perform meshing the CAD model

Step 8: Create a new Mesh scene to visualize the mesh

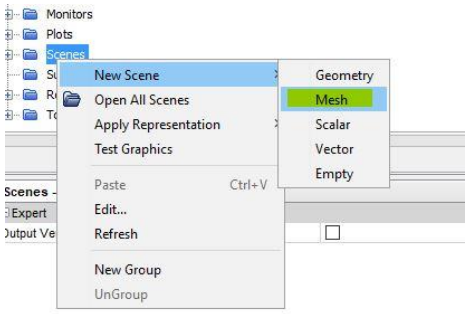

Step 9: Select Physics models

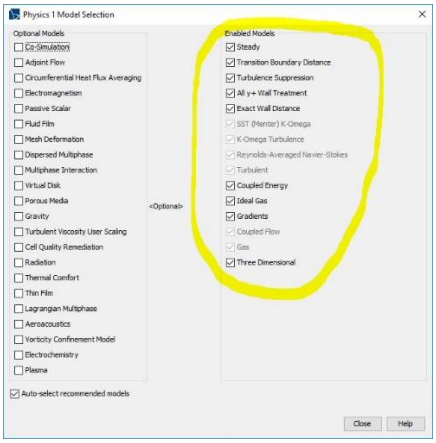

Step 10: Set proper physics at every region

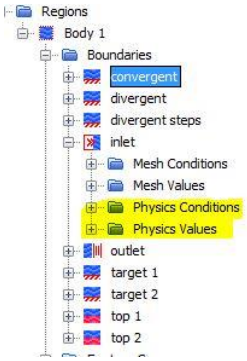

Step 11: Initialize the solution

Step 12: Run the Simulation